Peter S. Curtiss et al. “HVAC Design Calculations”
*Handbook of Heating, Ventilation, and Air Conditioning*
Ed. Jan F. Kreider
Boca Raton, CRC Press LLC. 2001

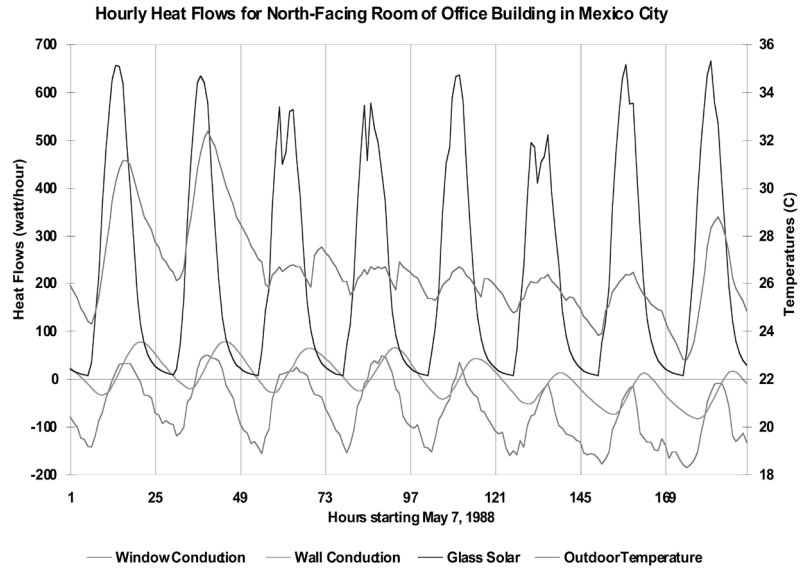


**FIGURE 6.2.16** Hourly plot of DOE-2 calculated conductive heat flows and solar heat gains in a typical north-facing office module in Mexico City.

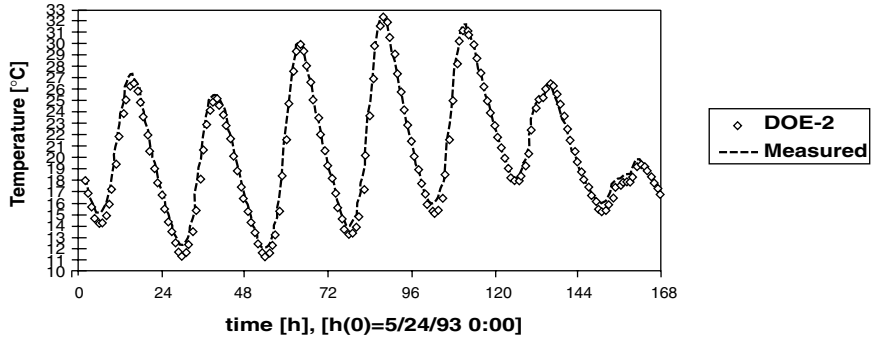


**FIGURE 6.2.17** Comparison of DOE-2 simulated and measured zone temperatures in an experimental test chamber in the U.K. (From Winkelmann, F. *The User's News*. With permission.)

buildings with sufficient information on building conditions and utility bills. In an International Energy Agency project that compared the results from various computer simulation programs to measured indoor temperatures for a well-monitored test cell in the U.K., the simulated indoor temperatures from DOE-2 were virtually identical to the measured results (see Figure 6.2.17).

In another project done at LBNL, DOE-2 simulations were done for several small unoccupied test houses in the San Diego area that were monitored in detail over several summers. The discrepancy in indoor temperatures was less than 0.3°C on average, and around 1°C maximum. In general, it seems that given sufficient time and effort to gather input parameters and calibrate (more truthfully, adjust) the building model, quite close agreements to measured data can be achieved. However, the same cannot be said for cases when there is no measured data for comparison. In such instances, there can be substantial discrepancies due to input errors, or user bias.

### *Future Developments in Building Energy Calculation Methods*

As mentioned previously, since 1996 the U.S. Department of Energy has been supporting the development of a new building energy simulation program, EnergyPlus, that aims to be an analysis platform for the next

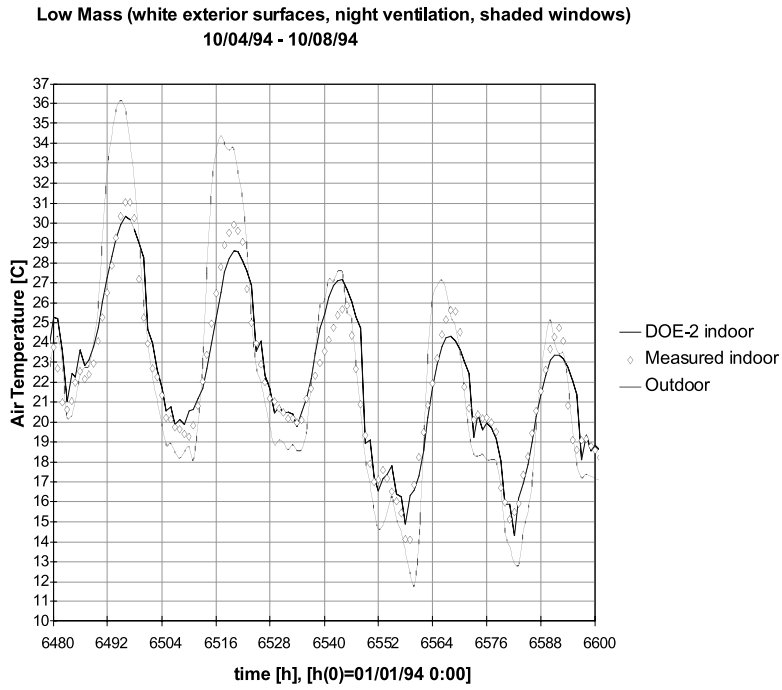


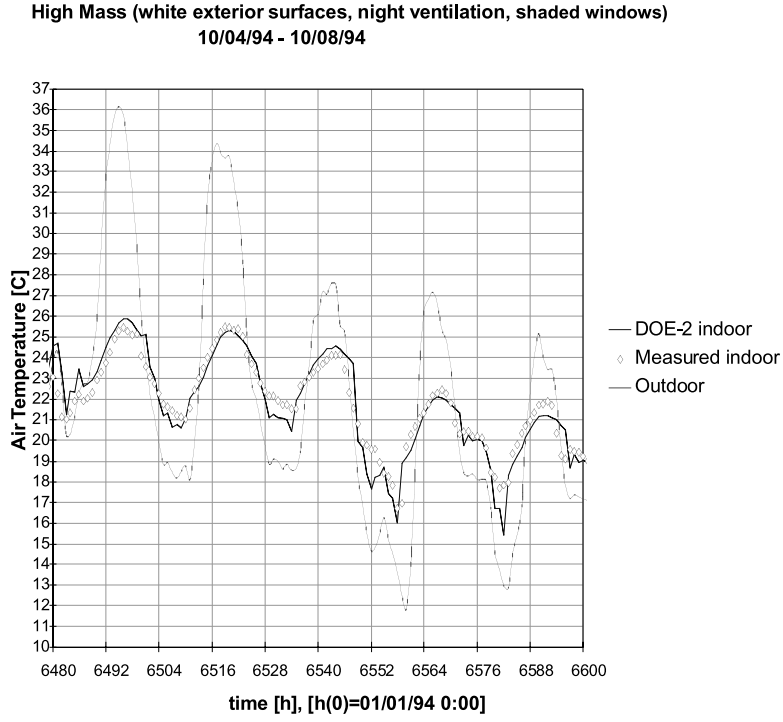


**FIGURE 6.2.18** Comparison of DOE-2 simulated and measured zone temperatures in unoccupied test houses in San Diego. (From Winkelmann, F. and Meldem, R. (1995). With permission.)

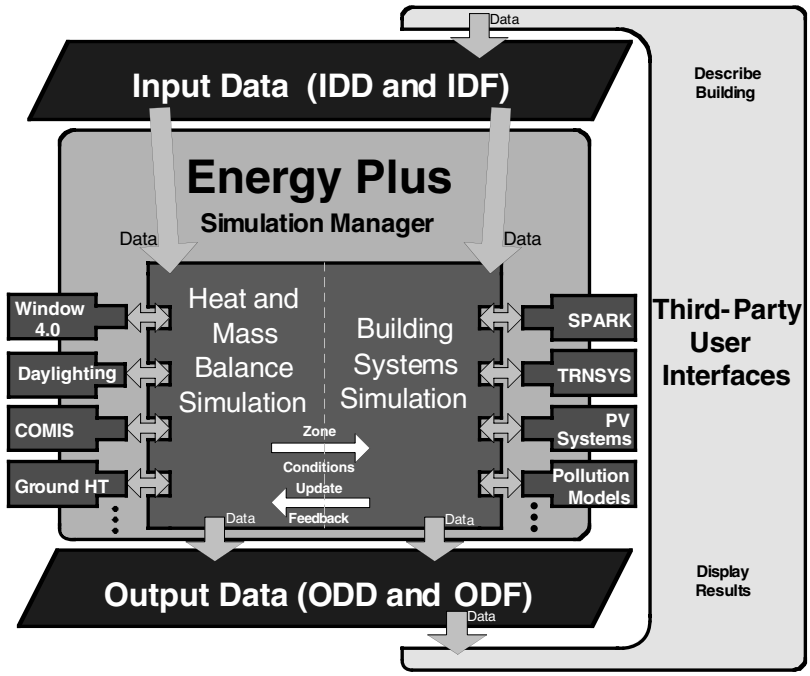


**FIGURE 6.2.19** Overall structure of the EnergyPlus program.

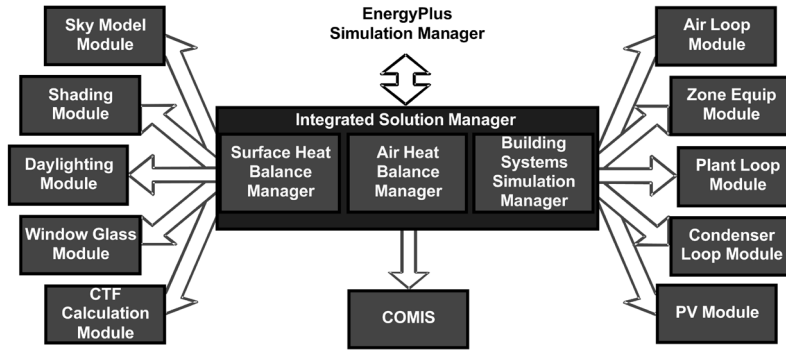


**FIGURE 6.2.20** EnergyPlus integrated simulation manager. (From Crawley, D.B. et al. (2000). With permission.)

decade or more. Figures 6.2.19 and 6.2.20 illustrate the structure and calculation sequence of this new simulation tool. A general description of this new program is given in an article by Crawley et al. (1999).

## 6.2.3 Inverse Modeling

At the present time there are many different methods for analyzing energy use in buildings. In general, the applications of these methods are driven by the motivation behind the investigation of a building's energy use, including retrofit energy savings analysis, diagnosing equipment malfunctions, energy auditing indices, component efficiency testing, and demand side management (DSM) evaluation. These methods can be divided into two basic approaches — forward modeling and inverse modeling — with a third approach that represents methods that contain aspects of both definitions — forward plus inverse (Rabl, 1988; Rabl and Riahle, 1992). Forward modeling was the subject of Sections 6.2.1 and 6.2.2.

In the inverse approach, the analysis is conducted on the empirical behavior of the building as it relates to one or more driving forces or parameters. This approach is referred to as a system identification,

parameter identification, or *inverse modeling*. In the inverse modeling approach, one assumes a structure or physical configuration of the building or system being studied and then attempts to identify the important parameters through the use of a statistical analysis (Rabl and Rialhe, 1992). In general, there are two basic types of inverse models: steady state inverse models and dynamic inverse models. A third category, hybrid models, includes models that have characteristics of both forward and inverse models.

Inverse modeling techniques have been successful in the following cases:

- Identifying the energy savings from building retrofits
- Estimating the performance of an existing building under future weather and occupancy conditions
- Predicting hourly (or subhourly) loads and energy use levels for optimal operation of HVAC systems under demand or real time pricing utility rates
- Constructing a model of HVAC subsystems for the optimal, adaptive control of that subsystem
- Faulting diagnosis of HVAC systems

## Steady State Inverse Models

The simplest form of an inverse model is a *steady state inverse model* of a building's energy use. The simplest steady state inverse model can be calculated by statistically regressing monthly utility consumption data against average billing period temperatures. Although simple in concept, the most accurate methods use sophisticated change-point regression procedures that simultaneously solve for several parameters including a weather independent base-level parameter, one or more weather dependent parameters, and the point or points at which the model switches from weather dependent to weather independent dependent behavior. In its simplest form, the 65°F (18.3°C) degree-day model is a change-point model that has a *fixed* change point at 65°F. Other examples include the three- and five-parameter Princeton Scorekeeping Methods* (PRISM) (Fels 1986) and a four-parameter model** (4P) developed by Ruch and Claridge (1991). An inverse bin method has also been proposed to handle more than four changepoints (Thamiseran and Haberl, 1995).

### *Models Using One Independent Variable*

Figure 6.2.21 shows several types of steady state, single variable inverse models. Figure 6.2.21a shows a simple one-parameter, or "average," model whose equation is given in the first line of Table 6.2.5. Figure 6.2.21b shows a steady state two-parameter (2P) model where $\beta_0$ is the y-axis intercept, and $\beta_1$ is the slope of the regression line for positive values of x, where x represents the ambient air temperature. The 2P model represents cases when either heating or cooling is always required.

Figure 6.2.21c shows a three-parameter, change point model. This is typical of natural gas energy use in a single family residence that utilizes gas for space heating and domestic water heating. In the equation in Table 6.2.5, $\beta_0$ represents the baseline energy use, and $\beta_1$ is the slope of the regression line for values of ambient temperature less than the change point $\beta_2$. In this type of notation, the exponent (+) indicates that only positive values of the parenthetical expression are considered. Figure 6.2.21d shows a three-parameter model for cooling energy.

Figures 6.2.21e and 6.2.21f illustrate four-parameter models for heating and cooling, respectively. In a four-parameter model, $\beta_0$ represents the baseline energy exactly at the change point $\beta_3$. $\beta_1$ and $\beta_2$ are the lower and upper region regression slopes for ambient air temperature below and above the change point $\beta_3$. Figure 6.2.21g illustrates a five-parameter model (Fels, 1986). Such a model is useful for modeling buildings that are electrically heated and cooled. The five-parameter model has two change points and a base level consumption value as shown in the final equation in Table 6.2.5.

* The three parameters include a weather independent base-level use, a change-point, and a temperature dependent parameter or slope of a line that is determined by regression.

** The four parameters include a change point, a slope above the change point, a slope below the change point, and the energy use associated with the change point.

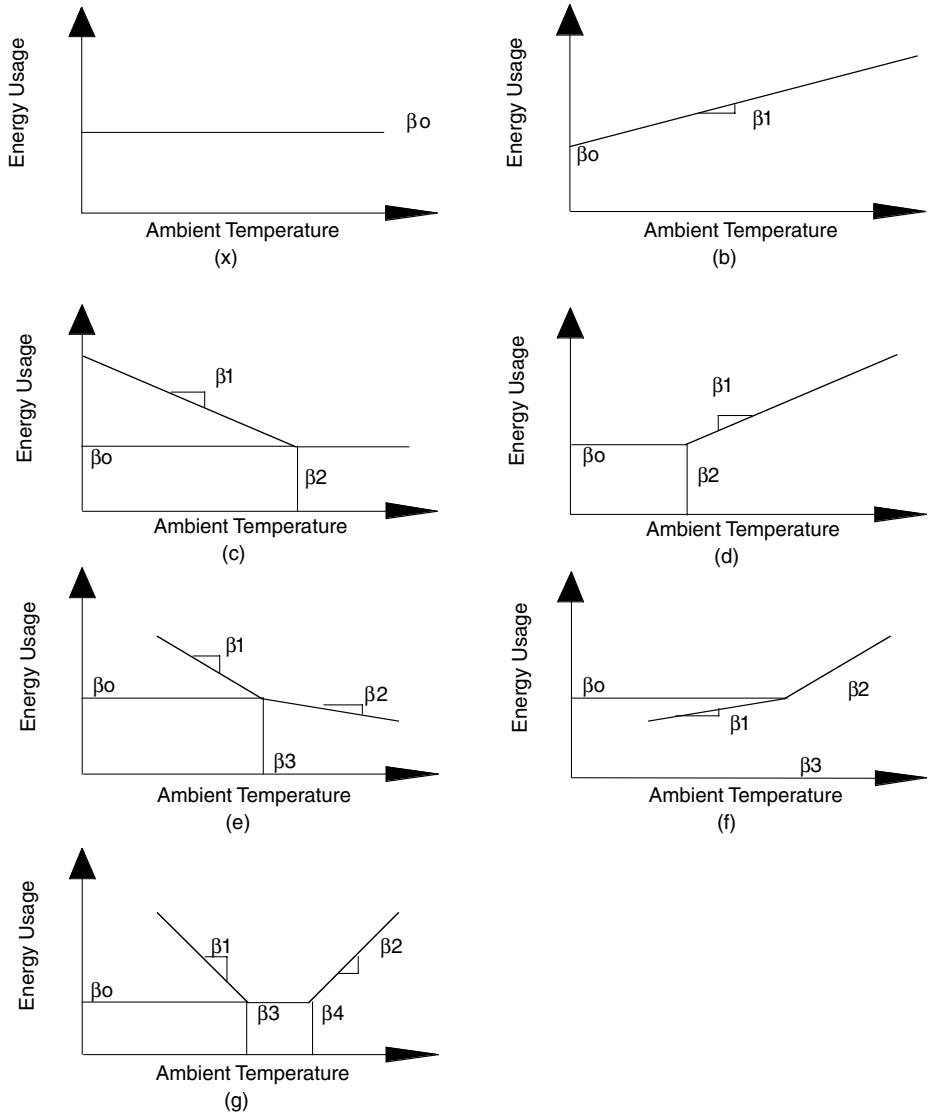


**FIGURE 6.2.21** Steady state, single variable models appropriate for commercial building energy use: (a) one-parameter model, (b) two-parameter model shown for cooling energy use, (c) three-parameter heating energy use model, (d) three-parameter cooling energy use model, (e) four-parameter heating energy use model, (f) four-parameter cooling energy use model, and (g) five-parameter heating and cooling model with separate change points.

The advantage of these simple steady state inverse models is that their use can be easily automated and applied to a large numbers of buildings where monthly utility billing data and average daily temperatures for the billing period are available. Steady state inverse models can also be applied to daily data, which allows one to compensate for differences in weekday and weekend use (Claridge et al., 1992).

The disadvantages of the steady state inverse models include

- An insensitivity to dynamic effects (i.e., thermal mass)
- Insensitivity to variables other than temperature (for example humidity and solar gain)
- Inappropriateness for certain building types, such as buildings that have strong on/off schedule dependent loads, or buildings that display multiple change points. In such cases, alternative models must be used.

**TABLE 6.2.5** Change Point (CP) Model Equations

$$E_{period} = \beta_0$$
(average model)

$$E_{period} = \beta_0 + \beta_1 T$$
(single CP model)

$$E_{period} = \beta_0 + \beta_1(\beta_2 - T)^+$$
(double CP model — heating)

$$E_{period} = \beta_0 + \beta_1(T - \beta_2)^+$$
(double CP model — cooling)

$$E_{period} = \beta_0 + \beta_1(\beta_3 - T)^+ - \beta_2(T - \beta_3)^+$$
(triple CP model — heating)

$$E_{period} = \beta_0 - \beta_1(\beta_3 - T)^+ + \beta_2(T - \beta_3)^+$$
(triple CP model — cooling

$$E_{period} = \beta_0 - \beta_1(\beta_3 - T)^+ + \beta_2(T - \beta_4)^+$$
(five-parameter model — cooling)

***Steady State Inverse Models Using More Than One Independent Variable***

Multiple regression techniques allow the analyst to investigate the influence of more than one independent variable (such as outdoor air temperature and humidity, solar radiation, and indicators of scheduling) on a response variable (such as building energy use). The form of the general linear regression model is

$$Y = \beta_0 + \beta_1 X_1 + \beta_2 X_2 + \ldots + \beta_P X_P + \varepsilon$$

where $Y$ is the response variable; $X_1, X_2, \ldots X_P$ are the independent variables; $\beta_0, \beta_1, \beta_2, \ldots, \beta_P$ are the p regression parameters; and ε is the error term. When $p$=2, the response surface is a plane. When $p > 2$, the response surface is called a hyperplane.

Interactions between independent variables can be considered by using the product of two independent variables. Curvature in the response surface can be introduced through the use of independent polynomial variables. The equation below demonstrates a model with two independent variables, each in quadratic form, with an interaction term:

$$Y = \beta_0 + \beta_1 X_1 + \beta_2 X_1^2 + \beta_3 X_2 + \beta_4 X_2^2 + \beta_5 X_1 X_2 + \varepsilon$$

The choice of the model should be guided by the analyst's understanding of the physical system and its expected response. Several standard statistical tests exist for evaluating the goodness-of-fit of the model and the degree of influence that each of the independent variables exerts on the response variable (Draper and Smith, 1981; Neter et al., 1989).

When modeling building energy use data, the independent variables are often linearly correlated with each other (as in the case of outdoor air temperature, humidity, and solar radiation). When multicolinearity exists, the regression coefficients may not indicate the relative importance of the independent variables. In addition, the uncertainties of the estimates of the regression parameters (reported as the standard error of each parameter estimate) may be so large that the model's usefulness for prediction purposes is comprised.

## Dynamic Inverse Models — Neural Networks

More advanced forms of inverse models include *dynamic inverse models.* Examples of dynamic inverse models include equivalent thermal network analysis (Sonderegger, 1977;), ARMA models (Subbarao, 1990; Reddy, 1989), Fourier series models (Dhar et al., 1995), and artificial neural networks (Kreider and

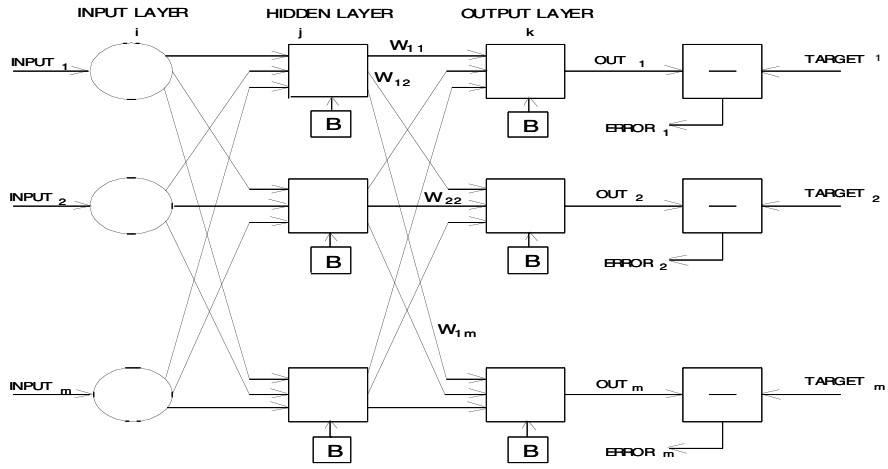


**FIGURE 6.2.22** Schematic diagram of a neural network showing input layer, hidden layers, and output along with target training values. Hidden and output layers consist of connected neurons; the input layer does not contain neurons.

Wang, 1991; Kreider and Haberl, 1994). Neural networks seem to hold considerable promise among those listed and are described in detail below.

The use of the term *dynamic* refers to the fact that these models are capable of capturing dynamic effects, such as mass dynamics, which traditionally have required the solution of a set of differential equations. These models are better suited for handling intercorrelated forcing functions or independent parameters. The advantages of dynamic inverse models include the ability to model complex systems which are dependent on more than one independent parameter. The disadvantages of dynamic inverse models include their increasing complexity and the need for more detailed measurements to "tune" the model. Unlike steady state inverse models, dynamic inverse models usually require a high degree of user interaction and knowledge of the building or system being modeled.

***Neural Network Construction***

An artificial neural network is a massively parallel, dynamic system of interconnected, interacting parts based loosely on some aspects of the brain. Neural networks are considered to be intuitive because they learn by example rather than by following programmed rules. The ability to "learn" is one of the key aspects of neural networks. A neural network consists of several layers of neurons that are connected to each other. A *connection* is a unique information transport link from one sending neuron to one receiving neuron. The structure of part of an NN is schematically shown in Figure 6.2.22. Any number of input, output, and hidden layer (only one hidden layer is shown) neurons can be used. One of the challenges of this technology is to construct a net with sufficient complexity to learn accurately without imposing a burden of excessive computational time.

The neuron is the fundamental building block of a neural network. A set of inputs is applied to each. Each element of the input set is multiplied by a weight, indicated by the *W* in Figure 6.2.22, and the products are summed at the neuron. The symbol for the summation of weighted inputs is termed *INPUT* and must be calculated for each neuron in the network. In equation form, this process for one neuron is

$$INPUT = \sum_{i} O_i W_i + B$$

where

$O_i$ are inputs to a neuron, i.e., outputs of the previous layer
$W$ are weights, and
$B$ are the biases.

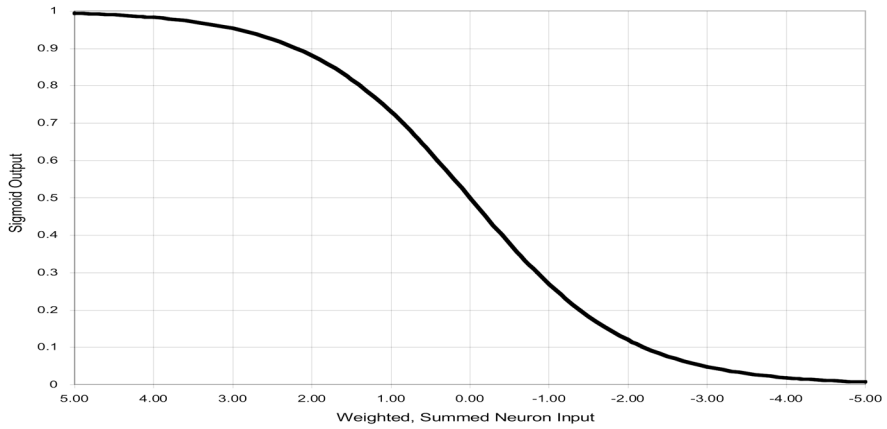


**FIGURE 6.2.23** Sigmoid function used to process the weighted sum of network inputs.

After *INPUT* is calculated, an activation function *F* is applied to modify it, thereby producing the neuron's output as described shortly.

Artificial networks have been trained by a wide variety of methods (McClelland and Rumelhart, 1988; Wasserman, 1989). Back-propagation is one systematic method for training multilayer neural networks. The weights of a net are initiated with small random numbers. The objective of training the network is to adjust the weights iteratively so that application of a set of inputs produces the desired set of outputs matching a training data set. Usually a network is trained with a data set that consists of many input-output pairs; these data are called a training set. Training the net using back-propagation requires the following steps:

1. Select a training pair from the training set and apply the input vector to the network input layer.
2. Calculate the output of the network, $OUT_i$.
3. Calculate the error $ERROR_i$ between the network output and the desired output (the target vector from the training pair).
4. Adjust the weights of the network in a way that minimizes the error.
5. Repeat steps 1 through 4 for each vector in the training set until the error for the entire set is lower than the user specified, preset training tolerance.

Steps 1 and 2 are the *forward pass*. The following expression describes the calculation process in which an activation function *F* is applied to the weighted sum of inputs *INPUT*:

$$OUT = F(INPUT) = F(\sum O_i W_i + B)$$

where *F* is the activation function, and *B* is the bias of each neuron.

A common activation function is the sigmoid function

$$F(INPUT) = \frac{1}{(1 + e^{-INPUT})}$$

A sigmoid function is shown in Figure 6.2.23. It has a value of 0.0 when *INPUT* is a large negative number and a value of 1.0 for large and positive *INPUT*, making a smooth transition between these limiting values. The bias *B* is the activation threshold for each neuron. The bias avoids the tendency of a sigmoid function to get "stuck" in the saturated, limiting value area.

Steps 3 and 4 above comprise the *reverse pass* in which the delta rule (McClelland and Rumelhart, 1988) is used as follows. For each neuron in the output layer, the previous weight *W(n)* is adjusted to a new value *W(n+1)* to reduce the error by the following rule:

$$W(n+1) = W(n) + (n\delta)OUT$$

where $W(n)$ is the previous value of a weight
$W(n+1)$ is the weight after adjusting
$\eta$ is the training rate coefficient
$\delta$ is calculated from

$$\delta = \left(\frac{\partial INPUT}{\partial OUT}\right)(TARGET - OUT) = OUT(1 - OUT)(TARGET - OUT)$$

in which *TARGET* (see Figure 6.2.22) is the training set target value. This method of correcting weights bases the magnitude of the correction on the error itself.

Of course, hidden layers have no target vector; therefore, back-propagation trains these layers by propagating the output error back through the network layer by layer, adjusting weights at each layer. The delta rule adjustment is calculated from

$$\delta_j = OUT(1 - OUT)\sum \delta_{j+1} W_{j+1}$$

This overall method of adjusting weights belongs to the general class of steepest descent algorithms. The weights and bias after training contain meaningful system information; before training the initial, random biases and random weights have no physical meaning.

***Neural Networks Applied to Buildings — Some Examples***

This section describes a number of applications of NNs to residential and commercial building systems. Two energy prediction cases are presented and one commercial building control demonstration is included. Anstett and Kreider (1993), Kreider and Wang (1991), and Wang and Kreider (1992) report additional case studies.

***Commercial Buildings —*** There are a number of reasons that an NN prediction of building energy use has been found to be useful in commercial buildings; among them are

- Prediction of what a properly operating building should be doing compared to actual operation — if there is a difference, it can be used in an expert system to produce early diagnoses of building operation problems.
- Prediction of what a building, prior to an energy retrofit, would have consumed under present conditions — when compared to the measured consumption of the retrofitted building, the difference represents a good estimate of the energy savings due to the retrofit. This represents one of the few ways that actual energy savings can be determined after the pre-retrofit building configuration has ceased to exist.

Figure 6.2.24 shows results typical of several hundred networks constructed on a number of commercial buildings. This building is an academic engineering center located in central Texas. The cooling load is created by solar gains, internal ("free") gains, outdoor air sensible heat, and outdoor air humidity loads. The NN is used to predict the pre-retrofit energy consumption for comparison with measured consumption of the retrofitted building. Six months of pre-retrofit data were available with which to train a network.

The known building consumption data are shown in the figure by the solid line while the NN predictions are shown by the dashes. The figure shows that NNs trained for one period (here, September 1989) can predict energy consumption well into the future (January 1990).

The network used for this prediction has two hidden layers. The input layer contains eight neurons that receive eight different types of input data as listed below. The output layer consists of one neuron that gives the output datum (chilled water consumption). Each training fact (i.e., training data set),

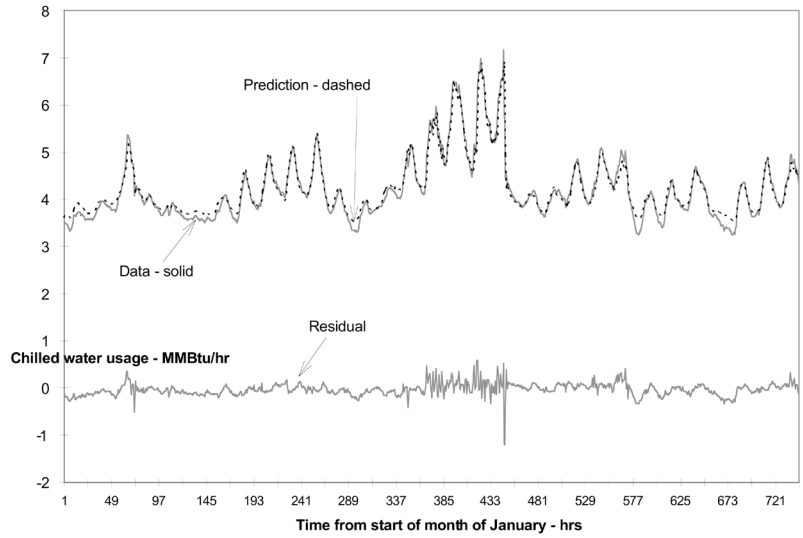


**FIGURE 6.2.24** NN prediction of whole building, hourly chilled water consumption, for example, commercial building.

therefore, contains eight input data (independent variables) and one pattern datum (dependent variable). The eight hourly input data used in each hour's data vector were selected on physical bases (Kreider, Rabl and Curtiss, 2001) as follows:

- Hour number (0–2300)
- Ambient dry-bulb temperature
- Horizontal insolation
- Humidity ratio
- Wind speed
- Weekday/weekend binary flag (0,1)
- Past hour's chilled water consumption
- Second past hour's chilled water consumption

These easily measured independent variables were able to predict the chilled water use to an RMS error of less than 4% (JCEM, 1992a, 1992b, 1992c).

The choice of an optimal network's configuration for a given problem remains an art. The number of hidden neurons and layers must be sufficient to meet the requirement of the given application. However, if too many neurons and layers are employed, the network becomes "brittle" and tends to memorize data rather than learning, that is, finding the underlying patterns within the data. Further, choosing an excessively large number of hidden layers significantly increases the required training time for certain learning algorithms.

The error and training time are two important training criteria. One measure of the accuracy of a network prediction is the root mean square error defined as

$$RMSE = \left\{ \frac{\sum (OUT - TARGET)}{\mathrm{N}} \right\}^{0.5}$$

where the network output *OUT* and target *TARGET* are both normalized before training to the closed interval [0-1]. The RMS error is dimensionless.

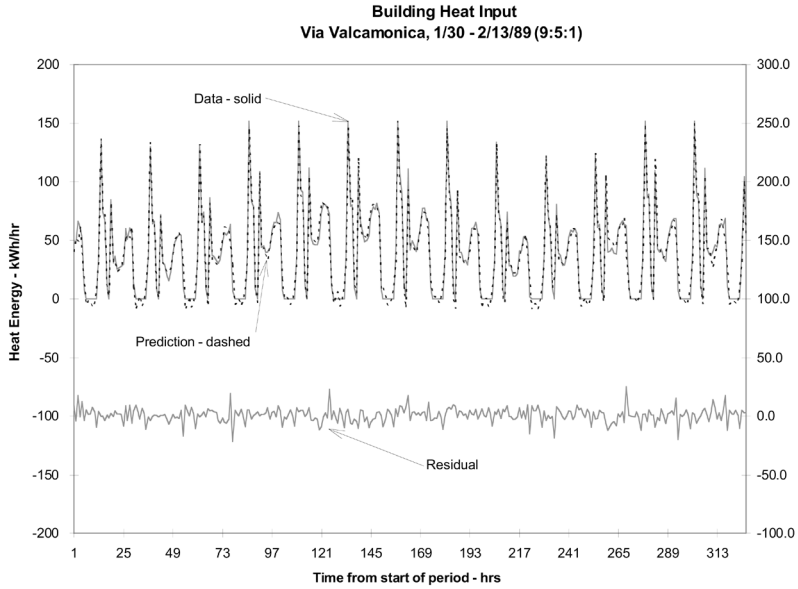


**FIGURE 6.2.25** NN prediction of residential heating energy for the first six weeks of 1989.

***Residential Buildings —*** Neural networks also have been applied to residential buildings. Figure 6.2.25 shows a typical prediction for a building in Varese, Italy. Hourly data collected by the Joint Research Center of the European Community included outdoor temperature and insolation, indoor temperature and heating energy consumption. The weather data and time information (hour of day, day of year) were used to make the predictions shown in the figure. It is seen that the diurnal patterns of heating energy usage are predicted well by the NN model.

## Application of Inverse Models

The principal applications of inverse models appear to be in the following areas:

- Evaluation of energy conservation programs
- Prescreening indices for energy auditing
- Building energy management
- Optimal control
- *In situ* characterization of HVAC

In each of these applications both steady state and dynamic inverse models have been applied. In general, steady state inverse models are used with monthly and daily data containing one or more independent variables. Dynamic inverse models are usually used with hourly or sub-hourly data in cases where the thermal mass of a building is significant enough to delay the heat gains or losses.

### *Evaluation of Energy Conservation Programs*

Aside from simply regressing energy use against temperature (e.g., often a two-parameter model with a slope and y-axis intercept), other widely-used steady state inverse methods for the evaluation of energy conservation retrofits include three-, four- and five-parameter change points models previously described (Fels, 1986; Ruch and Claridge, 1993). Such models have been shown to be useful for statistically determining average weather dependent and weather independent energy use for buildings. Three-parameter change point models can yield baseline energy use, the temperature at which weather dependent energy use begins to increase energy use above the baseline (i.e., the change point), and the linear slope of the temperature dependency above (cooling model) or below (heating model) the temperature change point.

The existence of a change point in heating or cooling data that is plotted against ambient temperature can be physically justified since most HVAC systems use a thermostat that turns systems on or off above or below a setpoint temperature. Change point regressions work best with heating data from buildings with systems that have few or no part-load nonlinearities (i.e., systems that become less efficient as they begin to cycle on-off with part-loads). In general change point regressions for cooling loads exhibit less of a good fit because of changes in outdoor humidity which influence latent coil loads. Other factors that decrease the goodness of fit of change point models include solar effects, thermal lags, and on-off HVAC schedules. In buildings with continuous, year-round cooling or heating, four-parameter models exhibit a better statistical fit over three-parameter models (i.e., grocery stores and office buildings with high internal loads). However, results of every modeling effort should be inspected for reasonableness (i.e., make sure that the regression is not falsely indicating an unreasonable relationship).

One of the main advantages of using a steady state inverse model to evaluate the effectiveness of energy conservation retrofits lies in its ability to factor out year-to-year weather variations. This can be accomplished by using a Normalized Annual Consumption or NAC (Fels, 1986). Basically, once the regression parameters have been calculated for both pre-retrofit and post-retrofit periods, the annual energy conservation savings can be calculated by comparing the difference one obtains by multiplying the pre-retrofit and post-retrofit parameters by the weather conditions for the average year. Typically, ten to twenty years of average daily weather data from a nearby National Weather Service site are used to calculate 365 days of average weather conditions which are then used to calculate the average pre-retrofit and post retrofit conditions.

***Energy Management***

Steady state and dynamic inverse models can be used by energy management and control systems to predict energy use (Kreider and Haberl, 1994). Hourly or daily comparisons of measured energy use against predicted energy use can be used to determine if systems are being left on unnecessarily or are in need of maintenance. Combinations of predicted energy use and a knowledge-based system have been shown to be capable of indicating above normal energy use and diagnosing the possible cause of the malfunction if sufficient historical information about malfunction signatures has been previously gathered (Haberl and Claridge, 1987). Hourly systems that utilize artificial neural networks have also been constructed (Kreider and Wang, 1991).

## 6.2.4 Hybrid Modeling

Forward plus inverse models or hybrid models encompass everything that does not neatly fit into the exact definition of forward or inverse models. For example, when a traditional fixed-schematic simulation program such as DOE-2 or BLAST (or even a component based model) is used to simulate the energy use of an existing building, then one has a *forward* analysis method that is being used in an *inverse* application, i.e., the forward simulation model is being calibrated or fit to the actual energy consumption data from a building in much the same way that one fits a linear regression of energy use to temperature. Such an application is a *hybrid model*.

Although at first this might appear to be a simple process, there are several practical difficulties in achieving a "calibrated simulation," including the measurement and adaptation of weather data for use by the simulation programs (i.e., converting global horizontal solar into beam and diffuse solar radiation), the choice of methods used to calibrate the model, and the choice of methods used to measure the required input parameters for the simulation (i.e., the weight of the building, infiltration coefficients, and shading coefficients). In the scientific sense, truly "calibrated" models have been achieved only in very few applications since they require a very large number of input parameters, a high degree of expertise, and enormous amounts of computing time, patience, and financial resources — much more than most practical applications would allow. However, examples exist in the literature of different methods employed to calibrate simulation models, including Bronson et al. (1992), Haberl et al. (1995), Kaplan et al. (1990), Corson (1992), Bou Saada and Haberl (1995a, 1995b), and Hsieh (1988).

**TABLE 6.2.6** Classification of Methods for the Thermal Analysis of Buildings

| Method | Forward | Inverse | Hybrid | Comments: |
|---|---|---|---|---|
| | | Steady State Methods | | |
| Simple linear regression | | X | | One dependent parameter, one independent parameter. May have slope and y-intercept. |
| Multiple linear regression | | X | X | One dependent parameter, multiple independent parameters. |
| Modified degree-day method | X | | | Based on fixed reference temperature of 65°F. |
| Variable base degree-day method | X | | | Variable reference temperatures. |
| ASHRAE bin method and inverse bin method | X | X | X | Hours in temperature bin times load for that bin. |
| Change point models: 3-parameter (PRISM CO, HO), 4-parameter, 5-parameter (PRISM HC). | | X | X | Uses daily or monthly utility billing data and average period temperatures. |
| ASHRAE TC 4.7 modified bin method | X | | X | Modified bin method with cooling load factors. |
| | | Dynamic Methods | | |
| Thermal network (Sonderegger, 1977) | X | X | X | Uses equivalent thermal parameters (inverse mode). |
| Response factors (Stephenson and Mitalas, 1967) | X | | | Tabulated or as used in simulation programs. |
| Fourier Analysis (Shurcliff, 1984; Dhar, 1995) | X | X | X | Frequency domain analysis convertible to time domain. |
| ARMA Model (Subbarao, 1986) | | X | | Autoregressive Moving Average model. |
| ARMA Model (Reddy, 1989) | | X | | Multiple-input autoregressive moving average model. |
| BEVA, PSTAR (Subbarao, 1986) | X | X | X | Combination of ARMA and Fourier series, includes loads in time domain. |
| Modal analysis (Bacot et al., 1984) | X | X | X | Bldg. described by diagonalized differential equation using nodes. |
| Differential equation (Rabl, 1988) | | X | | Analytical linear differential equation. |
| Computer simulation (DOE-2, BLAST) | X | | X | Hourly simulation programs with system models. |
| Computer emulation (HVACSIM+, TRNSYS) | X | | X | Sub-hourly simulation programs. |
| Artificial neural networks (Kreider and Wang, 1991; Kreider, 1992; Kreider and Haberl, 1994) | | X | X | Connectionist models. |

## 6.2.5 Classification of Methods

In Table 6.2.6 different methods of analyzing building energy use are classified using an expanded version of Rabl's definitions (Rabl, 1988). Simple linear regression and multiple linear regression are the most widely used forms of inverse analysis. In the proper application, multiple linear regression must adequately address intercorrelations among the independent parameters as discussed above.

## 6.2.6 How to Select an Approach

Table 6.2.7 presents a decision diagram for selecting an inverse model where usage of the model (diagnostics — D, energy savings calculations — ES, design — DE, and control — C), degree of difficulty in understanding and applying the model, time scale for the data used by the model (hourly — H, daily — D, monthly — M, and subhourly — S), calculation time, and input variables used by the models (temperature — T, humidity — H, solar — S, wind — W, time — t, thermal mass — tm) are the criteria used to determine the choice of a particular model.

**TABLE 6.2.7** Decision Diagram for Selection of Inverse Models

| Method | Usage[a] | Difficulty | Time[b] Scale | Calc. Time | Variables[c] | Accuracy |
|---|---|---|---|---|---|---|
| Simple linear regression | ES | Simple | D,M | Very Fast | T | Low |
| Multiple linear regression | D,ES | Moderate | D,M | Fast | T,H,S,W,t | Medium |
| ASHRAE bin method and inverse bin method | ES | Moderate | H | Fast | T | Medium |
| Change point models. | D,ES | Moderate | H,D,M | Fast | T | Medium |
| ASHRAE TC 4.7 modified bin method | ES,DE | Moderate | H | Medium | T,S,tm | Medium |
| Thermal network | D,ES,C | Complex | S,H | Fast | T,S,tm | High |
| Fourier Series Analysis | D,ES,C | Complex | S,H | Medium | T,H,S,W,t,tm | High |
| ARMA Model | D,ES,C | Complex | S,H | Medium | T,H,S,W,t,tm | High |
| Modal analysis | D,ES,C | Complex | S,H | Medium | T,H,S,W,t,tm | High |
| Differential equation | D,ES,C | Very Complex | S,H | Fast | T,H,S,W,t,tm | High |
| Computer Simulation (Component-based) | D,ES,C, DE | Very Complex | S,H | Slow | T,H,S,W,t,tm | Medium |
| Computer simulation (Fixed schematic) | D,ES,DE | Very Complex | H | Slow | T,H,S,W,t,tm | Medium |
| Computer emulation | D,C | Very Complex | S,H | Very Slow | T,H,S,W,t,tm | High |
| Artificial Neural Networks | D,ES,C | Complex | S,H | Fast | T,H,S,W,t,tm | High |

[a] Usage shown includes diagnostics (D), energy savings calculations (ES), design (DE), and control (C).
[b] Time scales shown are hourly (H), daily (D), monthly (M), and subhourly (S).
[c] Variables include temperature (T), humidity (H), solar (S), wind (W), time (t), thermal mass (tm).

## References


Anstett, M. and J.F. Kreider, (1993). Application of Artificial Neural Networks to Commercial Building Energy Use Prediction, *ASHRAE Trans.*, 99, (Part. 1), 505–517.

Bacot, P., A. Neveu, and J. Sicard, (1984). Analyse Modale Des Phenomènes Thermiques en Regime Variable Dans le Batiment, *Revue Generale de Thermique*, No. 267, 189.

Bou Saada, T. and J. Haberl, (1995a). A Weather-Daytyping Procedure for Disaggregating Hourly End-Use Loads in an Electrically Heated and Cooled Building from Whole-Building Hourly Data, *Proc. 30th IECEC*, 349–356.

Bou Saada, T., and J. Haberl, (1995b). An Improved Procedure for Developing Calibrated Hourly Simulation Models, *Proc. Int. Building Performance Simulation Assoc.*

Bronson, D., S. Hinchey, J. Haberl, and D. O'Neal, (1992). A Procedure for Calibrating the DOE-2 Simulation Program to Non-Weather Dependent Loads, 1992 *ASHRAE Trans.*, 98 (Part 1), 636–652.

Clarke, J.A., (1985). *Energy Simulation in Building Design*, Adam Hilger Ltd., Boston, MA.

Claridge, D.E., M. Krarti, and M. Bida, (1987). A Validation Study of Variable-Base Degree-Day Cooling Calculations, *ASHRAE Trans.*, 93(2), 90–104.

Claridge, D.E., J.S. Haberl, R. Sparks, R. Lopez, and K. Kissock, (1992). Monitored Commercial Building Energy Data: Reporting the Results. *ASHRAE Trans.*, 98 (Part 1), 636–652.

Clark, D.R., (1985). *HVACSIM+ Building Systems and Equipment Simulation Program: Reference Manual.* NBSIR 84-2996, U. S. Department of Commerce, Washington, D.C.

Cole, R.J., (1976). The Longwave Radiation Incident Upon the External Surface of Buildings. *The Building Services Engineer*, 44, 195–206.

Cooper, K.W. and D.R. Tree, (1973). A Re-evaluation of the Average Convection Coefficient for Flow Past a Wall. *ASHRAE Trans.*, 79, 48–51.

Corson, G.C. (1992). Input-Output Sensitivity of Building Energy Simulations, *ASHRAE Trans.*, 98 (Part 1), 618.

Crawley, D.B. et al., (1999). EnergyPlus: a New Generation Building Energy Simulation Program, in *Proceedings of the Renewable and Advanced Energy Systems for the 21st Century Conference*, April 11–15, 1999, Lahaina, Maui, Hawaii.

Crawley, D.B. et al., (2000). EnergyPlus: Energy simulation program, *ASHRAE Journal*, April.

Draper, N. and H. Smith, (1981). *Applied Regression Analysis*, 2nd edition, John Wiley & Sons, New York, NY.
Davies, M.G., (1988). Design Models to Handle Radiative and Convective Exchange in a Room. *ASHRAE Trans.*, 94 (Part. 2), 173–195.
Erbs, D. G., S. A. Klein, and W. A. Beckman, (1983). Estimation of Degree-Days and Ambient Temperature Bin Data from Monthly-Average Temperatures. *ASHRAE J.* 25(6), 60.
Fels, M., Ed. (1986). Measuring Energy Savings: The Scorekeeping Approach, *Energy and Buildings*, vol. 9.
Fels, M. and M. Goldberg, (1986). Refraction of PRISM Results in Components of Saved Energy, *Energy and Buildings*, 9:169.
Haberl, J.S. and P. Komor, (1990b). Improving Commercial Building Energy Audits: How Daily and Hourly Data Can Help, *ASHRAE J.*, 32 (9), 26–36.
Haberl, J.S., D. Bronson, D. O'Neal, (1993). An Evaluation of the Impact of Using Measured Weather Data Versus TMY Weather Data in a DOE-2 Simulation of an Existing Building in Central Texas. *ASHRAE Trans*.
Haberl, J.S. and D.E. Claridge, (1987). An Expert System for Building Energy Consumption Analysis: Prototype Results, *ASHRAE Trans.*, 93 (Part. 1), 979–998.
Huang, Y.J. et al., (1984), Home Energy Rating Systems: Sample Approval Methodology for Two Tools, LBL-18669, Lawrence Berkely Laboratory, Berkeley, CA.
Joint Center for Energy Management, (1992). *Interim Report: Artificial Neural Networks Applied to LoanSTAR Data*. Report No. TR/92/10, June.
Joint Center for Energy Management, (1992). *Second Interim Report: Artificial Neural Networks Applied to LoanSTAR Data*. Report No. TR/92/11, June.
Joint Center for Energy Management, (1992). *Final Report: Artificial Neural Networks Applied to LoanSTAR Data*. Report No. TR/92/15, September.
Kaplan, M., J. McFerran, J. Jansen, and R. Pratt, (1990). Reconciliation of a DOE2.1c Model with Monitored End-Use Data From a Small Office Building, *ASHRAE Trans.*, 96, (Part 1), 981.
Katipamula, S. and D.E. Claridge, (1993). Use of Simplified Models to Measure Retrofit Energy Savings, *ASME J. Solar Energy Engineering*, 115, 77–84.
Kreider, J.F. and X.A. Wang, (1992). Improved Artificial Neural Networks for Commercial Building Energy Use Prediction, *Solar Engineering,* 92, 361–366, ASME, New York.
Kreider, J.F. and J.S. Haberl, (1994). Predicting Hourly Building Energy Usage: The Great Predictor Shootout — Overview and Discussion of Results, *ASHRAE Trans*.
Kreider, J.F., A. Rabl, and P.S. Curtiss, (1994). *Heating and Cooling of Buildings*: *Design for Efficiency*, McGraw-Hill, New York, 890.
Kreider, J.F. and X.A. Wang, (1991). Artificial Neural Networks Demonstration for Automated Generation of Energy Use Predictors for Commercial Buildings. *ASHRAE Trans.*, 97, (Part 1).
Liu, M., and D. Claridge, (1995). Application of Calibrated HVAC System Models to Identify Component Malfunctions and To Optimize the Operation and Control Strategies, *Proc. of the 1995 ASME Solar Engineering Conf.*, 1, 209–218.
MacDonald, J.M. and D.M. Wasserman, (1989). *Investigation of Metered Data Analysis Methods for Commercial and Related Buildings*, ORNL Rept., ORNL/CON-279, May.
McClelland, J. L. and D. E. Rumelhart, (1988). *Exploration in Parallel Distributed Processing*. MIT Press, Cambridge, MA.
Neter, J., W. Wasserman, and M. Kutner, (1989). *Applied Linear Regression Models*, 2nd edition, Richard C. Irwin, Inc., Homewood, IL.
Rabl, A. (1988). Parameter Estimation in Buildings: Methods for Dynamic Analysis of Measured Energy Use, *J. Solar Energy Engineering*, 110, 52–66.
Rabl, A., A. Riahle, (1992). Energy Signature Model for Commercial Buildings: Test With Measured Data and Interpretation, *Energy and Buildings*, 19, 143–154.
Reddy, T., (1989). Application of Dynamic Building Inverse Models to Three Occupied Residences Monitored Non-Intrusively, *Proc. Thermal Performance of Exterior Envelopes of Buildings IV*, ASHRAE/DOE/BTECC/CIBSE.

Reddy, T. and D. Claridge, (1994). Using Synthetic Data to Evaluate Multiple Regression and Principle Component Analyses for Statistical Modeling of Daily Building Energy Consumption, *Energy and Buildings*. 24, 35–44.

Ruch, D., L. Chen, J. Haberl, and D. Claridge, (1993). A Change-Point Principal Component Analysis (CP/PCA) Method for Predicting Energy Usage in Commercial Buildings: The PCA Model, *J. Solar Energy Engineering*, 115, No. 2, May.

Ruch, D., and D. Claridge, (1991). A Four Parameter Change-Point model for Predicting Energy Consumption in Commercial Buildings, *Proc. ASME-JSES-JSME International Solar Energy Conf.*, 433–440.

Sonderegger, R.C., (1977). Dynamic Models of House Heating Based on Equivalent Thermal parameters, Ph.D. Thesis, Center for Energy and Environmental Studies Report No. 57, Princeton University, Princeton, NJ.

Thamilseran, S and J. Haberl, (1995). A Bin Method for Calculating Energy Conservation Retrofit Savings in Commercial Buildings, *Proc. 1995 ASME/JSME/JSES Intl. Solar Energy Conf.*, 111–124.

U.S. Air Force, (1978). *Engineering Weather Data, AF Manual* AFM 88-29, U.S. Government Printing Office, Washington, D.C.

U.S. Army, (1979). *BLAST, The Building Loads Analysis and System Thermodynamics Program — Users Manual*. U.S. Army Construction Engineering Research Laboratory Report E-153.

U.S. Department of Energy, (1981). *DOE Reference Manual Version 2.1A*. Los Alamos Scientific Laboratory Report LA-7689-M, Version 2.1A. Lawrence Berkeley Laboratory, Report LBL -8706 Rev. 2.

Wang, X.A. and J.F. Kreider, (1992). Improved Artificial Neural Networks for Commercial Building Energy Use Prediction, *Solar Engineering*.

Wasserman, P.D., (1989). *Neural Computing, Theory and Practice*. Van Nostrand Reinhold, New York, NY.

Winkelmann, F. and Meldem, R., Comparison of DOE-2 with measurements in the Pala Test Houses, *LBNL Report 37979*, July 1995.

Yuill, G.K., (1990). *An Annotated Guide to Models and Algorithms for Energy Calculations Relating to HVAC Equipment.* American Society of Heating, Refrigerating, and Air-Conditioning Engineers, Inc., Atlanta, GA.

## 6.3 Energy Conservation in Buildings

*Max Sherman and David Jump*

### 6.3.1 The Indoor Environment

The building sector is an important part of the energy picture. In the United States about 40% of all U.S. energy expenses are attributable to buildings. While buildings may consume about one-third of the fuel resources in the country, they consume over 65% of the electricity.

Residential buildings accounted for 17 quads of energy at a cost of 104 billion dollars, while commercial buildings (offices, stores, schools, and hospitals) accounted for about 13 quads and $68 of energy consumption in 1989. A breakdown by sector reveals where most of the energy is used in buildings and provides background for improving building energy efficiency. The OTA's estimate suggests that by 2010, more that 10 quads of energy could be saved with improved energy efficiency.

The energy consumed in residential and commercial building provides many services, including weather protection, thermal comfort, communications, facilities for daily living, esthetics, a healthy work environment, and so on. Since in a modern society, people spend the vast majority of their time inside buildings, the quality of the indoor (or built) environment is important to their comfort, and good thermal performance of buildings is important for energy efficiency as well as productivity of workers in commercial buildings.

This chapter first discusses issues that influence the quality of the indoor environment in terms of the occupants' comfort, health, and productivity. Most of the facets of providing an acceptable indoor environment involve energy-intensive services. Factors influencing space conditioning energy needs, such as the building envelope's thermal properties and ventilation requirements, are then discussed. Next, the

means of providing space conditioning to the building interior is examined. Thermal distribution systems are discussed in this section; the actual heating and cooling equipment is covered in Chapters 4.1–4.3. Where applicable, opportunities for energy conservation through improved efficiency are demonstrated. Finally, some building simulation tools are reviewed to provide the reader with the means necessary to complete the complicated analysis of building energy consumption.

### Thermal Comfort

The most fundamental building service is to protect the occupants of the building from the outdoor environment. The building structure keeps the wind and rain out, but energy is required to provide an acceptable thermal environment for the occupants. The amount of energy required depends in part on the optimum comfort conditions required by the occupants activity levels and clothing (Figure 6.3.1). Thermal comfort is discussed in Chapter 2.2.

### Lighting and Visual Comfort

After the HVAC system, lighting accounts for the largest energy consumption of the building services. Building occupants require sufficient light levels to go about their normal activities. Just as the building envelope protects the occupants from weather, it also reduces the amount of usable sunlight. The desire to continue activities at any time or place necessitates the use of electric lighting.

In the perimeter of buildings and throughout small buildings natural lighting or daylighting can provide a high-quality visual environment. Care must be taken in the design phase to control the admission of daylight as it varies over the day and throughout seasons. This is done primarily with the use of exterior overhangs, fins, awnings, blinds, and interior shades, drapes, or blinds. In the core areas of buildings, electric lighting must be continuously provided to meet the occupants' lighting requirements.

Achieving visual comfort requires more than providing average light levels. Glare from high-intensity sources, poor color rendition, or flickering can all cause discomfort or reduce visual performance.

### Indoor Air Quality

Good indoor air quality may be defined as air that is free of pollutants that cause irritation, discomfort or ill health to occupants, or premature degradation of the building materials, paintings, and furnishings or equipment. Thermal conditions and relative humidity also impact the perception of air quality in addition to their effects on thermal comfort. Focus on indoor air quality issues increased as reduced-ventilation energy-saving strategies, and consequently increased pollution levels, were introduced. A poor indoor environment can manifest itself as a sick building in which some occupants experience mild illness symptoms during periods of occupancy. More serious pollutant problems may result in long-term or permanent ill-health effects.

An almost limitless number of pollutants may be present in a space, of which many are at immeasurably low concentrations and have largely unknown toxicological effects. Sources of indoor air pollutants in the home and in offices and their typical concentrations are given in Table 6.3.1. The task of identifying and assessing the risk of individual pollutants has become a major research activity in the past 20 years. Some pollutants can be tolerated at low concentrations, while irritation and odor often provide an early warning of deteriorating conditions. Health-related air quality standards are typically based on risk assessment and are specified in terms of a maximum permitted exposure, which is determined by exposure time and pollutant concentration. Higher concentrations of pollutants are normally permitted for shorter term exposures.

Air quality needs for comfort are highly subjective and dependent on circumstances. Some occupations allow higher exposures than would be allowed for the home or office. Health-related air quality standards are normally set at minimum safety requirements and may not necessarily provide for adequate comfort or energy efficiency at work or in the home.

Pollution-free environments are a practical impossibility. Optimum indoor air quality relies on an integrated approach to managing exposures by the removal and control of pollutants and ventilating the occupied space. It is often useful to differentiate between unavoidable pollutants (such as human bioef-

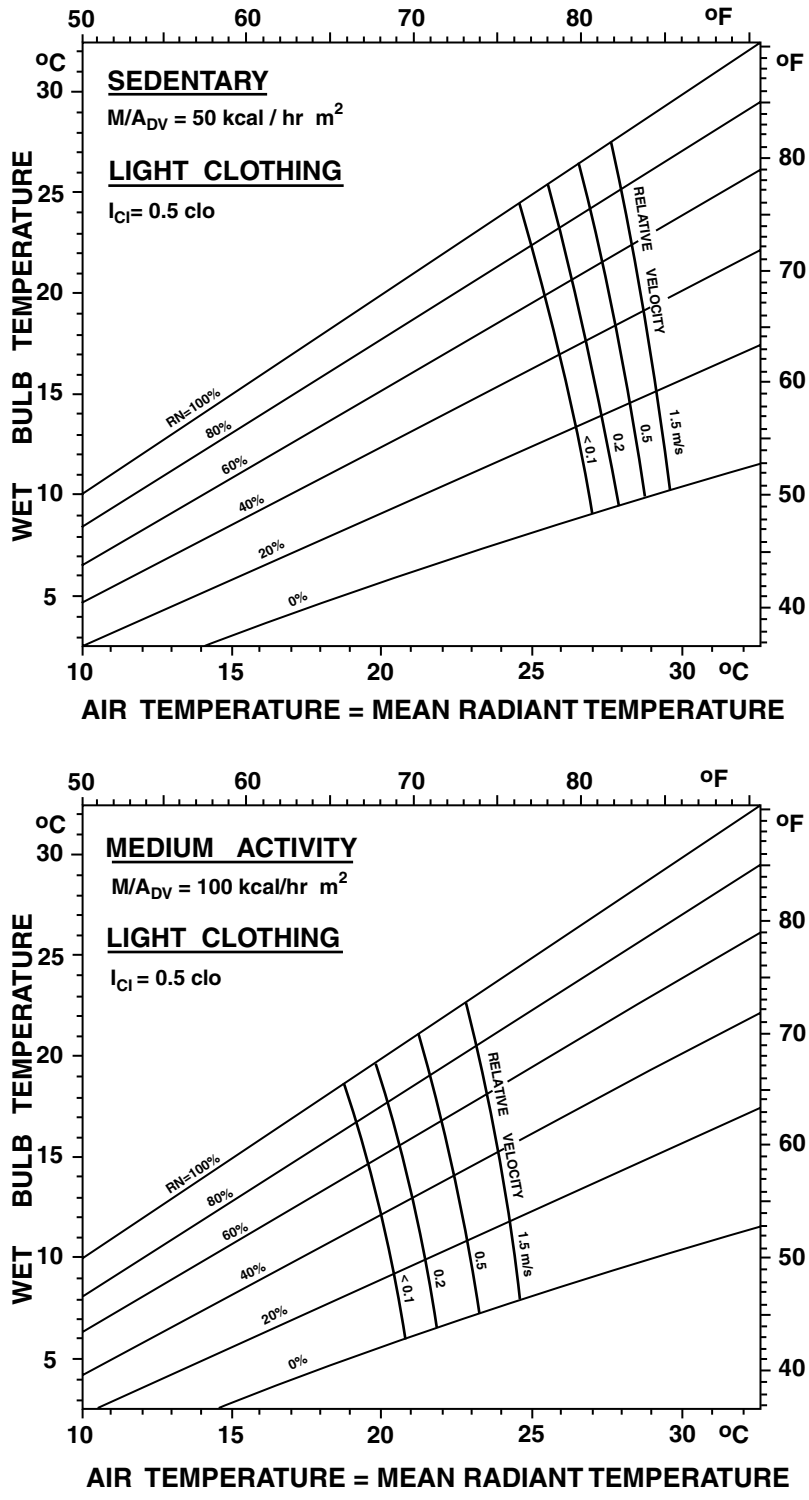


**FIGURE 6.3.1** Comfort lines for persons with light and medium clothing at two different activity levels. (From Fanger, P.O., *Thermal Comfort Analysis and Applications in Environmental Engineering,* McGraw-Hill, New York, 1970.)

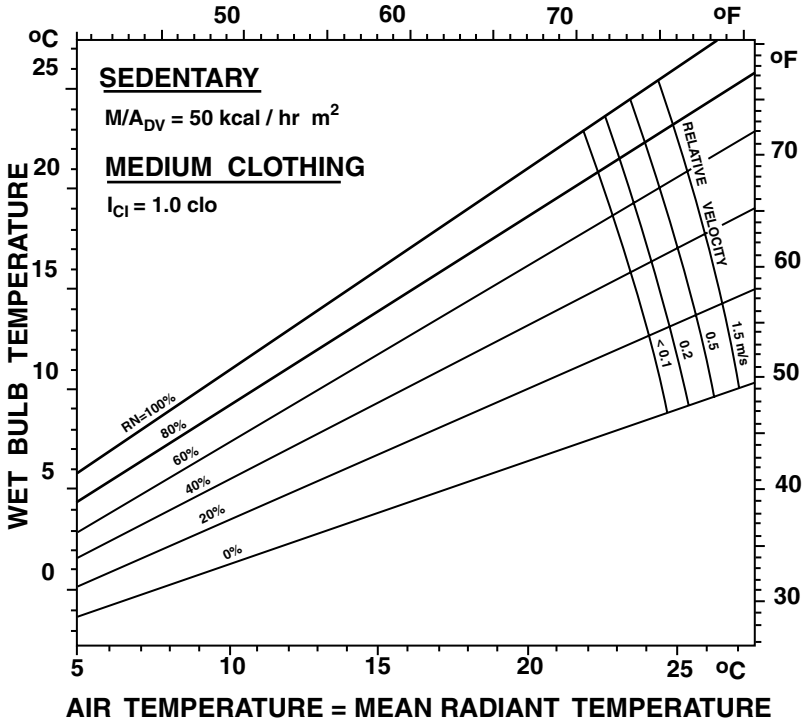


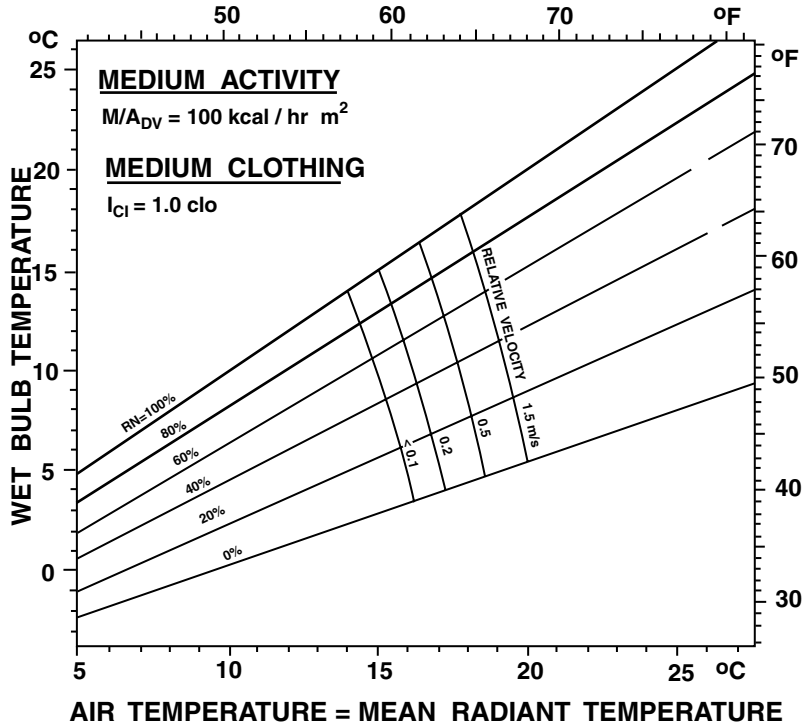


**FIGURE 6.3.1** (*continued*)

**TABLE 6.3.1** Principal Indoor Pollutants, Sources, and Typical Concentrations

| Pollutant | Source | Concentrations |
|---|---|---|
| Respirable particles | Tobacco smoke, unvented kerosene heaters, wood and coal stoves, fireplaces, outside air, occupant activities, attached facilities | >500 μg/m³ bars, meetings, waiting rooms with smoking<br>100–500 μg/m³ smoking sections of planes<br>10 to 100 μg/m³ homes<br>1,000 μg/m³ burning food or fireplaces |
| NO, $NO_2$ | Gas ranges and pilot lights, unvented kerosene and gas space heaters, some floor heaters, outside air | 25 to 75 ppb homes with gas stoves<br>100 to 500 ppb peak values for kitchens with gas stoves or kerosene gas heaters |
| CO | Gas ranges, pilot lights, unvented kerosene and gas space heaters, tobacco smoke, back drafting water heater, furnace, or wood stove, attached garages, street level intake vents, gasoline engines | >50 ppm when oven used for heating<br>>50 ppm attached garages, air intakes<br>2 to 15 ppm cooking with gas stove |
| $CO_2$ | People, unvented kerosene and gas space heaters, tobacco smoke, outside air | 320 to 400 ppm outdoor air<br>2,000 to 5,000 ppm crowded indoor environment, inadequate ventilation |
| Infectious, allergenic, irritating biological materials | Dust mites and cockroaches, animal dander, bacteria, fungi, viruses, pollens | >1,000 cfu/m³ homes with mold problems, offices with water damage<br>500 ± 200 cfu/m³ homes and offices without obvious problems |
| Formaldehyde | Urea Formaldehyde Foam Insulation (UFFI), glues, fiberboard, pressed board, plywood, particle board, carpet backing fabrics | 0.1 to 0.8 ppm homes with UFFI<br>0.5 ppm average in mobile homes |
| Radon and radon daughters | Ground beneath a home, domestic water, some utility natural gas | 1.5 pCi/l estimated average in homes<br>>6 pCi/l in 3 to 5% homes |
| Volatile organic compounds: benzene, styrene, tetrachloroethylene, dichlorobenzene, methylene chloride, chloroform | Outgassing from water, plasticizers, solvents, paints, cleaning compounds, mothballs, resins, glues, gasoline, oils, combustion, art materials, photocopiers, personal car products | Typical concentrations of selected compounds: benzene — 15 μg/m3; 1,1,1 trichloroethylene — 20 μg/m3; chloroform — 2 μg/m3; tetrachloroethylene — 5 μg/m3; styrene — 2 μg/m3; m, p-dichlorobenzene — 4 μg/m3; m,p-xylene — 15 μg/m3 |
| Semivolatile organics: chlorinated hydrocarbons, DDT heptachlor, chlordane, polycyclic compounds | Pesticides, transformer fluids, germicides, combustion of wood, tobacco, kerosene and charcoal, wood preservatives, fungicides, herbicides, insecticides | limited data |
| Asbestos | Insulation on building structural components, asbestos plaster around pipes and furnaces | >1,000 ng/m³ when friable asbestos, otherwise no systematic measurements |

*Note:* A cfu is a colony forming unit.
Source: From Samet, J.M. et al. (1988).

fluents) over which little source control is possible, and avoidable pollutants (such as emissions of volatile organic compounds) for which control is possible. Whole-building ventilation usually provides an effective measure to deal with the unavoidable emissions, but source control is the preferred and sometimes only practical method to address avoidable pollutant sources. Examples of source control are given in Table 6.3.3.

**TABLE 6.3.2** Methods of Controlling Sources of Indoor Pollution

| |
|---|
| Use of building materials, furnishings, and consumer products with low emissions rates |
| Physical removal of emitted pollutant |
| Isolating, encapsulating, or controlling emission sources |
| Local venting of pollutants at the point of emission (e.g., range hood, substructure radon control system) |

Source: From Nero, A.V. Jr., (1992). With permission.

## Productivity

The indoor environment contains and is affected by a variety of other issues that have indirect effects on thermal conservation in buildings. One of these that is of primary importance is worker productivity. Productivity is the workers' efficiency in performing their duties and responsibilities, which ultimately result in the economic well-being of the organization. In commercial buildings productivity has traditionally been viewed as the monetary return on employee compensation. Efforts to increase worker productivity have evolved from improving job satisfaction by various means (Stokes, 1978) and improving worker incentives (Lawler and Porter, 1967), to focusing on factors that negatively influence productivity, such as poor indoor environments.

Poor indoor environments can be generally described in three categories: inadequate thermal comfort, unhealthy environments, and poor lighting. Manifestations of poor productivity can be characterized by worker illness, absenteeism, distractions to concentration, and drowsiness or lethargy at work as well as by defects and mistakes in manufacturing and routine office work, and so forth. Primarily because of inadequate productivity measures, direct relationships between productivity and environmental factors are difficult to quantify (Daisey, 1989).

Examination of the cost of improving energy efficiency in buildings reveals that while significant energy cost savings are being achieved through retrofits, the relative savings may be dwarfed by savings due to increased worker productivity. Romm and Browning (1994) presented data based upon a national survey of office building stock in the United States showing that while energy costs are roughly $\$1.8/ft^2$ yr, the office workers' salaries amount to approximately $\$130/ft^2$ yr. As the authors state, "a 1% gain in productivity is equivalent to the entire annual energy cost." The point, often overlooked when considering an energy efficiency measure's cost-effectiveness, is that increased worker productivity can dramatically reduce the payback time of the retrofit.

## Envelope Thermal Properties

Some of the most important properties of building materials are their strength, weight, durability, and cost. In terms of energy conservation, their most important properties are their ability to absorb and transmit heat. The materials' thermal properties govern the rate of heat transfer between the inside and outside of the building, the amount of heat that can be stored in the material, and the amount of heat that is absorbed into the surface by heat conduction and radiation. The rate of heat transfer through the building materials in turn determines the magnitude of heat losses and gains in the building. This information is important in order to determine the proper and most efficient design of space heating equipment required to maintain the desired indoor environmental conditions.

Heat loss and gain through the building envelope is a complex process involving four main mechanisms: heat conductance through solid and porous parts of the building envelope; heat convection from air to walls, ceilings, floors, and exteriors; solar radiation absorbed on exterior surfaces and transmitted through windows; and heat transport through ventilation or infiltration of air. This section discusses the thermal properties associated with the first three mechanisms.

In order to take full advantage of different materials' thermal properties for energy conservation purposes, it is necessary first to determine the nature of building loads in each building sector. Residential, lightly loaded small commercial buildings and warehouses typically have low internal loads (e.g., heat from appliances, office equipment, lights, people, etc.), high infiltration loads, and high envelope transmission loads. The heat losses in these buildings are roughly proportional to the indoor-outdoor temperature difference. Depending on orientation and shading, solar heat gains can also be large. In large

commercial, industrial, and institutional buildings, envelope transmission loads are relatively lower than in houses and affect only the peripheral zones, not the building core. In these buildings, internal loads are dominant. Chapters 6.1 and 6.2 discuss additional details of thermal loads.

***Above-Grade Opaque Surfaces***

Steady-state heat transfer through the walls, floors and ceilings of a building depends on the indoor-outdoor temperature difference and the heat transmittance through each envelope component. Nothing can be done about the weather, and indoor conditions are constrained by occupant thermal comfort, but the conductance of the building envelope can be advantageously manipulated. Equation 6.3.1 shows the calculation required to determine envelope transmission heat losses, where the summation is taken over each component of the building envelope that separates the interior from the exterior.

$$Q_{tr} = \sum_i (UA)_i \, \Delta T \tag{6.3.1}$$

where

$\Delta T$ is the indoor-outdoor air temperature difference, in K (°F)
$A$ is the component's surface area, in m$^2$ (ft$^2$)
$U$ is the thermal transmittance of the component, in W/m$^2$K (Btu/hr ft$^2$°F)

The inverse of the transmittance $U$, is the component's resistance to heat flow, $R = 1/U$. Thermal resistance is analogous to electrical resistance when the heat transfer is one-dimensional, which is often the case in buildings. Thus, a very good approximate method of determining wall resistance to heat flow, for example, is to use electric circuit analogs. This is particularly useful when analyzing composite walls, ceilings, or floors made up of supporting framework, insulation, interior wallboard, exterior facing and so on, where the total resistance to heat flow can be determined from the individual resistances of each component. As an example, consider the composite wall of Figure 6.3.2(a), which represents the structure of a wall in a house, with insulation between wood studs on 46 cm (18 inches) centers. The interior wallboard is gypsum and the exterior facing is Douglas fir. The wall is represented by the electrical circuit shown in Figure 6.3.2(b).

The total thermal resistance of the wall is given by

$$R_{tot} = R_1 + T_2 + \left(R_5 R_6\right) / \left(R_5 + R_6\right) + R_3 + R_4$$

where $R_1 = 1/h_i$, $R_2 = a/k_1$, $R_3 = c/k_2$, $R_4 = 1/h_o$, $R_5 = b/\left(0.11 \cdot k_3\right)$, $R_6 = 1/\left(0.89 \cdot k_4\right)$

$R_1$ and $R_4$ are convective resistances, while all others are conductive resistances. $R_5$ and $R_6$ have been corrected for the fractional amount of area perpendicular to heat flow that they occupy. To show the effect of insulation, the calculation of the total wall resistance will be done first by assuming the insulation space is occupied by air. The calculation will be repeated with fiberglass installed in the insulation space.

Using thermal conductivity data from Table 6.3.3, and assuming typical values for the convection coefficients as shown:

$$h_i = 7.5 \text{ W/m}^2\text{K}, \; h_o = 15 \text{ W/m}^2\text{K},$$
$$k_1 = 0.48 \text{ W/m K}, \; a = 0.0127 \text{ m}$$
$$k_2 = 0.11 \text{ W/m K}, \; c = 0.0254 \text{ m}$$
$$k_3 = 0.17 \text{ W/m K}, \; b = 0.1016 \text{ m}$$

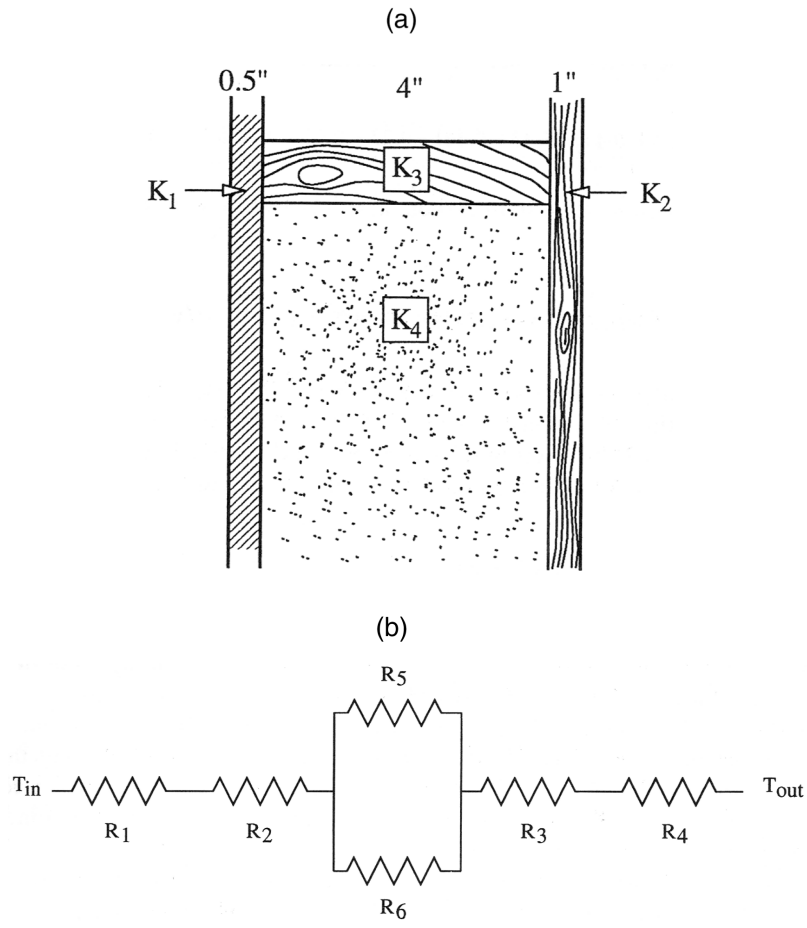


**FIGURE 6.3.2** (a) Schematic representation of a composite wall section. (b) Equivalent thermal resistance for wall section of (a).

for the airspace, $R_6 = 0.44$ Km²/W. Using these values, the total thermal resistance is

$$R_{tot} = 0.01 + 0.06 + \left(5.43 \cdot 0.44\right)\Big/\left(5.43 + 0.44\right) + 0.23 + 0.07 = 0.78 \text{ Km}^2/\text{W} \left(4.43°\text{F ft}^2 \text{ hr}/\text{Btu}\right)$$

If the air space is filled with cellulose insulation, $k_4 = 0.043$ W/m K, $R_4 = 0.1016/(.89*0.042) = 2.72$ K m²/W, and

$$R_{tot} = 0.01+0.06+\left(5.43\cdot 2.72\right)\Big/\left(5.43+2.72\right)+0.23+0.07 = 2.18 \text{ Km}^2/\text{W} \left(12.38°\text{F ft}^2 \text{ hr}/\text{Btu}\right)$$

which is more than double the thermal resistance of the wall with air between the studs.

The wood frame in the previous example acts as a thermal bridge between the wallboard and external facing. To further reduce heat losses a 2.54 cm (1 inch) layer of open-cell rigid foam can be added between the wood frame and exterior facing. This would result in a new total resistance of

$$R_{tot} = 2.18+0.0254/0.033 = 2.95 \text{ Km}^2/\text{W} \left(16.75°\text{F ft}^2 \text{ hr}/\text{Btu}\right)$$

**TABLE 6.3.3** Thermal Properties of Some Common Building Materials

| Material | Density kg/m³ (lb/ft³) | Conductivity W/m K (Btu/hr ft°F) | Specific Heat J/kg K (Btu/lb°F) | Emissivity Ratio |
|---|---|---|---|---|
| | | Wallboard | | |
| Douglas fir plywood | 140 (8.7) | 0.11 (0.06) | 2,720 (0.65) | |
| Gypsum board | 1,440 (90) | 0.48 (0.27) | 840 (0.20) | |
| Particle board | 800 (50) | 0.14 (0.08) | 1,300 (0.31) | |
| | | Masonry | | |
| Red brick | 1,200 (75) | 0.47 (0.27) | 900 (0.21) | 0.93 |
| White brick | 2,000 (125) | 1.10 (0.64) | 900 (0.21) | |
| Concrete | 2,400 (150) | 2.10 (121) | 1,050 (0.25) | |
| Hardwoods | | | 1,630 (0.39) | |
| Oak | 704 (44) | 0.17 (0.10) | | 0.09 (planed) |
| Birch | 704 (44) | 0.17 (0.10) | | |
| Maple | 671 (42) | 0.16 (0.09) | | |
| Ash | 642 (40) | 0.15 (0.09) | | |
| Softwoods | | | 1,630 (0.39) | |
| Douglas fir | 559 (35) | 0.14 (0.08) | | |
| Redwood | 420 (26) | 0.11 (0.06) | | |
| Southern pine | 614 (38) | 0.15 (0.09) | | |
| Cedar | 375 (23) | 0.11 (0.06) | | |
| Steel (mild) | 7,830 (489) | 45.3 (26.1) | 500 (0.12) | 0.12 (cleaned) |
| | | Aluminum | | |
| Alloy 1100 | 2,740 (171) | 221 (127.7) | 896 (0.21) | 0.09 (commercial sheet) |
| Bronze | 8,280 (517) | 100 (57.8) | 400 (0.10) | |
| Rigid Foam Insulation | 32.0 (2.0) | 0.033 (0.02) | | |
| Glass (soda-lime) | 2,470 (154) | 1.0 (0.58) | 750 (0.18) | 0.94 (smooth) |

*Sources: ASHRAE Handbook of Fundamentals*, 2001; Holman, J.P., 1976.

which is a 35% improvement. It is common practice in cold climates and in superinsulated houses to use an external insulation layer. However adding more insulation to the house exterior is not always beneficial. Adding insulation decreases envelope heat transmission losses; however, the percentage reduction diminishes quickly with increased insulation. After a certain point, the energy cost savings do not justify the cost of the added insulation. This point represents the economic optimum insulation thickness, and is determined by minimizing the life cycle and installation costs. This optimum varies by climate zone.

The application of insulation in internally loaded buildings must be analyzed on a case-by-case basis. For example, in a commercial building in a cool climate with outdoor temperatures below room temperatures more than half the time, adding insulation to the envelope would unnecessarily increase cooling costs. The optimum insulation thickness depends on the amount of internal and solar gains, hours of use, and so on. These factors vary between zones of the building.

The overall conductance of the building can be found by analyzing each component separately, then summing over all components. The process is cumbersome because the bookkeeping of all conductivities, thicknesses, resistances, and so on must be accurate. However, calculated values have been shown to agree well with measured data if the quality of installation is high.

Heat transmission through the building envelope is one of the major loss mechanisms in residences. Increasing the thermal resistance of the envelope by adding insulation reduces space heat loss on a long-term basis. This increases the building's thermal efficiency and also improves the occupants' thermal comfort by providing a more constant indoor temperature. Insulating walls and ceilings also keeps the inside surface of the exterior wall above the dewpoint temperature, thereby preventing condensation.

There are many types of insulation materials. Table 6.3.4 lists some of the various types of insulation, the various forms available, and the approximate thermal resistance per unit thickness.

**TABLE 6.3.4** Available Building Envelope Insulation

| Insulation Type | Blanket | Batt | Loose Fill | Rigid Panels | Formed-in-Place | R-Value/thickness $m^2$ K/W/m (°F $ft^2$ hr/Btu/in.) |
|---|---|---|---|---|---|---|
| Cellulose | √ | √ | √ | | | 25.7 (3.7) |
| Rock wool and fiberglass | √ | √ | (pellets) | (semirigid board) | 22.9 (3.3) | |
| Perlite | √ | | | | | 18.7 (2.7) |
| Polystyrene | | | | √ | | 24.3 (3.5) |
| Urea formaldehyde, urethane | | | | | √ | 31.2, 36.7 (4.5, 5.3) |

**TABLE 6.3.5** Appropriate Application of Insulation Forms

| | |
|---|---|
| Batts | Between joists, on unfinished attic floors or basement/crawl space ceilings |
| Blankets | Same as batts, but with longer continuous coverage |
| Loose fill | Poured in unfinished attic floor, useful around obstructions and hard-to-reach corners |
| Rigid boards | Interior or exterior basement walls |
| Foam | Between framing studs in wall, virtually anywhere in building |

*Sources:* From Jones, P. (1979).

While each type of insulation shows a high R-value, there are some disadvantages to some insulation types that must be mentioned. Both cellulose and perlite will pack down and lose their insulation value when they get wet. Rock wool and fiberglass irritate the skin. Polystyrene is moisture resistant, but combustible. Urea formaldehyde and urethane give off noxious gases during fire, even though they're fire resistant. They require specialized equipment to inject the foam into wall cavities, which makes them the most expensive type. If not installed correctly, they'll leave a lingering odor.

Reflective-type insulations are not mentioned in Table 6.3.4. These insulations generally have smooth and shiny surfaces and are installed with this surface facing the source of heat. Reflective insulations are generally installed over exposed studs in walls, attics, and floors, often enclosing an air space underneath. The thermal resistance of reflective insulations so installed depends on the orientation of the insulation and direction of heat flow. Some blanket and batt insulations have reflective backing, which also serves as a vapor barrier.

Currently the highest thermal resistance per unit thickness insulation is the blown polymer foam types as shown in Table 6.3.4. These foam insulations contain chlorofluorocarbons (CFCs), which have been identified with the depletion of the earth's ozone layer. Use of CFCs was discontinued in 1996 in the United States. The performance of blown foam insulations with CFC substitutes is expected to decrease by up to 25%.

Insulation technology is still evolving. A new type of insulation showing great promise is gas-filled panels (GFPs). These insulations are made up of a thin walled baffle structure with low-emittance coatings. The minimal solid construction prevents heat conduction; the baffle structure and coating reduce convection and radiation heat transfer. High-performance GFPs use low-conductivity gases such as argon and krypton in place of air in the baffle spaces. Originally designed for refrigerators and freezers, GFPs can be applied as a building insulation. The R-value per inch for argon filled units, R7.5/in, is twice as high as fiberglass insulation, and more expensive krypton filled units have achieved R12/in. Projected costs in 1992 for 3-inch R22 GFPs is \$0.60/$ft^2$. GFPs are in development (Griffith and Arashteh, 1992).

The various forms of insulation are convenient to use in different parts of the building. Table 6.3.5 shows where each form is typically installed.

Figure 6.3.3 shows a map of the United States roughly divided into climate zones. The recommended R-value has of residential ceiling, wall and floor insulation corresponding to the zones on the map are given in Table 6.3.6.

The thermal mass of a building material is the product of the material's specific heat and density. Judicious use of a building's thermal mass can also be used to increase its energy efficiency. For example, in winter, a building's thermal mass can store heat from solar radiation during the day and be made to

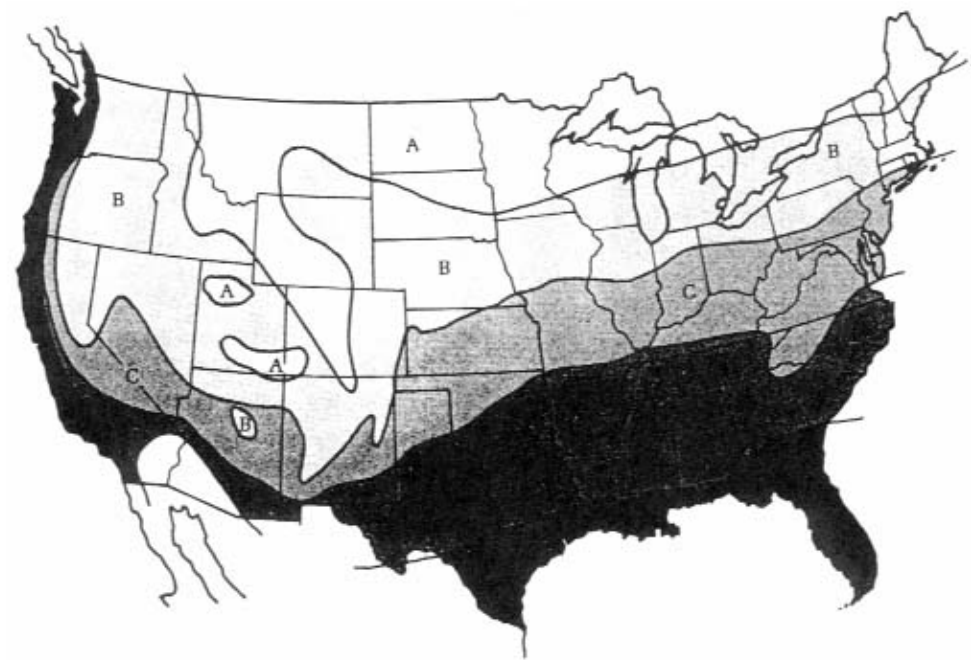


**FIGURE 6.3.3** U.S. zones based on insulation needs. (From Jones, P., *How to Cut Heating and Cooling Costs,* Butterick Publishing, New York, 1979.)

**TABLE 6.3.6** Recommended R-Value for U.S. Zones

| Zone | Ceiling | Wall | Floor |
|---|---|---|---|
| A | R-38 | R-19 | R-22 |
| B | R-33 | R-19 | R-22 |
| C | R-30 | R-19 | R-19 |
| D | R-26 | R-19 | R-13 |
| E | R-26 | R-13 | R-11 |

*Source:* Jones, P., *How to Cut Heating and Cooling Costs*, Butterick Publishing, New York, 1979.

release its heat to the interior at night, thereby reducing the need for space heating. These strategies are reviewed in the chapter on passive solar energy. Peak power shifting can also be accomplished with the use of a building's thermal mass by cooling the mass overnight and circulating indoor air over it to provide cooling during the day. Such strategies make use of lower utility rates during the night. Examples of materials with a high thermal mass are concrete, masonry, and cinder block. Gypsum board also serves as thermal mass in houses, though to a lesser degree. To use a building's thermal mass effectively, it should have a large exposed surface area to the interior.

***Foundations and Basements***

Foundations and basements of buildings raise other issues besides those of the rest of the building envelope. Unlike the ambient air, the ground temperature does not undergo large daily temperature swings. Problems with foundations and basements arise primarily in winter. For houses with uninsulated concrete slab foundations, the floor of the house can become very cold and water vapor diffusing through carpets can condense on the slab surface. This causes damage to the floors and carpets. The same problems can occur on uninsulated basement floors and walls. Also, pipes can freeze in uninsulated basements and the space is generally unusable. Moisture diffusion through concrete and cinder block and exposed soil in basements can be a problem. These problems can be mitigated by the proper placement of insulation and vapor barriers.

Insulating foundations and basements also has energy benefits. In a handbook on foundations and basements from Oak Ridge National Laboratory (ORNL, 1988), it was shown that both interior and exterior insulated masonry basement walls saved approximately the same amount of energy, while basement walls insulated only from the ground level to the frost line saved less energy. In regard to moisture problems, a vapor barrier between the soil and foundation can be used to keep condensing water vapors outside the building shell.

***Albedo and Shading***

In summer, solar radiation striking roofs and walls of houses and other buildings can be absorbed and transmitted to the building interior. For houses, attic temperatures can soar as a result of sunshine being absorbed on the roof and transmitted to the attic as heat. This increases the heat transmittance through the ceiling. One strategy to reduce ceiling heat gains is to increase attic insulation levels appropriately. In warmer climates such as the sun belt of the United States, attic insulation levels are being increased to the same levels as those found in the coldest climates of Table 6.3.6. This strategy can be expensive. Another strategy for preventing solar heat gains from penetrating the building envelope is to reflect the incoming solar radiation from building surfaces or by shading the surfaces from the sun with deciduous trees. These strategies are much more cost-effective.

Reflecting solar gains from building surfaces is a method with some precedence in history. In ancient Greece, whitewashed building walls reflected solar radiation to keep the interiors cool. This practice is being revisited in modern times. Recent studies have shown that increasing the albedo of the building roofs and walls can reduce air conditioner energy consumption. It was shown that a 22% reduction in the air conditioning bill was achieved by increasing the albedo from 0.2 to 0.6 of a residential roof in Sacramento (Akbari, et al. 1992).

Albedo is a measure of a surface's reflectance. Generally the higher the surface's reflectance, the lower its emissivity, but this does not always hold for paints, which can reflect visible light but absorb infrared radiation. The scale for both reflectivity and emissivity is from 0 to 1. Many paint manufacturers have begun listing the reflective properties on their products. Surface roughness and color also have an impact: rougher, darker surfaces generally have a lower albedo. Costs for retrofitting buildings with higher-albedo paints are minimal if the paint is used at the time of regular building maintenance.

Planting deciduous trees (i.e., broad-leaved trees that lose their leaves in the fall) near a house can provide the needed shading of buildings in summer, while allowing needed solar gains into the building in winter. There are many beneficial side effects as well: trees cool their surroundings by evapotranspiration, absorbing heat from the ambient air and evaporating up to 100 gallons of water per day, trees can filter air pollution, provide a windbreak for houses, reduce street noise, prevent soil erosion and provide habitat for wildlife. A study of the cooling effect of trees has shown that annual cooling costs of air conditioning were reduced by 10% by the addition of shade trees (Akbari, et al. 1994).

Air conditioning energy and cost savings can be further increased by combining the benefits of the use of shade trees, shrubs, and other greenery with raised albedo building surfaces and other surfaces in the urban environment as well. Figure 6.3.4 shows the typical albedo of various surfaces found in communities. When combining the shading properties of trees with high albedo surfaces, researchers estimate cooling costs to be reduced by 15 to 35% for the whole community. An excellent information source on the cooling effect of trees and high-albedo surfaces is listed in the bibliography (USEPA, 1992).

***Windows***

Windows, or building fenestration systems, influence building energy use in four ways. Heat is transmitted through windows in the same manner as through walls. Windows absorb and transmit direct and scattered solar radiation into the building, where it is absorbed on surfaces and convected to the inside air. Air leakage around windows increases infiltration loads. Windows also let in visible light, reducing the need for electric lighting.

Heat transmittance through building window systems is generally larger than through the opaque part of the building shell. A typical single pane of window glass has an insulating value of R-1. This value is low in comparison to typical R-15 wall thermal resistances. Adding a second or third pane of glass doubles

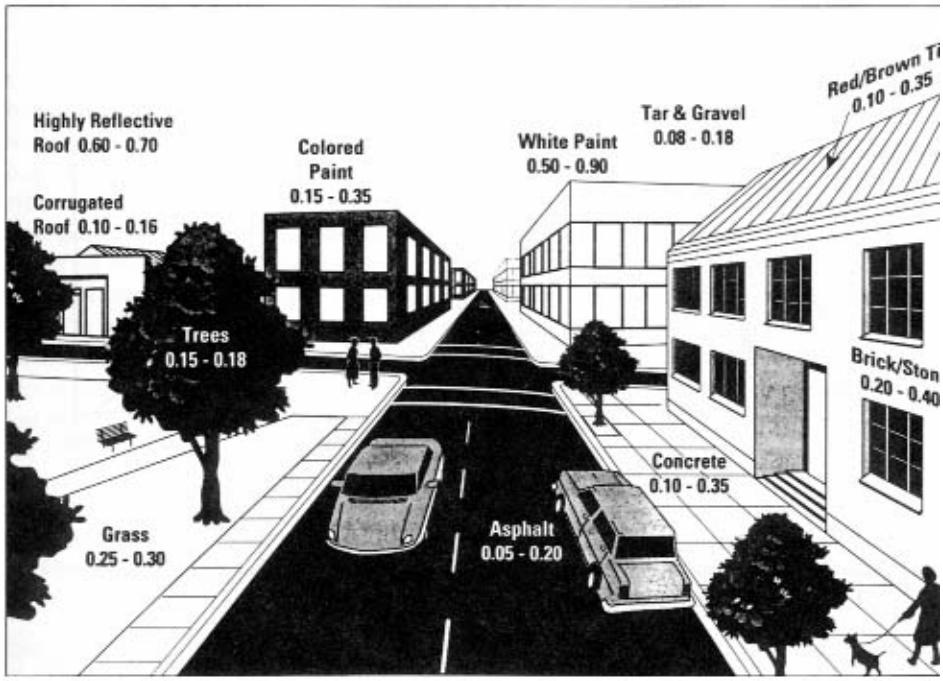


**FIGURE 6.3.4** Surface albedo values in a typical urban environment. (From the United States Environmental Protection Agency, "Coding Our Communities: A Guidebook on Tree Planting and Light-Colored Surfaces," USEPA Report No. 22p-2001, Office of Policy Analysis, Climate Change Division, Washington, D.C., January 1992.)

or triples the R-value respectively. Alternatively, filling the gap space between the window panes with argon gas and adding a transparent low emissivity coating can increase the resistance to R4. A triple layer window with two low-emissivity coatings and argon gas fill can achieve R8. Naturally, windows become more expensive with each step taken to increase the R-value.

The overall heat conductance of windows is made up of three parts: through the center of the glass, through the edge of the glass and through the window frame, as in Eq. (6.3.2)

$$_0 = \left(U_{cg}A_{cg} + U_{eg}A_{eg} + U_f A_f\right) \Big/ A_{pf} \tag{6.3.2}$$

where $U$ is the heat conductance, $A$ is the area of the surface, *cg* refers to the center of the glass, *eg* refers to the edge of the glass (defined by the area 2½ inches from the frame), *f* refers to the frame and $A_{pf}$ refers to the opening area of the wall. This methodology of determining the window $U$ value is preferred because of the different combinations of window and frame technologies possible in fenestration systems.

The National Fenestration Rating Council (NFRC, 1995) publishes a directory listing for over 20,000 commercially available windows.

Windows also allow radiative heat transmission through the glass. The amount of solar radiation passing through the glass during the day depends on the window's optical properties. Generally, clear glass is not spectrally selective and allows most incident solar radiation to pass through, with a small amount of absorptance (depending on thickness) and with about 8% reflected from each layer of glass. However, most architectural-quality glass is opaque to long wave radiation from surfaces at temperatures below 120°C. This tends to produce the greenhouse effect, in which radiation passing through the glass is absorbed on interior room surfaces and then re-radiated with long wave radiation to other interior surfaces, which warm the room air by convection. This re-radiated energy is unable to exit through the glass.

Figure 6.3.5 shows the relative intensity of solar radiation as a function of wavelength. Also shown in the figure is the region the human eye perceives as visible light. To make optimum use of daylighting,

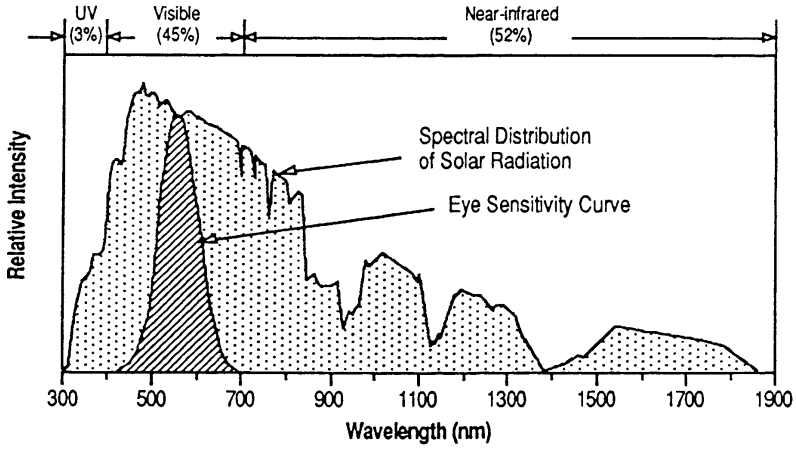


**FIGURE 6.3.5** Solar spectrum. (From Davids, B.J., "Taking the Heat out of Sunlight — New Advances in Glazing Technology for Commercial Buildings," Proc. ACEEE Summer Study on Energy Efficiency in Buildings, August 26–September 1, Asilomar Conference Center, Pacific Grove, CA, 1990.)

an ideal spectrally selective coating on the surface of a window would block out all solar radiation with wavelengths below about 450 nm and above about 690 nm. Such a coating would pass virtually all visible light through the window while blocking out approximately 50% of all solar radiation. Multilayer metal and dielectric coatings on glass approach this behavior, allowing more than 80% of visible light through and reflecting most of the rest of the sun's spectrum. Some types of green, blue-green, and blue absorbing glasses also provide spectral selectivity, although they are generally not as effective as reflective coatings.

Some of the nonreflected radiation is absorbed in the glass; the rest is transmitted through it. Part of the absorbed energy is conducted to the inside surface. Thus, the solar heat gain from a window is the sum of the transmitted radiation and the fraction of absorbed radiation that is conducted to the inside surface:

$$q_i = E_t\left(\tau_s + N_i\alpha_s\right) = E_t \times \text{SHGC} \tag{6.3.3}$$

where $E_t$ is the total solar radiation incident on the window, $\tau_s$ is the glass transmittance, $N_i$ is the fraction conducted inward and $\alpha_s$ is the glass absorbance. The fraction of the total radiation that finds its way to the interior is called the Solar Heat Gain Coefficient (SHGC). The SHGC and the window's overall *U*-value should be used in any description of a window's energy performance.

The total rate of heat transfer through a window is the sum of the normal heat transmittance due to the indoor-outdoor temperature difference, the solar gain, and an infiltration term as shown in Eq. (6.3.4)

$$q_{tot_i} = \text{SHGC}_i E_t + U_0 \Delta T + KQ_{\text{inf}} \Delta T \tag{6.3.4}$$

Cracks around window frames or loose sliding window sashes are sites for air infiltration in buildings. This topic is covered in the next section. In building design or retrofit, appropriate window selection depends on the climate and nature of the building. For heating-dominated buildings, it is desirable to have a high transmittance over the entire solar spectrum, but a high reflectivity (low emissivity) over the long wavelength infrared portion of the spectrum. This arrangement allows most solar radiation into the building, but traps low-temperature radiant heat inside the building. Many commercially available windows with low-emittance (low-e) coatings approach this performance. The opposite performance is desirable for cooling dominated buildings. The ideal in this case is to have a high reflectance (low emittance) over all solar wavelengths outside the visible portion of the spectrum. Depending on the spectral selectivity of the window, this would eliminate from 50 to 70% of the solar radiation from entering the building,

without loss in light transmission. Windows approximating this ideal behavior are available. Many absorbing glass and reflective coatings also block some portion of the visible spectrum which may be desirable to control glare from direct sun. These glazings may also change the color rendering properties of the transmitted light. This must also be considered in the selection of window systems.

Windows provide daylight, which aids visual comfort and reduces the need for artificial lighting, thus saving energy. An accurate evaluation of daylighting is beyond the purposes of this chapter. As a rule of thumb, properly designed windows can provide daylight adequate for typical indoor tasks for a depth $2^1/_2$ times the height of the window, based on normal sill height. In typical office buildings, if the effective aperture (visible transmittance of glass times fractional area of wall that is glazed) of a building is in the range of 0.2 to 0.35, daylighting can provide approximately 50% of annual electric lighting needs in perimeter zones adjacent to windows. In a skylighted building, an effective aperture of 0.04 can provide 50 to 70% of lighting needs. For more on the subject, the reader is referred to "Recommended Practices of Daylighting" (IES, 1979).

## Infiltration and Ventilation

Ventilation is the building service most associated with controlling the indoor air quality to provide a healthy and comfortable indoor environment. In large buildings ventilation is normally supplied through mechanical systems, but in smaller buildings such as single-family homes it is principally supplied by leakage through the building envelope (i.e., *infiltration*). Most U.S. buildings with mechanical ventilation systems also use the system for thermal energy distribution. We restrict our discussion here to ventilation of *outdoor* air.

Ventilation is the process by which clean air is provided to a space. It is needed to meet the metabolic requirements of occupants and to dilute and remove pollutants emitted within a space. Usually ventilation air must be conditioned by heating or cooling it to maintain thermal comfort and then it becomes an energy liability. Ventilation energy requirements can exceed 50% of the space conditioning load; thus excessive or uncontrolled ventilation can be a major contributor to energy costs and global pollution. Thus, in terms of cost, energy, and pollution, efficient ventilation is vital, but inadequate ventilation can cause comfort or health problems for the occupants.

### *Mechanically Dominated Ventilation*

Most medium and large buildings are ventilated by mechanical systems designed to bring in outside air, filter it, supply it to the occupants, and then exhaust an approximately equal amount of stale air.

Ideally these systems should be based on criteria that can be established at the design stage. After the systems are designed and installed, attempts to mitigate problems may lead to considerable expense and energy waste, and may not be entirely successful. The key factors that must be included in the design of ventilation systems are given in Table 6.3.7, along with suggested sources for more information.

These factors differ for various building types and occupancy patterns. For example, in office buildings pollutants tend to come from occupancy, office equipment, and automobile fumes. Occupant pollutants typically include metabolic carbon dioxide emission, odors, and sometimes smoking. When occupants are the prime source, carbon dioxide acts as a surrogate and can be used to cost-effectively modulate the ventilation, forming what is known as a *demand controlled ventilation* system.

**TABLE 6.3.7** Design Considerations for Mechanical Ventilation

| | |
|---|---|
| Code requirement, regulations or standards | ASHRAE Standard 55 |
| Ventilation strategy and system sizing | ASHRAE Standard 62-1989 |
| Climate and weather variations | ASHRAE *Handbook of Fundamentals*, (2001) |
| Air distribution, diffuser location, and local ventilation | ASHRAE *Handbook of Fundamentals*, (2001)<br>ASHRAE *Handbook of Systems and Equipment*, (2000) |
| Location of outdoor air inlets and outlets | ASHRAE *Handbook of Fundamentals*, (2001) |
| Ease of operations and maintenance | Equipment Manufacturer, ASHRAE *Handbook of Applications*, (1999) |
| Impact of system on occupants (e.g., acoustics and vibration) | ASHRAE *Handbook of Fundamentals*, (2001) |

Schools are dominated by high occupant loads, transient occupancy, and high levels of metabolic activity. Design ventilation in hospitals must aim at providing fresh air to patient areas, combined with clean room design for operating theaters. Ventilation in industrial buildings poses may special problems, which frequently have to be assessed on an individual basis. Contaminant sources are varied, but often well-defined, and limiting values are often determined by occupational standards. Poorly designed, operated or maintained ventilation systems, rather than the ventilation rate itself, may cause sick building syndrome (SBS). The causes of SBS were summarized earlier.

***Infiltration***

Infiltration is the process of air flowing in (or out) of leaks in the building envelope, thereby providing ventilation in an uncontrolled manner. All buildings are subject to infiltration, but it is more important in smaller buildings. In larger buildings there is less surface area to leak for a given amount of building volume, so the same leakage matters less. More important, the pressures in larger buildings are usually dominated by the mechanical ventilation system and the leaks in the building envelope have only a secondary impact on the ventilation rate. However, infiltration in larger buildings may affect thermal comfort, control, and system balance.

In low-rise residential buildings (most typically, single-family houses) infiltration is the dominant force. In these buildings mechanical systems contribute little (intentionally) to the ventilation rate.

Infiltration is made up of two parts: weather-induced pressures and envelope leakage. Since little of practical import can be done about the weather, it is the envelope leakage, or *air tightness*, that is the variable factor in understanding infiltration. Virtually all knowledge about the air tightness of buildings comes through making *fan pressurization* measurements, done most typically with a *blower door.*

*Blower door* is the popular name for a device that is capable of pressurizing or depressurizing a building and measuring the resultant air flow and pressure. The name comes from the common utilization of the technology, where there is a fan (i.e., blower) mounted in a door; the generic term is "fan pressurization." Blower door technology was first used around 1977 to test the tightness of building envelopes (Blomsterberg, 1977), but the diagnostic potential of the technology soon became apparent. Blower doors helped uncover hidden bypasses that accounted for a much greater percentage of building leakage than did the presumed culprits of window, door, and electrical outlet leakage. The use of blower doors as part of retrofitting and weatherization became known as *House Doctoring*. This led to the creation of instrumented audits and computerized optimizations (Blasnik and Fitzgerald, 1992). A brief description of a typical blower door test follows in the measurements section.

While it is understood that blower doors can be used to measure air tightness, the use of blower door data alone cannot be used to estimate real-time air flows under natural conditions or to estimate the behavior of complex ventilation systems. However, a rule of thumb relating blower door data to seasonal air change data exists (Sherman, 1987): namely, the seasonal air exchange can be estimated from the flow required to pressurize the building to 50 Pascal divided by 20. Ventilation and infiltration air flows are generally measured with a tracer gas, as described in the measurements section.

A more accurate description of infiltration rates can be found by separating the leakage characteristics of the building from the driving forces, which are wind- and temperature-induced pressures on the building shell. Modeling the leakage data from blower door tests as orifice flow, Sherman and Grimsrud (1980) developed the LBL infiltration model, Eq. (6.3.5):

$$Q = L\left(f_s \Delta T + f_w V_w^2\right)^{0.5} \tag{6.3.5}$$

Here $Q$ is the volumetric air flow rate, L is the effective leakage area of the house at 4 Pa, $\Delta T$ is the indoor-outdoor temperature difference, $V_w$ is the time-averaged wind speed, and $f_s$ and $f_w$ are the stack and wind coefficients, respectively, as determined from a fit of the data. The model was validated by Sherman and Modera (1984) and incorporated into the *ASHRAE Handbook of Fundamentals* (2001). Much of the subsequent work on quantifying infiltration is based on that model, including ASHRAE Standard 119 (1988) and ASHRAE Standard 136 (1993).

Blower doors are used to find and fix the leaks. A common method of locating leak sites is to hold a smoke source near the leak and to watch where the smoke exits the house. Depending on the leak site, different methods are used to stop the leakage.

Often, the values generated by blower door measurements are used to estimate infiltration for both indoor air quality and energy consumption analyses. These estimates in turn are used for comparison to standards or to provide program or policy decisions. Each specific purpose has a different set of associated blower door issues.

Compliance with standards, for example, requires that the measurement protocols be clear and easily reproducible, even if this reduces accuracy. Public policy analyses are more concerned with getting accurate aggregate answers than reproducible individual results. Measurements that might result in costly actions are usually analyzed conservatively, but "conservatively" for IAQ is diametrically opposed to "conservatively" for energy conservation.

Because infiltration depends on the weather, buildings that have much of it can have quite variable ventilation rates. Determining when there is insufficient infiltration to provide adequate indoor air quality or energy-wasteful excess infiltration is not a simple matter. The trade-off in determining optimal levels depends on various economic and climactic factors.

Individual variations notwithstanding, Sherman and Matson (1993) have shown that the stock of housing in the United States is significantly overventilated from infiltration and that there are 2 exajoules (1.9 quads) of potential annual savings that could be captured. Much of this savings could be captured by simple tightening, but a significant portion requires installation of a ventilation system or strategy to assure adequate ventilation levels.

### *Natural Ventilation*

Natural ventilation is a strategy suitable for use in mild climates or during mild parts of the year. As commonly interpreted, natural ventilation is the use of operable parts of the building envelope (e.g., windows, etc.) to allow natural airflow at the discretion of the occupants.

Natural ventilation shares many of the same properties as infiltration: it depends on weather for driving forces; it is a function of the leakage area of the buildings; and so on. The distinguishing feature of natural ventilation, however, is that it is under the control of the building occupants.

From the point of view of the HVAC designer, natural ventilation is quite bothersome, because a conservative ventilation designer cannot count on it, but one must consider its potential effects on the building load. From the perspective of the occupants, however, natural ventilation gives them more control of their environment and usually makes it more acceptable. Studies have shown that those in naturally ventilated buildings tend to suffer less sick building syndrome and less respiratory disease (e.g., colds) than buildings that are fully mechanically ventilated.

The designs of new commercial buildings have been curtailing the availability of natural ventilation as an option by removing operable windows. Natural ventilation still dominates in the residential sector.

### *Ventilative Cooling*

In dwellings, natural ventilation serves more than just a means to provide clean air; it serves to cool the building and its occupants and reduce the requirement for mechanical cooling. Fans are used to assist ventilative cooling by increasing the air change rates. These *whole house fans* are of much larger capacity than is needed for ventilation. A standard such fan may provide as much as 10 air changes per hour, compared with the ventilation requirement of no more than half an air change per hour.

Ventilative cooling removes internally generated heat as long as the outdoor temperature is less than the indoor temperature. When thermally massive elements are included in the structure, night ventilation can be used to store "coolth" and reduce the cooling requirements the following day.

The air motion caused by ventilative cooling provides additional cooling to the occupants of the building by removing more heat and lowering the apparent temperatures. Increased air motion raises the upper limit of acceptable air temperature from a thermal comfort perspective and therefore also reduces cooling demand.

In commercial buildings ventilative cooling is accomplished principally by the use of an *economizer*. Economizers are nothing more than dampers that allow outdoor air to be used instead of recycled (i.e., return) air in the building's thermal distribution system. This is usually done when there is a cooling load and the outdoor air is cooler than the indoor air.

A simple economizer works in lieu of the cooling system of the building. Because of the large internal loads of some commercial buildings it can be necessary to supply some mechanical cooling and also use outdoor air. Such a system is called an *integrated economizer* because it can do both. Not all systems are capable of running in this way. In buildings using cooling towers, *waterside economizers* can effectively use evaporative cooling to substitute for chiller operation.

***Heat Recovery***

Other than periods when ventilative cooling is useful, considerable energy is lost from a building through the departing air stream. When air change is dominated by infiltration, little can be done to recapture this energy, but if the departing air stream is centrally collected, a variety of methods for recovering or recycling the waste heat become possible (AIVC TN 45, 1994).

Ventilation heat recovery is the process by which sensible and latent heat is recovered from the air stream. Methods have been developed for air-to-air systems, in which the energy in the departing air stream is transferred directly to the entering air stream. Heat recovery can also be accomplished with heat-pump systems, in which heat from the exhaust air is pumped to another system such as the domestic hot water.

While the heat recovery process can be efficient at collecting the heat, benefits must always be weighed against the energy needed to drive the recovery, the capital costs of the equipment, and the maintenance. Induced losses such as infiltration or duct leakage must be understood. Without careful design and construction of the building envelope the system total performance can be considerably impaired and in some cases could increase the total energy costs.

The efficiency of all systems can be defined in terms of the proportion of outgoing ventilation energy that is recovered. Quoted efficiencies can be quite high (e.g., 65–75%), and the attractiveness therefore quite strong. For various reasons, however, field studies do not always come up to expectations. Basically, if poor attention is given to planning and installation, then the level of heat recovery can be quite disappointing.

***Measurement Methods***

A brief description of a blower door test follows. The reader is referred to ASTM Standard E779 for a complete description. Shown in Figure 6.3.6 is a sketch of a fan mounted in a doorway of a single-family house. A means of measuring the pressure difference between the house and outside is provided in this case by a digital manometer. Other pressure measuring instruments are acceptable as long as they are accurate over the measured pressure range: 0 to 100 Pascal. Volumetric air flow through the fan must also be determined. The air flow through most blower door fans is calibrated against fan speed in revolutions per minute or the pressure drop across the fan (range of approximately 0 to 500 Pa). The latter method is shown in Figure 6.3.6. The test is performed after ensuring that all windows and fireplace dampers in the house are closed. Some protocols also require exhaust vents in the kitchen and bathrooms to be sealed. The general procedure is to depressurize the house in steps of about 12 Pascal to about 50 Pascal, recording the house pressure and fan air flow at each step. The air flow direction through the fan is then reversed and the procedure is repeated for house pressurization measurements.

The air flow is plotted against the house pressure and a power law relationship of the type $Q = c(\Delta P)^n$ is fitted to the data ($c$ and $n$ are determined from the chosen curve fitting procedure). Using this relationship and modeling the house leakage as orifice flow, the effective leakage area of the house is determined by Eq. (6.3.6)

$$\text{ELA} = CQ_r\left(\rho/\left(2\Delta P\right)\right)^{0.5} \tag{6.3.6}$$

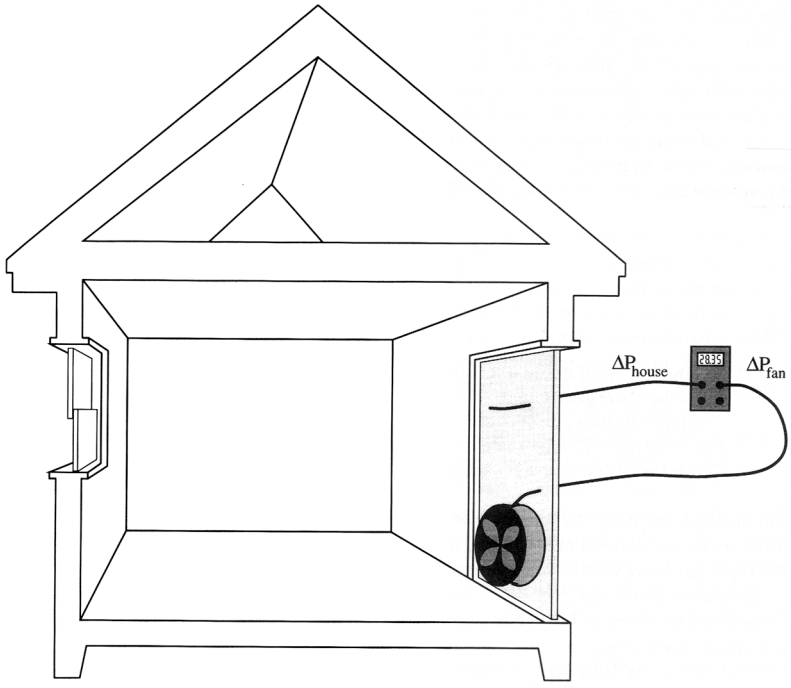


**FIGURE 6.3.6** Sketch of a typical blower door test setup.

where ELA is the effective leakage area at the reference pressure $\Delta P_r$, usually 4 Pa, $Q_r$ is the reference pressure air flow, ρ is the air density, and $C$ is a conversion constant. At 4 Pascal, the ELA is a good estimate of the equivalent area of holes in the envelope that provide the same leakage. Note that the ELA at 4 Pa is determined by extrapolation of measured data.

Other indications of a house's air tightness are often used. Two of these are CFM50 and ACH50. CFM50 is the flow in cubic feet per minute at a house pressure of 50 Pa. ACH 50 is the air change rate at 50 Pa, which is obtained by dividing CFM50 by the house volume in cubic feet. Unlike ELA measurements, which require an entire range of air flow and house pressure data, both CFM50 and ACH50 can be determined from one measurement. This simplifies testing. On the other hand, normalizing ELAs with house floor area enables comparisons between houses—to determine if one house is unusually leaky, for example. These air tightness indications are used for comparisons to standards, to provide background for program or policy decisions, or to estimate the energy load caused by the infiltration.

Tracer gas techniques have become widely used to measure the ventilation rates in buildings. The basic principle involved is that of conservation of mass (of tracer gas) as expressed in the continuity equation. By monitoring the injection and concentration of the tracer, one can infer the exchange of air. Although there is only one continuity equation, there are many different experimental injection strategies and analytical approaches. These different techniques may result in different estimates of infiltration due to uncertainties and biases of the procedures.

An ideal tracer gas is one which is inert, safe, mixes well, does not adhere to surfaces and its concentration in air is easily measurable. A mass balance of tracer gas within the building, assuming the outdoor concentration is zero, takes the form of Eq. (6.3.7):

$$\frac{dc(t)}{dt} = F(t) - Q(t)c(t) \tag{6.3.7}$$

where

$V$ is the volume of the interior space
$c(t)$ is the tracer gas concentration at time $t$
$dc(t)/dt$ is the time rate of change of tracer concentration
$F(t)$ is the tracer injection rate at time $t$
$Q(t)$ is the airflow rate of the building at time $t$

The development of Eq. (6.3.7) made use of a number of assumptions: the airflow out of the building accounts for the removal of tracer gas, not chemical reactions or absorption onto surfaces, and the tracer gas concentration is uniform throughout the interior space.

There are a number of methods to use in determining infiltration and ventilation rates with a tracer gas. The choice of method in a given situation will depend on the practical details of the experiment as well as the reason for measuring the air change in the first place. A standardization method (ASTM 1990) is the decay method, which requires the least time and usually the least preparation.

In the decay method, a small amount of tracer gas is mixed with the interior air. The injection is then stopped and the concentration of tracer gas is monitored. The air change rate is then determined from the solution of Eq. (6.3.7):

$$c(t) = c_0 e^{-\mathrm{ACH}_t} \tag{6.3.8}$$

where $c_0$ is the concentration at time = 0 and ACH = $Q/V$ is the air change rate.

The advantages of the decay method are numerous: the injection rate $F$ need not be measured, the concentration of tracer gas can be measured on site or collected in sample containers and analyzed elsewhere, and the test can be performed with a minimum of equipment and time. Disadvantages include errors introduced by the nonuniform mixing of tracer gas with air, large uncertainties in the air change rate unless the precision of the measuring equipment is high, and biased estimates of the average air change rate.

Other experimental techniques, such as the constant concentration and constant injection techniques are used. The constant concentration technique can be both accurate and precise, but it requires the most equipment as well as sophisticated control systems and real-time data acquisition. The constant injecting technique (without charge-up) can be considered a somewhat simpler version of the constant concentration technique, in that no active control of the injection rate is needed.

As more detailed information is required for both energy and indoor air quality purposes, researchers are turning to complex, multizone tracer strategies. Both single-gas and multigas techniques are being utilized, but only multigas techniques are capable of uniquely determining the entire matrix of air flows.

Tracer gases are used for a wide range of diagnostic techniques including leak detection and atmospheric tracing. In cases (e.g., mechanically ventilated rooms) in which ventilation rates are known, tracer gases can be used to measure the ventilation efficiency within the zone. Age of air concepts are often used to describe the spatial variation of ventilation. Sandberg (1983) summarizes the definitions and some of the tracer techniques for determining the efficiency (e.g., by seeding inlet streams or monitoring exhaust streams). Further discussion of intrazonal air flows and ventilation efficiency is beyond the scope of this chapter.

## 6.3.2 Review of Thermal Distribution Systems

Thermal distribution systems are the ductwork, piping or other means used to transport heat or cooling effect from the heating or cooling equipment (furnaces, boilers, compressors, etc.) to the building space where it is needed. This section focuses on the distribution system connected to the heating/cooling equipment, rather than on the equipment itself. For a review of air distribution equipment, refer to

Chapter 4.3. Energy efficiency research in buildings has been primarily focused on the building shell, lighting, appliances, or the space-conditioning equipment. Although the need for improved efficiency in thermal distribution systems has been often cited (Modera, 1989, Cummings and Tooley, 1989), this need has received more attention only in recent years.

Thermal distribution systems are primarily characterized by two transport mediums, air and water. Andrews and Modera (1991) classify the type of distribution system used in residential and small commercial buildings and estimate the potential energy savings possible. In residential applications they found that 85% of the primary energy used for space conditioning was in forced-air systems, with the remainder in hydronic systems. In small commercial buildings the authors reported that 69% of all small commercial buildings in 1986 were heated or cooled with forced air systems, and that the fraction was continually increasing. The focus of this section will be on forced air systems, because this type of system is the largest fraction in buildings and because they have the most potential for efficiency improvements.

There are three primary modes of energy loss associated with air distribution. One is direct air leakage from the ducts to unconditioned spaces or to outside via holes or cracks in the ductwork. This mechanism is mainly a function of the quality and durability of the duct installation. Another is heat conduction through the duct walls resulting from inadequate insulation. The third mode is increased infiltration resulting from increased pressures across building shell leakage sites, pressures which are generated by the operating forced air system. Infiltration is also increased when the system is not operating because the leakage sites in the duct system add to the building's overall leakage area.

The magnitude of the energy loss depends on many factors: level and location of duct leakage sites, insulation level, location of ducts, space conditioning system sizing, and climate region are a few examples. Typically, the inefficiencies of ducts are at their worst at the time of day when they are needed most. This is due to the extreme temperature differences between the ducts and their surroundings, which increase the conduction losses through the duct walls and worsen return-side leakage losses. This is true in both residential and commercial buildings where the ducts can be located in attics or on rooftops, for example. Because the demand for space conditioning is highest during these peak hours, inefficient ducts exacerbate the problem electric utilities have in meeting the power demand.

## Measurement Methods

Measurement techniques available to use in the analysis of distribution efficiencies and to characterize the existing stock of forced air systems are outlined here. Duct leakage area (DLA) is an important parameter used to characterize both direct duct leakage losses and additional envelope leakage area. The most common measurement methods are listed in Table 6.3.8.

The blower door subtraction method utilizes two blower door tests, a normal blower door test as described in a previous section, and a second test with the duct system sealed from the house by taping over the duct registers. The DLA is then determined from the difference between the ELAs measured in each test. This method yields duct leakage to outside values only, as the total leakage area of ducts may also include leakage sites to inside the conditioned space. The accuracy of this method is low because the DLA is determined by the subtraction of two large numbers.

In the blower door plus flow hood measurement, the method is similar to a normal blower door test except that a flow capture hood is placed over one unsealed register, usually a return register, and the airflow into the ducts is measured during the test. Simultaneous measurements of house and duct pressure are made, and with the measured flow through the flow capture hood an orifice model is used to determine the DLA. This method has been shown to be more accurate than the subtraction technique.

**TABLE 6.3.8** Duct Leakage Area Measurement Methods

| No. | Primary Equipment | Result | Accuracy | Reference |
|---|---|---|---|---|
| 1 | Blower door | DLA (to outside) | low | (Proctor et al., 1993) |
| 2 | Blower door + flow hood | DLA (to outside) | medium | (Proctor et al., 1993) |
| 3 | Duct pressurizing fan | DLA (total) | high | (Energy Conservatory, 1995) |
| 4 | Duct fan + blower door | DLA (to outside) | high | (Energy Conservatory, 1995) |

The third measurement of DLA is the most versatile and is gaining acceptance as the preferred method in field measurements: the fan pressurization technique. The procedure is similar to the determination of the house ELA. In this method, all registers are taped except one, where a fan is connected. The fan has been previously calibrated for volumetric flow rate. With this technique, airflow and duct pressurization measurements are made and the total duct leakage of the supply side, return side, or entire system is determined. Measurements of duct leakage to the outside are made with the help of a blower door. Besides being the most accurate of the three methods, this method has advantages when sealing ducts in retrofit applications.

Actual duct air leakage rates during system operation can be measured by individually measuring the fan air flow rate and air flow through the supply and return registers. The volumetric leakage rate of supply air is then the difference between the fan air flow rate and the sum of the air flow out the supply registers. The method is similar on the return side. Fan air flow rates can be measured with a tracer gas technique (ASTM Standard E741). Air flow rates out of registers can be measured with a flow capture hood or a modified version of a flow capture hood as done in June and Modera (1994).

An indication of duct conduction losses can be obtained by measuring temperatures in the supply and return plenums and in each supply register. The percentage of energy lost due to duct conduction is the temperature difference between the supply plenum and register temperature divided by the difference between the supply and return plenum temperatures. Measurement of the distribution system's impact on the building infiltration rate can be measured by the tracer gas or blower door techniques outlined previously.

Alternatively, a duct system's efficiency can be determined by an electric coheating method. This method compares the energy used by the heating equipment (furnace, heat-pump, etc.) and duct system to maintain a set indoor temperature with the energy consumed by electric heaters placed inside the conditioned space to maintain the same indoor temperature. This method requires extensive data acquisition and measurement equipment, but has revealed much insight on the factors that influence a duct system's energy impacts. An example of this method is found in Palmiter and Francisco (1994).

As research into the energy efficiency of air distribution systems has only recently begun, development of standard methods of testing to determine distribution system efficiencies is not yet complete. ASHRAE is currently sponsoring the development of such tests. There are three test pathways currently in development. The first is the design pathway, and it will rely on computer modeling of the building, equipment, and duct system. The other two pathways involve field measurements. The research pathway is intended to obtain the most complete description of the *in situ* performance of a duct system. The diagnostic pathway is intended to rely on field measurements which may be obtained quickly and at minimal cost. Each field measurement pathway will contain descriptions of the recommended procedures to analyze an air distribution system's performance. First versions of the ASHRAE test methods were available in 1997.

## Residential Ducts

Forced air heating and cooling systems are used in approximately 50% of existing single family housing in the United States (Andrews and Modera, 1991). In the Northeast and Midwest, 52% of all homes have forced air systems, with 44% of those homes having ducts in unconditioned spaces such as attics or crawl spaces, and 50% having them in partly conditioned spaces, such as basements. In the southern and western United States, 46% of all homes have forced air systems, with 82% of their ducts located in unconditioned spaces.

Field work on existing housing has revealed the potential for efficiency improvements. Modera et al. (1992) measured DLAs (at 4 Pa) of 0.90 $cm^2/m^2$ (normalized for house floor area) in 19 California houses built before 1980, and 0.92 $cm^2/m^2$ in post-1980 construction (12 houses). Jump and Modera (1994) measured 1.57 $cm^2/m^2$ leakage area (at 25 Pa) in 13 houses in Sacramento, California. In terms of conduction losses, Modera et al. reported that 23% of the energy delivered to the air at the coil was lost due to conduction before it arrived at the registers. In the Sacramento houses, Jump and Modera reported a 13% loss. In terms of distribution system induced air infiltration, Gammage (1986) reported an average

increase of 80% in the infiltration rate of 31 Tennessee houses when the air handler fan was operating. In five Florida houses, Cummings and Tooley (1989) determined that the infiltration rate tripled when the air handler fan was on and internal doors in the house were open, and that rate further tripled when internal doors were closed. The former effect was attributed to duct system leakage, while the latter effect was attributed to pressure imbalances in the house due to inadequate return-air pathways.

Palmiter and Francisco (1994) measured the system and delivery efficiencies in 24 all-electric homes in the Pacific Northwest. They found that delivery efficiencies averaged 56% for 22 of those homes, which had ducts in unconditioned spaces. The corresponding system efficiency was 71%. In the 2 homes with 50% or more of the ducts in conditioned spaces, they found that delivery efficiencies were 67%, with system efficiencies of 98% on average.

The majority of new single-family housing construction is housing with solid concrete foundations. This practice usually results in duct placement in the attic. This is the most unfavorable local for the distribution system because of the extreme temperature differences that exist between ducts and attics, particularly in the summer. In designing homes for energy efficiency, care must be taken to either seal and insulate the ducts well, or locate them in a less harsh environment, preferably inside the conditioned space. Efficiency-conscious home builders use techniques such as fan pressurization to verify minimum leakage levels in the duct system. Stum (1993) has other advice for duct installation in new construction.

Efficiency improvements in existing housing is mainly accomplished by duct sealing and insulation retrofits. Monitoring of duct system retrofits has shown a reduction of space conditioning energy use of up to 20% for the houses studied (Jump and Modera, 1994; Palmiter and Francisco, 1994). The average cost per house in the Jump and Modera study was $600. This cost is approximately $1\frac{1}{2}$ as much as adding R19 attic insulation.

In new construction, the savings potential is much larger. Actual energy savings are much larger if care is taken at the time of installation, ensuring airtight duct systems and adequate insulation levels. Other efficiency improvements which can be incorporated into new construction are the inclusion of zoned air distribution systems and installing the ducts inside the conditioned space. In the latter case, energy losses from the duct system will not be lost to outside the home.

### Commercial Buildings

Commercial building air distribution systems have received far less attention as compared to residential systems. Small commercial buildings have received some attention because of their similarities with residential systems. Andrews and Modera (1991) determined that 69% of small commercial buildings used forced air systems for heating and cooling.

Large commercial building air distribution systems are characterized by extensive networks of ducts, mixing boxes, dampers, in-line fans, and controls. They operate at higher pressures and serve many different building zones and often the building's ventilation system is included. Unlike residential systems, the duct location in large commercial buildings is not typically in a severe environment. Two sources of energy losses in these systems come from warming the conditioned air with the in-line fans and leaky air dampers. Efficiency problems with large commercial duct systems has not received as much attention as residential and small commercial systems.

### Advanced Systems

A new application of an existing technology is being developed for energy-efficient cooling, thermal comfort, and high indoor air quality in commercial buildings (Feustel, 1993). These systems provide cooling effect through radiative exchange between humans and water-cooled ceilings or ceiling panels. There are several advantages to radiant hydronic systems. The first is that water is a far better thermal medium than air. Water systems in general do not leak, and when they do, the problem is quickly noted and repaired. Second, the preferred thermal comfort arrangement of a cool head and warm feet is maintained in these systems. Overhead plenum space need no longer be provided. High indoor air quality is maintained by the continual supply of fresh air, eliminating the need to mix fresh and recirculated air as is the case in all air systems. Such systems are more common in Europe, but small studies have shown their high application potential in the United States. (Feustel, 1993; Feustel and Stetiu, 1995).

### 6.3.3 Tools

A variety of tools and reference materials are available to help estimate the issues discussed in this chapter.

#### Whole-Building Simulation Tools

Chapters 6.1 and 6.2 describe building thermal analysis tools in detail. Computer-based building energy simulation tools allow architects, engineers, and researchers much-needed flexibility in analyzing a buildings energy performance while preserving accuracy. These tools serve a variety of functions, from relatively uncomplicated algorithms that are used to predict a building's peak loads and system requirements to comprehensive room-by-room analysis packages that yield information about the load impacts of specific building components, the performance of heating or cooling equipment, and life cycle costs.

Both BLAST and DOE-2, as well as many other energy simulation tools are now being used as the energy analysis engines behind user-friendly computer interfaces. This is an attempt to make these valuable tools more accepted among architects and design engineers, as well as researchers. A more recent innovation involves linking these engines with CAD software.

#### Air Flow and Air Quality Simulation Tools

Air flow models are used to simulate the rates of incoming and outgoing air flows for a building with known leakage under given weather and shielding conditions. Air flow models can be divided into two main categories: single-zone models and multizone models. Single-zone models assume that the structure can be described by a single, well-mixed zone. The major application for this model type is the single-story, single-family house with no internal partitions. A large number of buildings, however, have structures that would characterize them more accurately as multizone structures. Therefore, more detailed models have been developed, which also take internal partitions into account.

Multizone airflow network models deal with the complexity of flows in a building by recognizing the effects of internal flow restrictions. They require extensive information about flow characteristics and pressure distribution.

As for their single-zone counterparts, these models are based on the mass-balance equation. Unlike the single-zone approach, where there is only one internal pressure to be determined, the multizone model must determine one pressure for each of the zones. This adds considerably to the complexity of the numerical solving algorithm, but by the same token, the multizone approach offers great potential in analyzing infiltration and ventilation airflow distribution.

The advantage of multizone models, besides being able to simulate air flows for larger buildings, is their ability to calculate mass flow interactions between the different zones. Understanding the air mass flow in buildings is important for several reasons:

- Exchange of outside air with inside air necessary for building ventilation
- Energy consumed to heat or cool the incoming air to inside comfort temperature
- Air needed for combustion
- Airborne particles and germs transported by air flow in buildings
- Smoke distribution in case of fire

Literature reviews undertaken in 1985 and 1992 (Fuestel and Kendon, 1985; Fuestel and Dieris, 1992) showed a large number of different multizone airflow models. One of the first models found was already published in 1970 (Jackman, 1970). Newer airflow models (e.g., CONTAM 93 [Walton, 1993] and COMIS [Feustel and Raynor-Hoosen, 1990]) include pollutant transport models, are more user-friendly and run on personal computers. Furthermore, faster and more robust solvers guarantee shorter calculation times and allow integration of all kinds of flow resistance (e.g., large vertical openings with two-way flows) besides the basic crack flow resistance. The limits of zones and flow paths per zone a model can handle depends on the computer storage.

One of the most bothersome exercises for the modeler is to provide the characteristic parameters for the flow resistance and the outside pressure field for different wind directions. In COMIS, the wind

pressure distribution for rectangular shaped buildings can be calculated using an algorithm derived from a parametric study based on wind tunnel results (Feustel and Raynor-Hoosen, 1990).

## Thermal Distribution Simulation Tools

### *Air Distribution Systems*

Air distribution system leakage, conduction losses, and the associated impact on whole-building air infiltration has received little attention in building energy simulation tools. The widely known building simulation program DOE-2 uses a simple efficiency multiplier of approximately 0.9 (Lawrence Berkeley Laboratory, 1984) to compensate for duct energy losses. Other simulation tools such as the Thermal Analysis Research Program (TARP) (Walton, 1983) and TRNSYS (University of Wisconsin, 1978) ignored the space conditioning equipment and associated distribution system when calculating building thermal loads.

In more recent times, researchers have begun to consider air distribution systems and their impact on building thermal loads in simulations. An ASHRAE special projects committee (Jakob et al., 1986) showed a reduction of up to 40% in the overall system efficiency in the heating mode. Parker et al. (1993) used a simulation tool, FSEC 2.1 (Kerestecioglu and Gu, 1990), coupled with a detailed duct model to predict duct system impacts on building loads and associated energy consumption. Details considered in the duct model were duct leakage flows based upon duct leakage areas and operating pressures, infiltration impacts across the return ducts and building envelope and heat storage and heat transfer losses across the duct walls. They found that the impacts of duct leakage were of the largest magnitude and that electrical demand during summer peak hours were significantly increased.

Modera and Jansky (1992) developed a simulation tool to analyze air distribution system energy impacts in residences. The tool is based upon the DOE-2 thermal simulation code (Birdsall et al. 1990), the COMIS airflow network code (Feustel and Raynor-Hoosen, 1990), and a duct performance model developed specifically for the simulation tool. The duct performance model calculates the combined impacts of duct leakage and conduction on duct performance and also acts as the interface between COMIS and DOE-2. One of the major findings of their study was the identification of a thermalsiphon loop with a heat exchange rate of more than four times larger than that due to system-off duct leakage. Modera and Treidler (1995) improved the simulation tool in order to look at the thermal siphon effect in more detail and improve the modeling of the duct thermal mass and its effects on duct losses and model duct impacts on multispeed space conditioning equipment. They estimated thermal siphon loads to be between 5 and 16% of the heating load, and that duct thermal mass effects decrease the energy delivery efficiency of the duct system by 1 to 6%. Most significantly, multispeed air conditioners were shown to be more sensitive to duct efficiency than single-speed equipment, because their efficiency decreases with increasing building load. Subsequent field measurements have shown the simulation tool to be accurate.

### *Hydronic Systems*

Energy savings and peak load impacts of radiant hydronic systems have not been studied as systematically. Stetiu and Feustel (1995), developed a simulation tool to perform sensitivity analyses of nonresidential radiantly cooled buildings. The model is based on a methodology for describing and solving the dynamic, nonlinear equations that correspond to complex physical systems as found in buildings. Accurate simulation of the dynamic performance of hydronic radiant cooling systems is described. The model calculates loads, heat extraction rates, room air temperature and room surface temperature distributions, and can be used to evaluate issues such as thermal comfort, controls, system sizing, system configuration, and dynamic response. The authors present favorable comparisons with available field data.

### *Window Thermal Analysis and Daylighting/Fenestration Tools*

Fenestration software programs are used to determine the windows thermal performance and daylighting capabilities. The software can be either stand alone or used as a front end of a whole building energy simulation program. To facilitate their use in the building design stage, window analysis software often has CAD-compatible inputs for geometric details or graphics displays. Software developers are continually

**TABLE 6.3.9** Sample of Fenestration Software

| Software | Analysis | CAD | Building Simulation | Platform | Developer |
|---|---|---|---|---|---|
| ADELINE | thermal/ lighting | yes | yes | DOS | Lawrence Berkeley National Laboratory, International Energy Agency |
| AGI | lighting | yes | no | DOS | Lighting Analysis Corporation |
| CALA | lighting | yes | no | DOS | Holophane Corporation |
| Building Design Advisor | thermal/ lighting | yes | yes | WINDOWS | Lawrence Berkeley National Laboratory |
| Lumen-Micro | lighting | yes | no | DOS | Lighting Technologies Inc. |
| LUXICON | lighting | yes | no | WINDOWS | Cooper Lighting |
| Radiance | lighting | yes | no | UNIX | Lawrence Berkeley National Laboratory |
| RESFEN | thermal | no | yes | DOS | Lawrence Berkeley National Laboratory |
| SUPERLITE | lighting | no | no | DOS | Lawrence Berkeley National Laboratory, International Energy Agency |
| WINDOW 4.1 | thermal | no | no | DOS | Lawrence Berkeley National Laboratory |

improving the user interface to make the programs more accessible to building designers, who may not have time or design fees to use less friendly tools.

The thermal performance of a window is characterized by its overall *U*-value, solar heat gain coefficient, and shading coefficient. These factors depend on the number of panes, gas-filled spaces, low-emittance coatings, frame material and construction, and so on. Window thermal performance software does the required bookkeeping and calculations to determine the parameters important to a window's impact on the thermal loads in a building. Such programs can be used to design and develop new window products and compare the performance characteristics of different types of windows.

The daylighting capabilities of windows are important to consider in the design phase. Some fenestration programs are designed to demonstrate a window's ability to illuminate a space. Some of these programs can calculate the interreflection of light from surfaces in the space and present the results in high-resolution photorealistic graphical displays using a variety of ray-tracing and radiosity techniques. This offers a significant advantage over traditional software that provides simple numerical results or isolux contours. The results tell the designer where the room is under- or overilluminated and where glare problems may exist. These programs can also be integrated into whole building energy simulation programs and thus present a complete picture of the impacts of the windows on the building's energy efficiency and comfort. Table 6.3.9 presents a sample of available lighting or fenestration software. A more complete review of the lighting or daylighting design software can be found in (IESNA, 1995).

## Conclusion

This chapter presented the issues that determine the quality of the indoor environment and the energy issues that affect them. Many facets of building properties and energy services that affect comfort levels of occupants, their health, and their productivity were reviewed. These included conductive, convective, and radiant heat transmission through the building envelope, ventilation and infiltration, and thermal distribution. It was demonstrated how improvements in the building envelope or thermal distribution system can provide the same services, but much more efficiently. Technical advances in construction materials, insulation, windows, and paint provide the means to control building loads or use them to advantage. This reduces the requirements of heating or cooling in the building, thus reducing energy consumption, operating costs, and peak power demand. Whole building simulation programs allow the building designer or retrofitter to evaluate an energy service or shell technology's impact on a building's energy efficiency. These tools give architects the information and means necessary to evaluate a proposed building's thermal and visual comfort, heating and cooling equipment, energy budgets, design cost-effectiveness, and so on. The benefit to society is reduced pressure on limited natural resources, independence from foreign fuel supplies, less demand for new power plants, and reduced air pollution and groundwater contamination.

## References


Akbari, H., S. Bretz, H. Taha, D. Kurn, and J. Hanford, "Peak Power and Cooling Energy Savings of High-Albedo Roofs," Submitted to *Energy and Bulidings.* Excerpts from Lawrence Berkely National Laboratory Report LBL-34411, Berkeley, CA, 1992.

Akbari, H., S. Bretz, H. Taha, D. Kurn, and J. Hanford, "Peak Power and Cooling Energy Savings of Shade Trees," Submitted to *Energy and Bulidings.* Excerpts from Lawrence Berkely National Laboratory Report LBL-34411, Berkeley, CA, 1994.

AIVC, "A Review of Building Airtightness and Ventilation Standards," TN 30, Air Infiltration and Ventilation Centre, UK, 1990.

AIVC, "Air-to-Air Heat Recovery in Ventilation," TN 45, Air Infiltration and Ventilation Centre, UK, 1990.

ASHRAE Standard 119, "Air Leakage Performance for Detached Single-Family Residential Buildings," American Society of Heating, Refrigerating and Air conditioning Engineers, 1988.

ASHRAE Standard 62, "Air Leakage Performance for Detached Single-Family Residential Buildings," American Society of Heating, Refrigerating and Air conditioning Engineers, 1989.

ASHRAE Handbooks, American Society of Heating, Refrigerating and Air conditioning Engineers, 2001.

ASHRAE Standard 55, "Thermal Environmental Conditions for Human Occupancy," American Society of Heating, Refrigerating and Air conditioning Engineers, 1992.

ASHRAE Standard 119, "Air Leakage Performance for Detached Single-Family Residential Buildings," American Society of Heating, Refrigerating and Air conditioning Engineers, 1988.

ASHRAE Standard 136, "A Method of Determining Air Change Rates in Detached Dwellings," American Society of Heating, Refrigerating and Air conditioning Engineers, 1993.

ASTM STP 1067, "Air Change Rate and Airtightness in Buildings, American Society of Testing and Materials," M.H. Sherman, Ed., 1990.

ASTM Standard E741-83, "Standard Test Method for Determining Air Leakage Rate by Tracer Dilution," *ASTM Book of Standards,* American Society of Testing and Materials, Vol. 04.07, 1994.

ASTM Standard E779-87, "Test Method for Determining Air Leakage by Fan Pressurization," *ASTM Book of Standards,* American Society of Testing and Materials, Vol. 04.07, 1991.

ASTM Standard E1186-87, "Practices for Air Leakage Site Detection in Building Envelopes," *ASTM Book of Standards,* American Society of Testing and Materials, Vol. 04.07, 1991.

Andrews, J.W. and M.P. Modera, "Energy Savings Potential for Advanced Thermal Distribution Technology in Residential and Small Commercial Buildings," Prepared for the Building Equipment Division, Office of Building Technologies, U.S. Dept. of Energy, Lawrence Berkeley Laboratory Report, LBL-31042, 1991.

Andrews, J.W. and M.P. Modera, "Thermal Distribution in Small Buildings: A Review and Analysis of Recent Literature," Brookhaven National Laboratory Report, BNL-52349, September 1992.

Birdsall, B., W.F. Buhl, K.L. Ellington, A.E. Erdem, and F.C. Winkelmann, "Overview of the DOE-2 Building Energy Analysis Program, Version 2.1D," Lawrence Berkeley Laboratory Report LBL-19735 Rev.1, Lawrence Berkeley Laboratory, Berkeley, CA, July 1992.

Blasnik, M. and J. Fitzgerald, "In Search of the Missing Leak," *Home Energy,* Vol. 9, No. 6, November/December 1992.

Blomsterberg, A., "Air Leakage in Dwellings," Dept. Bldg. Constr. Report No. 15, Swedish Royal Institute of Technology, 1977.

Cummings, J.R. and J.J. Tooley Jr., "Infiltration and Pressure Differences Induced by Forced Air Systems in Florida Residences," *ASHRAE Trans.,* Vol. 95, Pt. 2, 1989.

Daisey, J.M., "Buildings of the 21st Century: A Perspective on health and Comfort and Work Productivity," presented at the International Energy Agency's Workshop on Buildings of the 21st Century: "Developing Innovative Research Agendas," Gersau, Switzerland, May 16–18, 1979.

Davids, B.J., "Taking the Heat Out of Sunlight—New Advances in Glazing Technology for Commercial Buildings," Proc. ACEEE Summer Study on Energy Efficiency in Buildings, August 26–September 1, Asilomar Conference Center, Pacific Grove, CA, 1990.

Energy Conservatory, "Minneapolis Duct Blaster Operation Manual," The Energy Conservatory, 5158 Bloomington Ave, S, Minneapolis, MN 55417. 1995.

Fuestel, H.E., "Hydronic Radiant Cooling—Preliminary Performance Assessment," Lawrence Berkeley Laboratory Report, LBL-33194, 1993.

Fuestel, H.E. and C. Stetiu, "Hydronic Radiant Cooling—Preliminary Assessment," *Energy and Buildings,* Vol. 8, 1985.

Feustel, H.E. and V.M. Kendon, "Infiltration Models for Multicellular Structures—A Literature Review," *Energy and Bulidings,* Vol. 8, 1985.

Feustel, H.E. and A. Raynor-Hoosen, "Fundamentals of the Multizone Airflow Model COMIS," Technical Note 29, Air Infiltration and Ventilation Centre, Warwick, UK, 1990, also Lawrence Berkeley National Laboratory Report LBNL-28560, 1990.

Feustel, H.E. and J. Dieris, "A Survey of Airflow Models for Multizone Structures," *Energy and Buildings,* Vol. 18, 1992.

Gammage, R.B., A.R. Hawthorne, and D.A. White, "Parameters Affecting Air Infiltration and Air Tightness in Thirty-One East Tennessee Homes," In *Measured Air Leakage of Buildings, ASTM STP 904,* H.R. Trechsel and P.L. Lagus, Eds., pp. 61–69, American Society for Testing and Materials, Philadelphia, 1986.

Griffith, B. and D. Arasteh, "Gas Filled Panels: A Thermally Improved Building Insulation," Proc. ASHRAE/DOE/BTECC Conference: Thermal Performance of the Exterior Envelopes of Buildings V, Clearwater Beach, FL, December 1992.

Holman, J.P., *Heat Transfer,* 4th Edition, McGraw-Hill, New York, 1976.

IES, "Recommended Practices of Daylighting," IES RP-5, Illuminating Engineering Society of North America, 120 Wall St., 17th Floor, New York, NY 10005, 1979.

IESNA, "1995 Software Summary, Lighting Design and Applications,"

Vol. 25, No. 7, Illuminating Engineering Society of North America, 120 Wall St., 17th Floor, New York, NY 10005, July 1995.

Jackman P.J. "A Study of Natural Ventilation of Tall Office Buildings," *J. Inst. Heat. Vent. Eng.,* 38, 1970.

Jakob, F.E., D.W. Locklin, P.E. Fisher, L.J. Flanigan, and R.A. Cudnick, "SP43 Evaluation of Systems Options for Residential Forced Air Heating," *ASHRAE Transactions,* Vol. 92, Pt. 2, Atlanta, GA, 1986.

Jones, P., *How to Cut Heating and Cooling Costs,* Butterick Publishing, New York, 1979.

Jump, D.A. and M.P. Modera, "Energy Impacts of Attic Duct Retrofits in Sacramento Houses," Proc. ACEEE 1994 Summer Study, Pacific Grove, CA, August 28–September 3, 1994, American Council for an Energy Efficient Economy, 1001 Connecticut Av., NW, Suite 801, Washington, DC 20036, 1994.

Keresteciogiu, A. and L. Gu, "Theoretical and Computational Investigation of Heat and Moisture Transfer in Buildings: Evaporation and Condensation Theory," *ASHRAE Trans.,* Vol. 96, Pt. 1, 1990.

Lawler, E.E. III and L.W. Porter, "The Effect of Performance on Job Satisfaction," *Industrial Relations,* Vol. 7, pp. 20–28, 1967.

Lawrence Berkeley Laboratory, "DOE 2.1 Supplement, Version 2.1C," Building Energy Simulation Group, Lawrence Berkeley Laboratory, Berkeley, CA, 1984.

Modera, M.P., "Residential Duct System Leakage: Magnitude, Impacts, and Potential for Reduction," *ASHRAE Trans.,* Vol. 95, Pt. 2, 1989, also LBL-26575.

Modera, M.P., D.J. Dickerhoff, R.E. Jansky, and B.V. Smith, "Improving the Energy Efficiency of Residential Air Distribution Systems in California—Final Report: Phase 1," Lawrence Berkeley Laboratory Report, LBL-30886, 1991.

Modera, M.P. and E.B. Treidler, "Improved Modeling of HVAC System/Envelope Interactions in Residential Buildings," Proc. 1995 ASME International Solar Energy Conference (March 19–24), 1995.

Modera, M.P. and R. Jansky, "Residential Air-Distribution Systems: Interactions with the Building Envelope," Lawrence Berkeley Laboratory Report LBL-31311, UC-350, Lawrence Berkeley Laboratory, Berkeley, CA, July 1992.

Modera, M.P., J.C. Andrews, and E. Kweller, "A Comprehensive Yardstick for Residential Thermal Distribution Efficiency," Proc. ACEEE 1992 Summer Study, Pacific Grove, CA, August 30–September 5, 1992, American Council for an Energy Efficient Economy, 1001 Connecticut Ave., NW, Suite 801, Washington, DC 20036, 1992.

Modera, M.P. and D.A. Jump, "Field Measurement of the Interactions Between Heat Pumps and Duct Systems in Residential Buildings," Proc. 1995 ASME International Solar Energy Conference (March 19–24), 1995; also LBL-36047.

National Fenestration Rating Council (NFRC), "Certified Products Directory," 4th Edition, Silver Springs, MD, January 1995.

Nero, A.V. Jr., "Personal Methods of Controlling Exposure to Indoor Air Pollution," *Principles and Practice of Environmental Medicine,* Plenum Medical Book Company, New York, 1992.

Oak Ridge National Laboratory (ORNL), "Building Foundation Design Handbook," ORNL/SUB/86-72143/1, Oak Ridge National Laboratory, Oak Ridge, TN, 37831, May 1988.

Palmiter, L.E. and P.W. Francisco, "Measured Efficiency of Forced-Air Distribution Systems in 24 Homes," Proc. ACEEE 1994 Summer Study, Pacific Grove, CA, August 28–September 3, 1994, American Council for an Energy Efficient Economy, 1001 Connecticut Ave. NW, Suite 801, Washington, DC 20036, 1992.

Parker, D., P. Fairey, and L. Gu, "Simulation of the Effects of Duct Leakage and Heat Transfer on Residential Space-Cooling Energy Use," *Energy and Buildings,* Vol. 20, No. 2, 1993.

Proctor, J., M. Blasnik, B. Davis, T. Downey, M.P. Modera, G. Nelson, and J.J. Tooley, Jr., "Leak Detectors: Experts Explain the Techniques," *Home Energy,* Vol. 10, No. 5, pp. 26–31, September/October 1993.

Romm, J.J. and W.D. Browning, "Greening the Building and the Bottom Line: Increasing Productivity Through Energy Efficient Design," Proc. ACEEE 1994 Summer Study on Energy Efficiency in Buildings, Panel 9, Demonstrations and Retrofits, Pacific Grove, CA, September 1994.

Samet, J.M., M.C. Marbury, and J.D. Spengler, "Health Effects and Sources of Indoor Air Pollution. Part II," *Am. Rev. Respir. Dis.,* Vol. 137, pp. 221–242, 1988.

Sandberg, M. and M. Sjoberg, "The Use of Moments for Assessing Air Quality in Ventilated Rooms," *Building & Environment,* Vol. 18, p. 181, 1983.

Sherman, M.H., "Estimation of Infiltration from Leakage and Climate Indicators," *Energy and Buildings,* Vol. 10, No. 1, p. 81, 1987.

Sherman, M.H., D.T. Grimsrud, "The Measurement of Infiltration using Fan Pressurization and Weather Data," Proc. First International Air Infiltration Centre Conference, London, England. Lawrence Berkeley Laboratory Report, LBL-10852, October 1980.

Sherman, M.H., N.E. Matson, "Ventilation-Energy Liabilities in U.S. Dwellings," Proc. 14th AIVC Conference, pp. 23–41, 1993, LBL Report No. LBL-33890, 1994.

Sherman, M.H., M.P. Modera, "Infiltration Using the LBL Infiltration Model," Special Technical Publication No. 904, "Measured Air Leakage Performance of Buildings," pp. 325–347. ASTM, Philadelphia, PA, 1984.

Stetiu, C. and H.E. Feustel, "Development of a Model to Simulate the Performance of Hydronic Radiant Cooling Ceilings," presented at the ASHRAE Summer Meeting, San Diego, CA, June 1995.

Stokes, B., "Worker Participation—Productivity and the Quality of Work Life," Worldwatch Paper 25, Worldwatch Institute, December 1978.

Stum, K., "Guidelines for Designing and Installing Tight Duct Systems," *Home Energy,* Vol. 10, No. 5, pp. 55–59, September/October 1993.

Treidler, E.B. and M.P. Modera, "Peak Demand Impacts of Residential Air-Conditioning Conservation Measures," Proc. ACEEE 1994 Summer Study, Pacific Grove, CA, August 28–September 3, 1994, American Council for an Energy Efficient Economy, 1001 Connecticut Ave. NW, Suite 801, Washington, DC20036, 1992.

United States Congress, Office of Technology Assessment, "Building Energy Efficiency," OTA-E-518, Washington, D.C.: U.S. Government Printing Office, May, 1992.

United States Environmental Protection Agency, "Cooling Our Communities: A Guidebook on Tree Planting and Light-Colored Surfaces," USEPA Report No. 22P-2001, Office of Policy Analysis, Climate Change Division, Washington, D.C., January 1992.
University of Wisconsin, "TRNSYS, A Transient Simulation Program," University of Wisconsin Experiment Station, Report 38-9, Madison WI, 1978.
Walton, G.N., "Thermal Analysis Research Program," National Bureau of Standards, NSBIR 83-2655, Washington, D.C., 1983.
Walton, G. "CONTAM 93, User Manual," NISTIR 5385, National Institute of Standards and Technology, 1993, Chapter 53. "Thermal Insulation and Airtightness Building Regulations," Royal Ministry of Local Government and Labor, Norway, 27 May, 1987.

## 6.4 Solar Energy System Analysis and Design

*T. Agami Reddy*

Successful solar system design is an iterative process involving consideration of many technical, practical, reliability, cost, code, and environmental considerations (Mueller Associates, 1985). The success of a project involves identification of and intelligent selection among trade-offs, for which a proper understanding of goals, objectives, and constraints is essential. Given the limited experience available in the solar field, it is advisable to keep solar systems as simple as possible and not be lured by the promise of higher efficiency offered by more complex systems. Because of the location-specific variability of the solar resource, solar systems offer certain design complexities and concerns not encountered in traditional energy systems.

The objective of this chapter is to provide energy professionals with a fundamental working knowledge of the scientific and engineering principles of solar collectors and solar systems relevant to both the feasibility study and schematic design of a solar project. Conventional equipment such as heat exchangers, pumps, and piping layout is but briefly described. Because of space limitations, certain equations/correlations had to be omitted, and proper justice could not be given to several concepts and design approaches. Effort has been made to provide the reader with pertinent references to textbooks, manuals, and research papers.

A detailed design of solar systems requires in-depth knowledge and experience in (1) the use of specially developed computer programs for detailed simulation of solar system performance, (2) designing conventional equipment, controls, and hydronic systems, (3) practical aspects of equipment installation, and (4) economic analysis. These aspects are not addressed here, given the limited scope of this chapter. Readers interested in acquiring such details can consult manuals such as SERI (1989) or Mueller Associates (1985).

It is obvious that the rather lengthy process just outlined pertains to large solar installations. The process is much less involved when a small domestic hot water system or unitary solar equipment or single solar appliances such as solar stills, solar cookers, or solar dryers are to be installed. Not only do such appliances differ in engineering construction from region to region, there are also standardized commercially available units whose designs are already more or less optimized by the manufacturers, normally as a result of previous experimentation, both technical or otherwise. Such equipment is not described in this chapter.

The design concepts described in this chapter are applicable to domestic water heating, swimming pool heating, active space heating, industrial process heat, convective drying systems, and solar cooling systems.

### 6.4.1 Solar Collectors

#### Collector Types

A solar thermal collector is a heat exchanger that converts radiant solar energy into heat. In essence this consists of a receiver that absorbs the solar radiation and then transfers the thermal energy to a working

**TABLE 6.4.1** Advantages and Disadvantages of Liquid and Air Systems

| Characteristics | Liquid | Air |
|---|---|---|
| Efficiency | Collectors generally more efficient for a given temperature difference | Collectors generally operate at slightly lower efficiency |
| System configuration | Can be readily combined with service hot water and cooling systems | Space heat can be supplied directly but does not adapt easily to cooling. Can preheat hot water. |
| Freeze protection | May require antifreeze and heat exchangers that add cost and reduce efficiency | None needed |
| Maintenance | Precautions must be taken against leakage, corrosion and boiling | Low maintenance requirements. Leaks repaired readily with duct tape, but leaks may be difficult to find. |
| Space requirements | Insulated pipes take up nominal space and are more convenient to install in existing buildings | Duct work and rock storage units are bulky, but ducting is a standard HVAC installation technique. |
| Operation | Less energy required to pump liquids | More energy required by blowers to move air; noisier operation. |
| Cost | Collectors cost more. | Storage costs more. |
| State of the art | Has received considerable attention from solar industry | Has received less attention from solar industry |

*Source:* From SERI, 1989.

**TABLE 6.4.2** Types of Solar Thermal Collectors

| Nontracking Collectors | Tracking Collectors |
|---|---|
| Basic flat-plate | Parabolic troughs |
| Flat-plate enhanced with side reflectors or V-troughs | Fresnel reflectors |
| Tubular collectors | Paraboloids |
| Compound parabolic concentrators (CPCs) | Heliostats with central receivers |

fluid. Because of the nature of the radiant energy (its spectral characteristics, its diurnal and seasonal variability, changes in diffuse to global fraction, etc.) as well as the different types of applications for which solar thermal energy can be used, the analysis and design of solar collectors present unique and unconventional problems in heat transfer, optics, and material science. The classification of solar collectors can be made according to the type of working fluid (water, air, or oils) or the type of solar receiver used (nontracking or tracking).

Most commonly used working fluids are water (glycol being added for freeze protection) and air. Table 6.4.1 identifies the relative advantages and potential disadvantages of air and liquid collectors and associated systems. Because of the poorer heat transfer characteristics of air with the solar absorber, the air collector may operate at a higher temperature than a liquid-filled collector, resulting in greater thermal losses and, consequently, a lower efficiency. The choice of the working fluid is usually dictated by the application. For example, air collectors are suitable for space heating and convective drying applications, while liquid collectors are the obvious choice for domestic and industrial hot water applications. In certain high-temperature applications, special types of oils that provide better heat transfer characteristics are used.

The second criterion of collector classification is according to the presence of a mechanism to track the sun throughout the day and year in either a continuous or discreet fashion (see Table 6.4.2). The stationary flat-plate collectors are rigidly mounted, facing toward the equator with a tilt angle from the horizontal roughly equal to the latitude of the location for optimal year-round operation. The compound parabolic concentrators (CPCs) can be designed either as completely stationary devices or as devices that need seasonal adjustments only. On the other hand, Fresnel reflectors, paraboloids, and heliostats need two-axis tracking. Parabolic troughs have one axis tracking either along the east–west direction or the north–south direction. These collector types are described in other chapters.

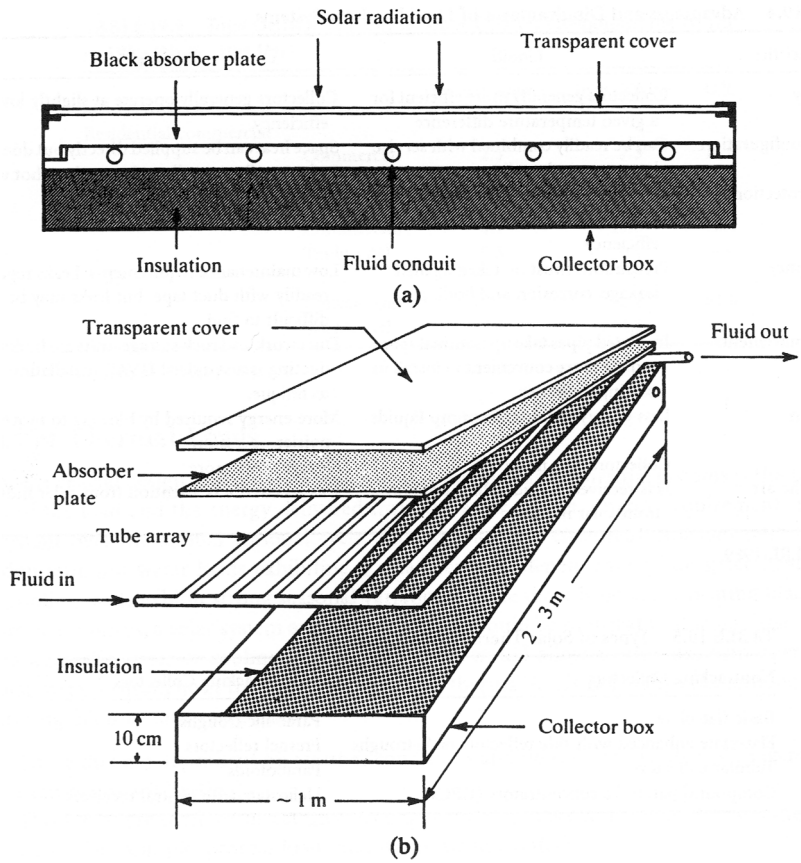


**FIGURE 6.4.1** Cross-section of a flat-plate collector.

A third classification criterion is to distinguish between nonconcentrating and concentrating collectors. The main reason for using concentrating collectors is not that *more energy* can be collected but that the thermal energy is obtained at higher temperatures. This is done by decreasing the area from which heat losses occur (called the receiver area) with respect to the aperture area (i.e., the area that intercepts the solar radiation). The ratio of the aperture to receiver area is called the *concentration ratio*.

## Flat-Plate Collectors

### Description

The flat-plate collector is the most common conversion device in operation today, since it is most economical and appropriate for delivering energy at temperatures up to about 100°C. The construction of flat-plate collectors is relatively simple, and many commercial models are available.

Figure 6.4.1 shows the physical arrangements of the major components of a conventional flat-plate collector with a liquid working fluid. The blackened absorber is heated by radiation admitted via the transparent cover. Thermal losses to the surroundings from the absorber are contained by the cover, which acts as a black body to the infrared radiation (this effect is called the *greenhouse* effect), and by insulation provided under the absorber plate. Passages attached to the absorber are filled with a circulating fluid, which extracts energy from the hot absorber. The simplicity of the overall device makes for long service life.

The absorber is the most complex portion of the flat-plate collector, and a great variety of configurations are currently available for liquid and air collectors. Figure 6.4.2 illustrates some of these concepts

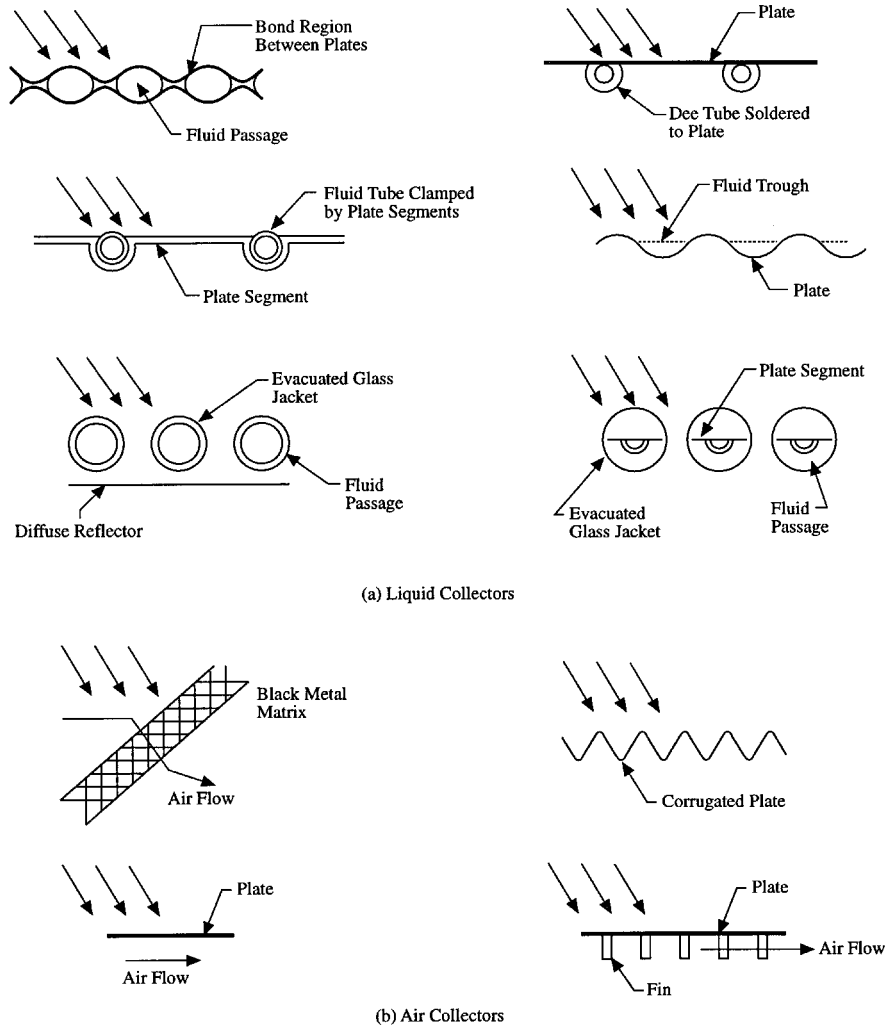


**FIGURE 6.4.2** Typical flat-plate absorber configurations.

in absorber design for both liquid and air absorbers. Conventional materials are copper, aluminum, and steel. The absorber is either painted with a dull black paint or can be coated with a *selective surface* to improve performance (see "Improvements to Flat-Plate Collector Performance" for more details). Bonded plates having internal passageways perform well as absorber plates because the hydraulic passageways can be designed for optimal fluid and thermal performance. Such collectors are called *roll-bond* collectors. Another common absorber consists of tubes soldered or brazed to a single metal sheet, and mechanical attachments of the tubes to the plate have also been employed. This type of collector is called a *tube-and-sheet* collector. Heat pipe collectors have also been developed, though these are not as widespread as the previous two types. The so-called *trickle type* of flat-plate collector, with the fluid flowing directly over the corrugated absorber plate, dispenses entirely with fluid passageways. Tubular collectors have also been used because of the relative ease by which air can be evacuated from such collectors, thereby reducing convective heat losses from the absorber to the ambient air.

The absorber in an air collector normally requires a larger surface than in a liquid collector because of the poorer heat transfer coefficients of the flowing air stream. Roughness elements and producing turbulence by way of devices such as expanded metal foil, wool, and overlapping plates have been used as a means for increasing the heat transfer from the absorber to the working fluid. Another approach to

enhance heat transfer is to use packed beds of expanded metal foils or matrices between the glazing and the bottom plate.

***Modeling***

A particular modeling approach and the corresponding degree of complexity in the model are dictated by the objective as well as by experience gained from past simulation work. For example, it has been found that transient collector behavior has insignificant influence when one is interested in determining the long-term performance of a solar thermal system. For complex systems or systems meant for non-standard applications, detailed modeling and careful simulation of system operation are a must initially, and simplifications in component models and system operation can subsequently be made. However, in the case of solar thermal systems, many of the possible applications have been studied to date and a backlog of experience is available not only concerning system configurations but also with reference to the degree of component model complexity.

Because of low collector time constants (about 5 min), heat capacity effects are usually small. Then the instantaneous (or hourly, because radiation data are normally available in hourly time increments only) steady-state useful energy $q_C$ in Watts delivered by a solar flat-plate collector of surface area $A_C$ is given by

$$q_c = A_c F' \left[ I_T \eta_0 - U_L \left( T_{Cm} - T_a \right) \right]^+ \tag{6.4.1}$$

where $F'$ is the plate efficiency factor, which is a measure of how good the heat transfer is between the fluid and the absorber plate; $\eta_0$ is the optical efficiency, or the product of the transmittance and absorptance of the cover and absorber of the collector; $U_L$ is the overall heat loss coefficient of the collector, which is dependent on collector design only normally expressed in W/(m$^2$ °C); $T_{Cm}$ is the *mean* fluid temperature in the collector (in °C); and $I_T$ is the radiation intensity on the plane of the collector (in W/m$^2$). The + sign denotes that only positive values are to be used, which physically implies that the collector should not be operated when $q_C$ is negative (i.e., when the collector loses more heat than it can collect).

However, because $T_{cm}$ is not a convenient quantity to use, it is more appropriate to express collector performance in terms of the fluid *inlet* temperature to the collector ($T_{Ci}$). This equation is known as the classical Hottel–Whillier–Bliss (HWB) equation and is most widely used to predict instantaneous collector performance:

$$q_c = A_c F_R \left[ I_T \eta_0 - U_L \left( T_{Ci} - T_a \right) \right]^+ \tag{6.4.2}$$

where $F_R$ is called the heat removal factor and is a measure of the solar collector performance as a heat exchanger, since it can be interpreted as the ratio of actual heat transfer to the maximum possible heat transfer. It is related to F′ by

$$\frac{F_R}{F'} = \frac{\left( mc_p \right)_C}{A_C F' U_L} \left\{ 1 - \exp\left[ - \frac{A_C U_L F'}{\left( mc_p \right)_C} \right] \right\} \tag{6.4.3}$$

where $m_c$ is the total fluid flow rate through the collectors and $c_{pc}$ is the specific heat of the fluid flowing through the collector. The variation of $(F_R/F')$ with $[(mC_p)_c/A_C U_L F']$ is shown graphically in Figure 6.4.3. Note the asymptotic behavior of the plot, which suggests that increasing the fluid flow rate more than a certain amount results in little improvement in $F_R$ (and hence in $q_C$) while causing a quadratic increase in the pressure drop.

Factors influencing solar collector performance are of three types: (1) constructional, that is related to collector design and materials used, (2) climatic, and (3) operational, that is, fluid temperature, flow rate, and so on. The plate efficiency factor $F'$ is a factor that depends on the physical constructional

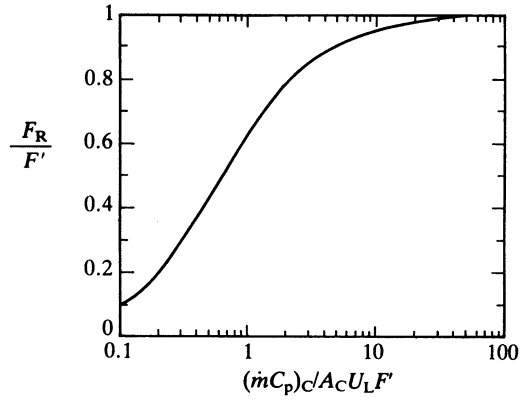


**FIGURE 6.4.3** Variation of $F_R/F'$ as a function of $[(mc_p)_c/(A_cU_LF')]$ (From Duffie, J.A. and Beckman, W.A., *Solar Engineering of Thermal Processes*, Wiley Interscience, New York. Copyright 1980. Reprinted with permission of John Wiley & Sons, Inc.)

features and is essentially a constant for a given liquid collector. (This is not true for air collectors, which require more careful analysis.) Operational features involve changes in $m_C$ and $T_{Ci}$. While changes in $m_C$ affect $F_R$ as per Eq. (6.4.3), we note from Eq. (6.4.2) that to enhance $q_C$, $T_{Ci}$ needs to be kept as low as possible. For solar collectors that are operated under more or less constant flow rates, specifying $F_R\,\eta_0$ and $F_R\,U_L$ is adequate to predict collector performance under varying climatic conditions.

There are a number of procedures by which collectors have been tested. The most common is a *steady-state procedure*, where transient effects due to collector heat capacity are minimized by performing tests only during periods when radiation and ambient temperature are steady. The procedure involves simultaneous and accurate measurements of the mass flow rate, the inlet and outlet temperatures of the collector fluid, and the ambient conditions (incident solar radiation, air temperature and wind speed). The most widely used test procedure is the ASHRAE Standard 93-77 (1978), whose test setup is shown in Figure 6.4.4. Though a solar simulator can be used to perform indoor testing, outdoor testing is always more realistic and less expensive. The procedure can be used for nonconcentrating collectors using air or liquid as the working fluid (but not two phase mixtures) that have a single inlet and a single outlet and contain no integral thermal storage.

Steady-state procedures have been in use for a relatively long period and though the basis is very simple the engineering setup is relatively expensive (see Figure 6.4.4). From an overall heat balance on the collector fluid and from Eq. (6.4.2), the expressions for the instantaneous collector efficiency under normal solar incidence are

$$\eta_C \equiv \frac{q_C}{A_C I_T} = \frac{\left(mc_p\right)_C \left(T_{Co} - T_{Ci}\right)}{A_C I_T} \tag{6.4.4}$$

$$= \left[ F_R \eta_n - F_R U_L \left( \frac{T_{Ci} - T_a}{I_T} \right) \right] \tag{6.4.5}$$

where $\eta_n$ is the optical efficiency at normal solar incidence.

From the test data, points of $\eta_c$ against reduced temperature $[(T_{Ci} - T_a) / I_T]$ are plotted as shown in Figure 6.4.5. Then a linear fit is made to these data points by regression, from which the values of $F_R\,\eta_n$ and $F_R\,U_L$ are easily deduced. It will be noted that if the reduced term were to be taken as $[(T_{Cm} - T_a) /I_T]$, estimates of $F'\eta_n$ and $F'U_L$ would be correspondingly obtained.

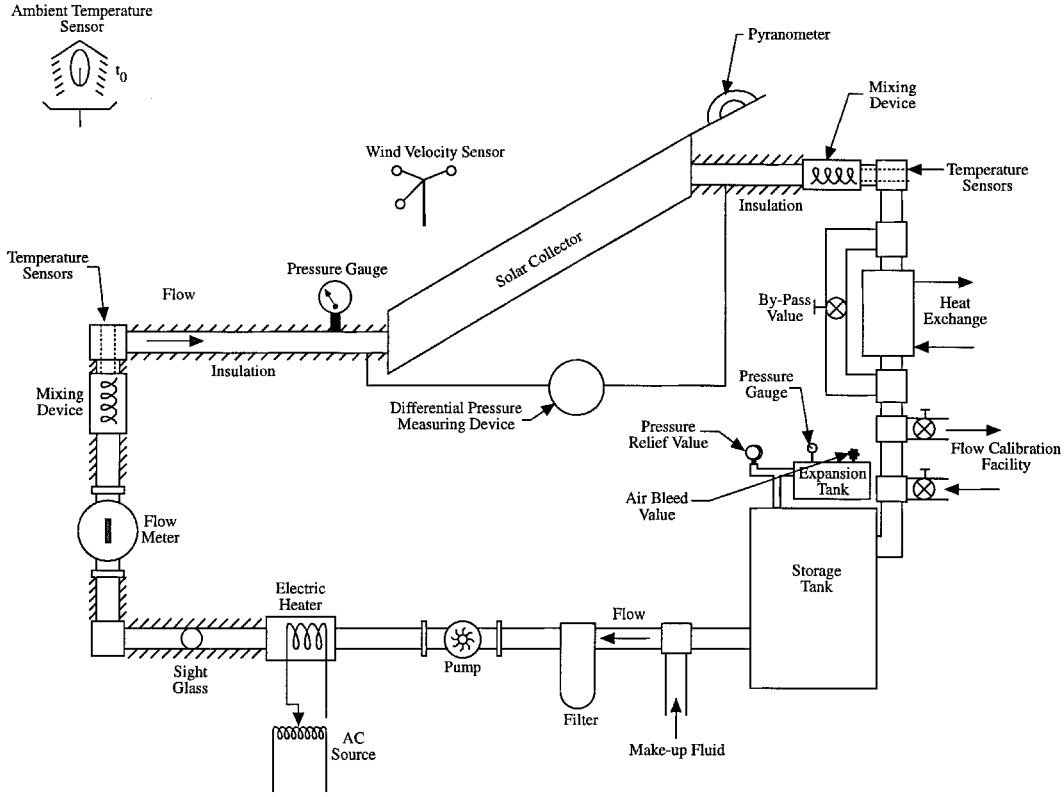


**FIGURE 6.4.4** Set up for testing liquid collectors according to ASHRAE Standard 93-72.

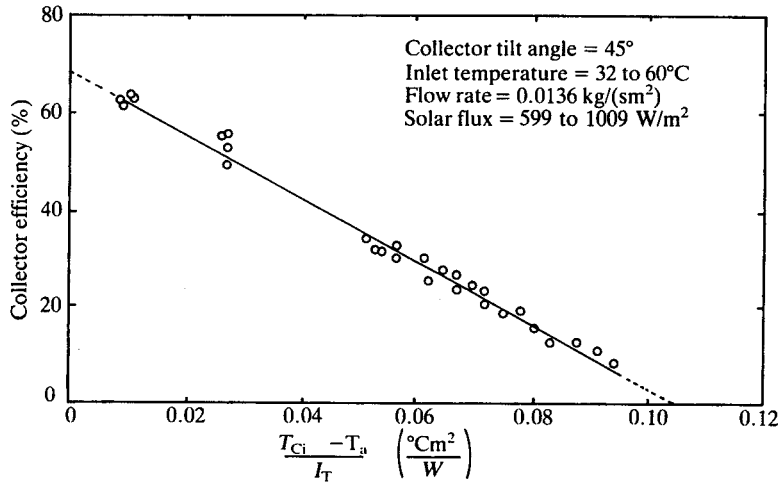


**FIGURE 6.4.5** Thermal efficiency curve for a double glazed flat-plate liquid collector (ASHRAE 1978). Test conducted outdoors on a 1.2 m by 1.25 m panel with 10.2 cm of glass fiber back insulation and a flat copper absorber with black coating of emissivity of 0.97.

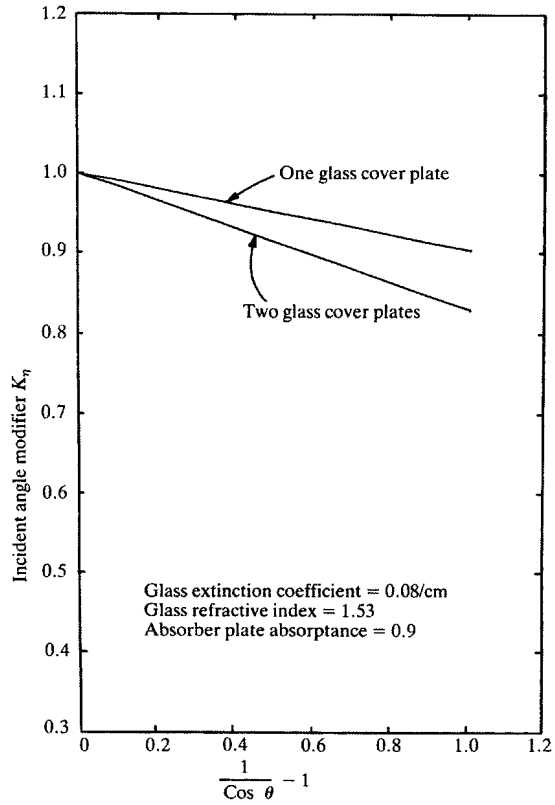


**FIGURE 6.4.6** Incident angle modifiers for two flat-plate collectors with non-selective coating on the absorber. (Adapted from ASHRAE, 1978.)

***Incidence Angle Modifier***

The optical efficiency $\eta_0$ depends on the collector configuration and varies with the angle of incidence as well as with the relative values of diffuse and beam radiation. The incidence angle modifier is defined as $K_\eta \equiv (\eta_0/\eta_n)$. For flat plate collectors with 1 or 2 glass covers, $K_\eta$ is almost unchanged up to incidence angles of 60°, after which it abruptly drops to zero.

A simple way to model the variation of $K_\eta$ with incidence angle for flat plate collectors is to specify $\eta_n$, the optical efficiency of the collector at normal beam incidence, to assume the entire radiation to be beam, and to use the following expression for the angular dependence (ASHRAE, 1978)

$$K_\eta = 1 + b_0\left(\frac{1}{\cos\theta} - 1\right) \tag{6.4.6}$$

where $\theta$ is the solar angle of incidence on the collector plane (in degrees) and $b_0$ is a constant called the incidence angle modifier coefficient. Plotting $K_\eta$ against $[(1/\cos\theta)-1]$ results in linear plots (see Figure 6.4.6), thus justifying the use of Eq. (6.4.6). We note that for one-glass and two-glass covers, approximate values of $b_0$ are –0.10 and –0.17, respectively.

In case the diffuse solar fraction is high, one needs to distinguish between beam, diffuse, and ground-reflected components. Diffuse radiation, by its very nature, has no single incidence angle. One simple way is to assume an equivalent incidence angle of 60° for diffuse and ground-reflected components. One would then use Eq. (6.4.6) for the beam component along with its corresponding value of $\theta$ and account for the contribution of diffuse and ground reflected components by assuming a value of $\theta = 60°$ in

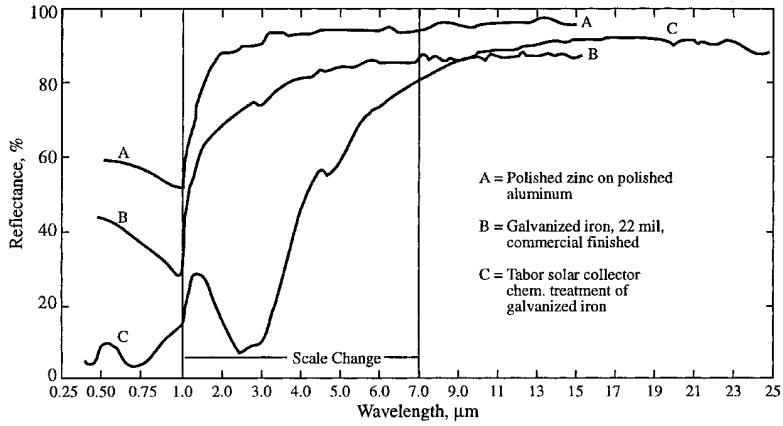


**FIGURE 6.4.7** Spectral reflectance of several surfaces. (From Edwards, D.K. et al., 1960.)

Eq. (6.4.6). For more accurate estimation, one can use the relationship between the effective diffuse solar incidence angle versus collector tilt given in Duffie and Beckman (1980). It should be noted that the preceding equation gives misleading results with incidence angles close to 90°. An alternative functional form for the incidence angle modifier for both flat-plate and concentrating collectors has been proposed by Rabl (1981).

## Improvements to Flat-Plate Collector Performance

There are a number of ways by which the performance of the basic flat-plate collectors can be improved. One way is to enhance optical efficiency by treatment of the glass cover thereby reducing reflection and enhancing performance. As much as a 4% increase has been reported (Anderson, 1977). Low-iron glass can also reduce solar absorption losses by a few percent.

These improvements are modest compared to possible improvements from reducing losses from the absorber plate. Essentially, the infrared upward reradiation losses from the heated absorber plate have to be decreased. One could use a second glass cover to reduce the losses, albeit at the expense of higher cost and lower optical efficiency. Usually for water heating applications, radiation accounts for about two-thirds of the losses from the absorber to the cover with convective losses making up the rest (conduction is less than about 5%). The most widely used manner of reducing these radiation losses is to use selective surfaces whose emissivity varies with wavelength (as against matte-black painted absorbers, which are essentially gray bodies). Note that 98% of the solar spectrum is at wavelengths less than 3.0 μm, whereas less than 1% of the black body radiation from a 200°C surface is at wavelengths less than 3.0 μm. Thus selective surfaces for solar collectors should have high solar absorptance (i.e., low reflectance in the solar spectrum) and low long-wave emittance (i.e., high reflectance in the long-wave spectrum). The spectral reflectance of some commonly used selective surfaces is shown in Figure 6.4.7. Several commercial collectors for water heating or low-pressure steam (for absorption cooling or process heat applications) that use selective surfaces are available.

Another technique to simultaneously reduce both convective and radiative losses between the absorber and the transparent cover is to use honeycomb material (Hollands, 1965). The honeycomb material can be reflective or transparent (the latter is more common) and should be sized properly. Glass honeycombs have had some success in reducing losses in high-temperature concentrating receivers, but plastics are usually recommended for use in flat-plate collectors. Because of the poor thermal aging properties, honeycomb flat-plate collectors have had little commercial success. Currently the most promising kind seems to be the simplest (both in terms of analysis and construction), namely collectors using horizontal rectangular slats (Meyer, 1978). Convection can be entirely suppressed provided the slats with the proper aspect ratio are used.

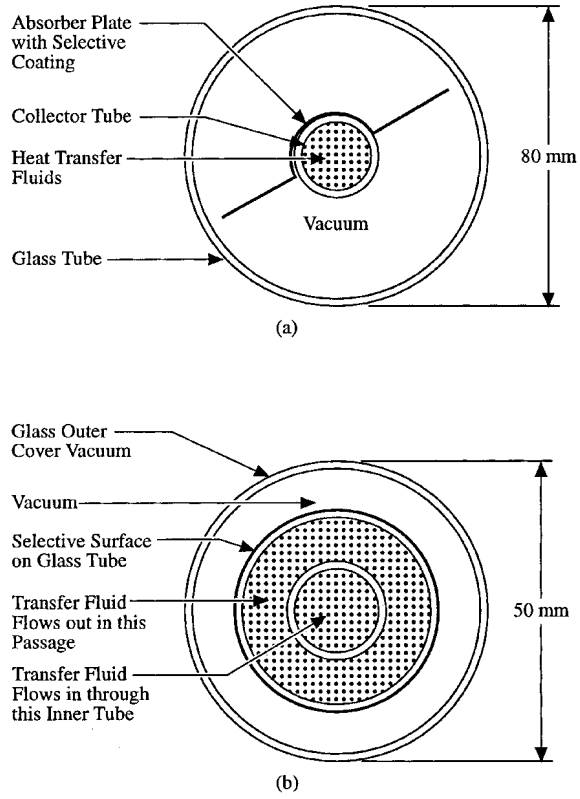


**FIGURE 6.4.8** Evacuated tubular collectors. (From Charters, W.W.S. and Pryor, T.L., 1982.)

Finally, collector output can be enhanced by using side reflectors, for instance a sheet of anodized aluminum. The justification in using these is their low cost and simplicity. For instance, a reflector placed in front of a tilted collector cannot but increase collector performance because losses are unchanged and more solar radiation is intercepted by the collector. Reflectors in other geometries may cast a shadow on the collector and reduce performance. Note also that reflectors would produce rather nonuniform illumination over the day and during the year, which, though not a problem in thermal collectors, may drastically penalize the electric output of photovoltaic modules. Whether reflectors are cost-effective depends on the particular circumstances and practical questions such as aesthetics and space availability. The complexity involved in the analysis of collectors with planar reflectors can be reduced by assuming the reflector to be long compared to its width and treating the problem in two dimensions only. How optical performance of solar collectors are affected by side planar reflectors is discussed in several papers, for example Larson (1980) and Chiam (1981).

## Other Collector Types

### *Evacuated Tubular Collectors*

One method of obtaining temperatures between 100°C and 200°C is to use evacuated tubular collectors. The advantage in creating and being able to main a vacuum is that convection losses between glazing and absorber can be eliminated. There are different possible arrangements of configuring evacuated tubular collectors. Two designs are shown in Figure 6.4.8. The first is like a small flat-plate collector with the liquid to be heated making one pass through the collector tube. The second uses an all-glass construction with the glass absorber tube being coated selectively. The fluid being heated passes up the middle of the absorber tube and then back in contact with the hot absorber surface. Evacuated tubes can collect both direct and diffuse radiation and do not require tracking. Glass breakage and leaking

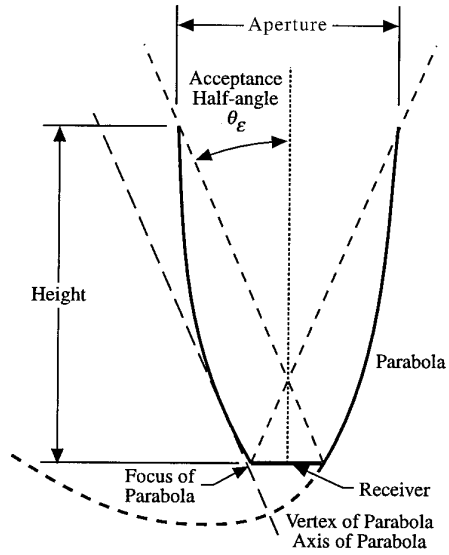


**FIGURE 6.4.9** Cross-section of a symmetrical non-truncated CPC. (From Duffie, J.A. and Beckman, W.A., *Solar Engineering of Thermal Processes*, Wiley Interscience, New York. Copyright 1980. Reprinted with permission of John Wiley & Sons, Inc.)

joints due to thermal expansion are some of the problems which have been experienced with such collector types. Various reflector shapes (like flat-plate, V-groove, circular cylindrical, involute, etc.) placed behind the tubes are often used to usefully collect some of the solar energy, which may otherwise be lost, thus providing a small amount of concentration.

***Compound Parabolic Concentrators (CPCs)***

The CPC collector, discovered in 1966, consists of parabolic reflectors that funnel radiation from aperture to absorber rather than focusing it. The right and left halves belong to different parabolas (hence the name *compound*) with the edges of the receiver being the foci of the opposite parabola (see Figure 6.4.9). It has been proven that such collectors are *ideal* in that any solar ray, be it beam or diffuse, incident on the aperture within the acceptance angle will reach the absorber while all others will bounce back to and fro and re-emerge through the aperture. CPCs are also called *nonimaging* concentrators because they do not form clearly defined images of the solar disk on the absorber surface as achieved in classical concentrators. CPCs can be designed both as low-concentration devices with large acceptance angles or as high-concentration devices with small acceptance angles. CPCs with low concentration ratios (of about 2) and with east–west axes can be operated as stationary devices throughout the year or at most with seasonal adjustments only. CPCs, unlike other concentrators, are able to collect all the beam and a large portion of the diffuse radiation. Also they do not require highly specular surfaces and can thus better tolerate dust and degradation. A typical module made up of several CPCs is shown in Figure 6.4.10. The absorber surface is located at the bottom of the trough, and a glass cover may also be used to encase the entire module. CPCs show considerable promise for water heating close to the boiling point and for low-pressure steam applications. Further details about the different types of absorber and receiver shapes used, the effect of truncation of the receiver and the optics, can be found in Rabl (1985). In order to justify the significant investment in a solar heating system, the HVAC designer must weigh costs against energy production (Section 3.2). This section outlines how to calculate the energy production.

## 6.4.2 Long-Term Performance of Solar Collectors

### Effect of Day-to-Day Changes in Insolation

Instantaneous or hourly performance of solar collectors has been discussed in "Flat-Plate Collectors." For example, one would be tempted to use the HWB equation (Eq. 6.4.2) to predict long-term collector

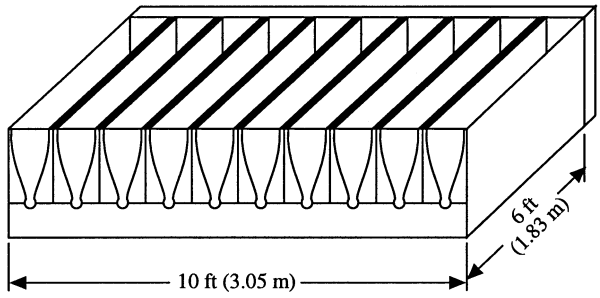


**FIGURE 6.4.10** A CPC collector module. (From SERI, 1989.)

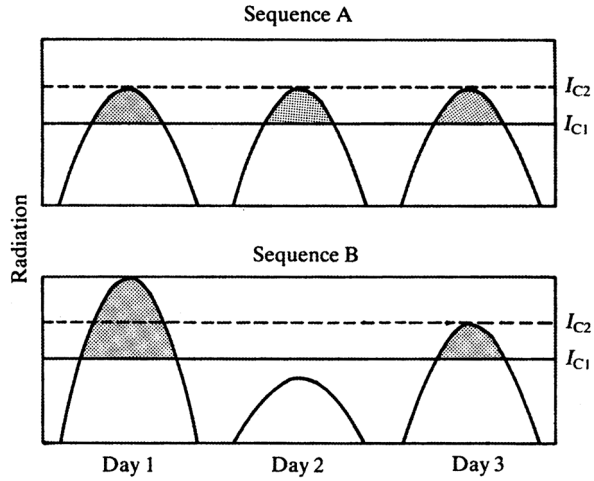


**FIGURE 6.4.11** Effect of radiation distribution on collector long-term performance. (From Klein, S.A., Calculation of flat-plate collector utilizability, *Solar Energy*, 21, 393, 1978. With permission.)

performance at a prespecified and constant fluid inlet temperature $T_{Ci}$ merely by assuming average hourly values of $I_T$ and $T_a$. Such a procedure would be erroneous and lead to underestimation of collector output because of the presence of the control function, which implies that collectors are turned on only when $q_C > 0$, that is when radiation $I_T$ exceeds a certain critical value $I_C$. This critical radiation value is found by setting $q_C$ in Eq. (6.4.2) to zero:

$$I_C = U_L\left(T_{Ci} - T_a\right)/\eta_0 \tag{6.4.7a}$$

To be more rigorous, a small increment $\delta$ to account for pumping power and stability of controls can also be included if needed by modifying the equation to

$$I_C = U_L\left(T_{Ci} + \delta - T_a\right)/\eta_0 \tag{6.4.7b}$$

Then, Eq. (6.4.2) can be rewritten in terms of $I_C$ as

$$q_C = A_C F_R \eta_0 \left[I_T - I_C\right]^+ \tag{6.4.8}$$

Why one cannot simply assume a mean value of $I_T$ in order to predict the mean value of $q_C$ will be illustrated by the following simple concept (Klein, 1978). Consider the three identical day sequences shown in sequence A of Figure 6.4.11. If $I_{C1}$ is the critical radiation intensity, and if it is constant over the whole

day, the useful energy collected by the collector is represented by the sum of the shaded areas. If a higher critical radiation value shown as $I_{C2}$ in Figure 6.4.11 is selected, we note that no useful energy is collected at all. Actual weather sequences would not look like that in sequence A but rather like that in sequence B, which is comprised of an excellent, a poor, and an average day. Even if both sequences have the same average radiation over 3 days, a collector subjected to sequence B will collect useful energy when the critical radiation is $I_{C2}$. Thus, neglecting the variation of radiation intensity from day to day over the long term and dealing with mean values would result in an underestimation of collector performance.

Loads are to a certain extent repetitive from day to day over a season or even the year. Consequently, one can also expect collectors to be subjected to a known diurnal repetitive pattern or mode of operation, that is, the collector inlet temperature $T_{Ci}$ has a known repetitive pattern.

### Individual Hourly Utilizability

In this mode, $T_{Ci}$ is assumed to vary over the day but has the same variation for all the days over a period of $N$ days (where $N = 30$ days for monthly and $N = 365$ for yearly periods). Then from Eq. (6.4.8), *total* useful energy collected over $N$ days during individual hour $i$ of the day is

$$q_{CN}(i) = A_C F_R \overline{\eta}_0 \bar{I}_{Ti} \sum_{i=1}^{N} \frac{\left[I_T - I_C\right]^+}{\bar{I}_{Ti}} \tag{6.4.9}$$

If we define the radiation ratio

$$X = I_{Ti} / \bar{I}_{Ti} \tag{6.4.10}$$

then the critical radiation ratio

$$X_C = I_C / \bar{I}_{Ti}$$

The HWB equation (Eq. 6.4.8) can be rewritten as

$$q_{CN}(i) = A_C F_R \overline{\eta}_0 \bar{I}_{Ti} \overline{N} \phi_i \tag{6.4.11}$$

where the individual hourly utilizability factor $\phi_i$ is identified as

$$\phi_i(X_C) = \frac{1}{N} \sum_{i=1}^{N} (X_i - X_C)^+ \tag{6.4.12}$$

Thus $\phi_i$ can be considered to be the fraction of the incident solar radiation that can be converted to useful heat by an ideal collector (i.e., whose $F_R \eta_0 = 1$. The utilizability factor is thus a *radiation statistic* in the sense that it depends solely on the radiation values at the specific location. As such, it is in no way dependent on the solar collector itself. Only after the radiation statistics have been applied is a collector dependent significance attached to $X_C$.

Hourly utilizability curves on a *monthly* basis that are independent of location were generated by Liu and Jordan (1963) more than 30 years ago for flat-plate collectors (see Figure 6.4.12). The key climatic parameter which permits generalization is the *monthly clearness index* $\overline{K}$ of the location defined as

$$\overline{K} = \overline{H} / \overline{H}_0 \tag{6.4.13}$$

where $\overline{H}$ is the monthly mean daily global radiation on the horizontal surface and $\overline{H}_0$ is the monthly mean daily extraterrestrial radiation on a horizontal surface.

Extensive tables giving monthly values of $\overline{K}$ for several different locations worldwide can be found in several books, for example, Duffie and Beckman (1980) or Reddy (1987). The curves apply to

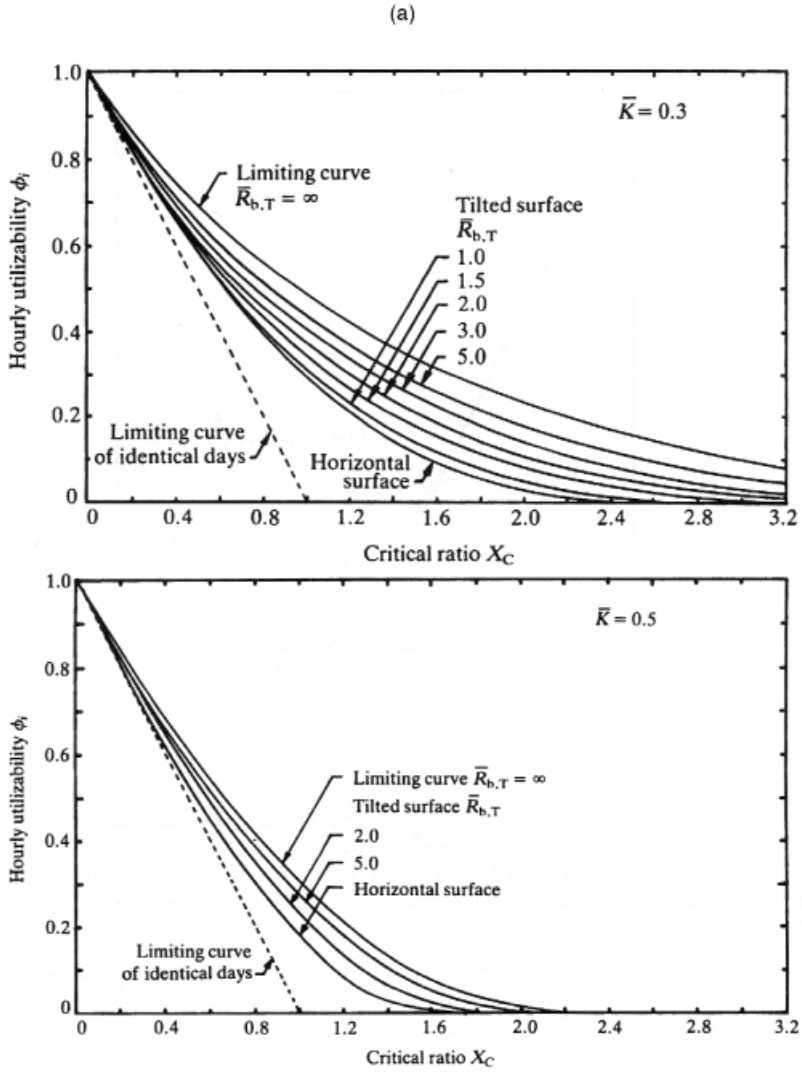


**FIGURE 6.4.12(a)** Generalized hourly utilizability curves of Liu and Jordan (1963) for three different monthly mean clearness indices $\bar{K}$.

equator-facing tilted collectors with the effect of collector tilt accounted for by the factor $\bar{R}_{b,T}$ which is the ratio of the monthly mean daily extraterrestrial radiation on the tilted collector to that on a horizontal surface. Monthly mean daily calculations can be made using the 15th of the month, though better accuracy is achieved using slightly different dates (Reddy, 1987). Clark et al. (1983), working from measured data from several U.S. cities, have proposed the following correlation for individual hourly utilizability over monthly time scales applicable to *flat-plate collectors only*:

$$\begin{aligned} \phi_i &= 0 && \text{for } X_C \geq X_{max} \\ &= \left(1 - X_C / X_{max}\right)^2 && \text{for } X_{max} = 2 \\ &= \left| |a| - \left[ a^2 + (1+2a)\left(1 - X_C / X_{max}\right)^2 \right]^{1/2} \right| && \text{otherwise} \end{aligned} \tag{6.4.14}$$

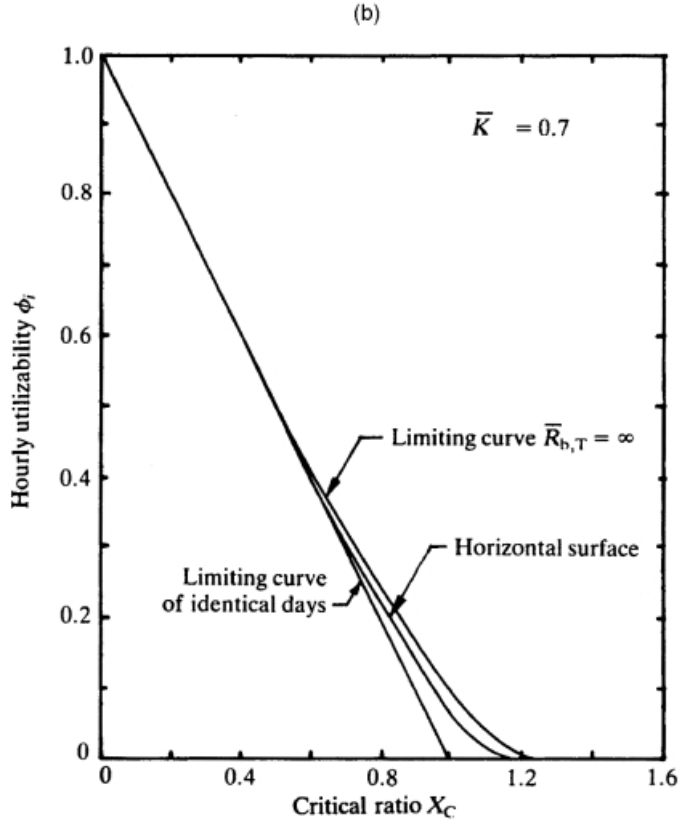


**FIGURE 6.4.12(b)**

where

$$a = \left(X_{\max} - 1\right)\left(2 - X_{\max}\right) \tag{6.4.15}$$

and

$$X_{\max} = 1.85 + 0.169\left(\bar{r}_T/\bar{k}^2\right) - 0.0696\ \cos\beta/\bar{k}^2 - 0.981\ \bar{k}/\left(\cos\ \delta\right)^2 \tag{6.4.16}$$

where $\bar{k}$ is the monthly mean *hourly* clearness index for the particular hour, $\delta$ is the solar declination, $\beta$ is the tilt angle of the collector plane with respect to the horizontal, and $\bar{r}_T$ is the ratio of monthly average hourly global radiation on a tilted surface to that on a horizontal surface for that particular hour. For an isotropic sky assumption, $\bar{r}_T$ is given by

$$\bar{r}_T = \left(1 - \frac{\bar{I}_d}{\bar{I}}\right) r_{b,T} + \left(\frac{1 + \cos\ \beta}{2}\right)\frac{\bar{I}_d}{\bar{I}} + \left(\frac{1 - \cos\ \beta}{2}\right)\rho \tag{6.4.17}$$

where $\bar{I}_d$ and $\bar{I}$ are the hourly diffuse and global radiation on the horizontal surface, $r_{b,T}$ is the ratio of hourly beam radiation on the tilted surface to that on a horizontal surface (this is a purely astronomical quantity and can be calculated accurately from geometric considerations), and $\rho$ is the ground albedo.

## Daily Utilizability

### *Basis*

In this mode, $T_{Ci}$, and hence the critical radiation level is assumed constant during all hours of the day. The *total* useful energy over $N$ days that can be collected by solar collectors operated all day over $n$ hours is given by

$$Q_{CN} = A_C F_R \overline{\eta}_0 \overline{H}_T N \overline{\phi} \tag{6.4.18}$$

where $\overline{H}_T$ is the average daily global radiation on the collector surface, and $\overline{\phi}$ (called "phibar") is the daily utilizability factor, defined as

$$\overline{\phi} = \sum^{N}\sum^{n}\left(I_T - I_C\right)^{+} \Big/ \sum^{N}\sum^{n} I_T = \frac{1}{Nn}\sum^{N}\sum^{n}\left(X_i - \overline{X}_C\right)^{+} \tag{6.4.19}$$

Generalized correlations have been developed both at monthly time scales and for annual time scales based on the parameter $\overline{K}$. Generalized (i.e., location and month independent) correlations for $\overline{\phi}$ on a *monthly* time scale have been proposed by Theilacker and Klein (1980). These are strictly applicable for flat-plate collectors only. Collares-Pereira and Rabl (1979) have also proposed generalized correlations for $\overline{\phi}$ on a monthly time scale which, though a little more tedious to use are applicable to concentrating collectors as well. The reader may refer to Rabl (1985) or Reddy (1987) for complete expressions.

### *Monthly Time Scales*

The phibar method of determining the daily utilizability fraction proposed by Theilacker and Klein (1980) is based on correlating $\overline{\phi}$ to the following factors:

1. A geometry factor $\overline{R}_T/\bar{r}_{T,noon}$, which incorporates the effects of collector orientation, location, and time of year. $\overline{R}_T$ is the ratio of monthly average global radiation on the tilted surface to that on a horizontal surface. $\bar{r}_{T,noon}$ is the ratio of radiation at noon on the tilted surface to that on a horizontal surface for the average day of the month. Geometrically, $\bar{r}_{T,noon}$ is a measure of the maximum height of the radiation curve over the day, whereas $\overline{R}_T$ is a measure of the enclosed area. Generally the value $(\overline{R}_T/\bar{r}_{T,noon})$ is between 0.9 and 1.5.
2. A dimensionless critical radiation level $\overline{X}_{C,K}$ where

$$\overline{X}_{C,K} = I_C \big/ \bar{I}_{T,noon} \tag{6.4.20}$$

with $\bar{I}_{T,noon}$, the radiation intensity on the tilted surface at noon, given by

$$\bar{I}_{T,noon} = \bar{r}_{noon}\,\bar{r}_{T,noon}\overline{H} \tag{6.4.21}$$

where $\bar{r}_{noon}$ is the ratio of radiation at noon to the daily global radiation on a horizontal surface during the mean day of the month which can be calculated from the following correlation proposed by Liu and Jordan (1960):

$$r(W) = \frac{I(W)}{H} = \frac{\pi}{24}(a + b\ \cos W)\frac{\left(\cos W - \cos W_S\right)}{\left(\sin W_S - \frac{\pi}{180}W_S\ \cos W_S\right)} \tag{6.4.22}$$

with

$$a = 0.409 + 0.5016\ \sin(W_s - 60)$$

$$b = 0.6609 - 0.4767\ \sin(W_s - 60)$$

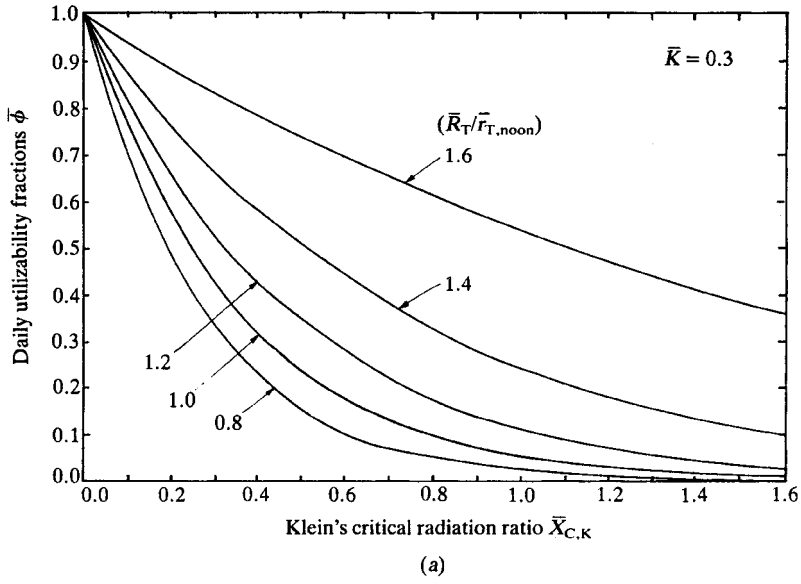


(a)

**FIGURE 6.4.13** Generalized daily utilizability curves of Theilacker and Klein (1980) for three different $K$ values.

where $W$ is the hour angle corresponding to the midpoint of the hour (in degrees) and $W_S$ is the sunset hour angle given by

$$\cos W_S = -\tan L \tan \delta \tag{6.4.23}$$

The fraction $r$ is the ratio of hourly to daily global radiation on a horizontal surface. The factors $\bar{r}_{T,noon}$ and $\bar{r}_{noon}$ can be determined from Eqs. (6.4.17) and (6.4.22) respectively with $W = 0°$.

The Theilacker and Klein correlation for the daily utilizability for equator-facing flat-plate collectors is

$$\bar{\phi}\left(X_{C,K}\right) = \exp\left\{\left[a' + b'\left(\bar{r}_{T,noon}/\bar{R}_T\right)\right]\left[X_{C,K} + c' \; X_{C,K}^2\right]\right\} \tag{6.4.24}$$

where

$$a' = 7.476 - 20.0 \; \bar{K} + 11.188 \; \bar{K}^2 \tag{6.4.25}$$

$$b' = -8.562 + 18.679 \; \bar{K} - 9.948 \; \bar{K}^2$$

$$c' = -0.722 + 2.426 \; \bar{K} + 0.439 \; \bar{K}^2$$

How $\bar{\phi}$ varies with the critical radiation ratio $\bar{X}_{C,K}$ for three different values of $\bar{K}$ is shown in Figure 6.4.13.

***Annual Time Scales***

Generalized expressions for the *yearly* average energy delivered by the principal collector types with constant radiation threshold (i.e., when the fluid inlet temperature is constant for all hours during the day over the entire year) have been developed by Rabl (1981) based on data from several U.S. locations. The correlations are basically quadratic of the form

$$\frac{Q_{CY}}{A_C F_R \eta_n} = \tilde{a} + \tilde{b} I_C + \tilde{c} I_C^2 \tag{6.4.26}$$

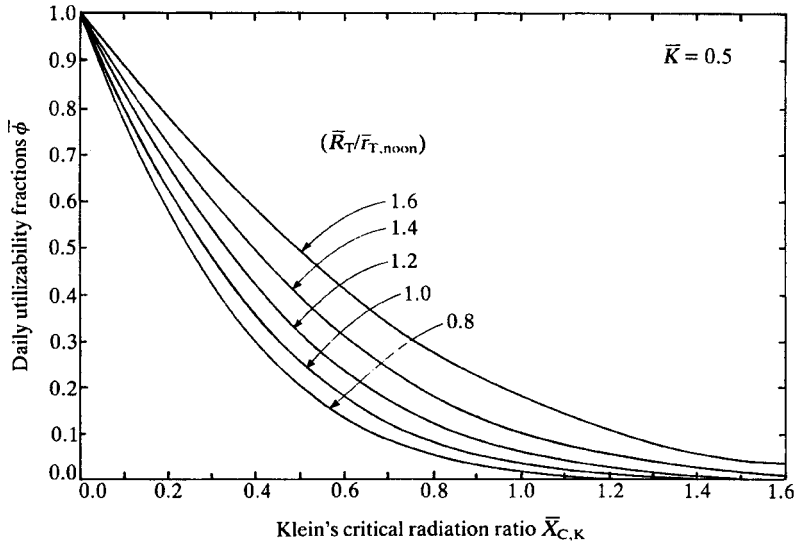


(*b*)

**FIGURE 6.4.13(b)**

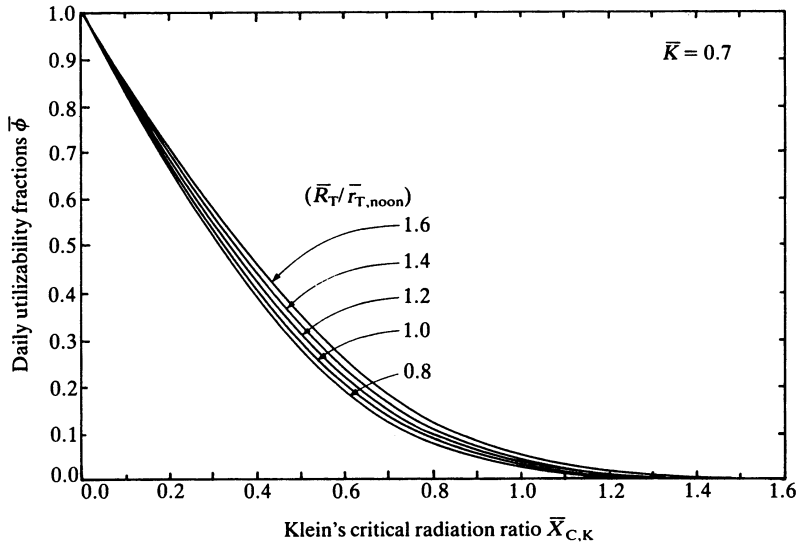


(*c*)

**FIGURE 6.4.13(c)**

where the coefficients $\tilde{a}$, $\tilde{b}$, and $\tilde{c}$ are function of collector type and/or tracking mode, climate, and in some cases, latitude. The complete expressions as revised by Gordon and Rabl (1982) are given in Reddy (1987). Note that the yearly *daytime* average value of $T_a$ should be used to determine $I_C$. If this is not available, the yearly mean *daily* average value can be used. Plots of $Q_{CY}$ versus $I_C$ for flat-plate collectors that face the equator with tilt equal to the latitude are shown in Figure 6.4.14. The solar radiation enters these expressions as $\tilde{I}_{bn}$, the annual average beam radiation at normal incidence. This can be estimated from the following correlation

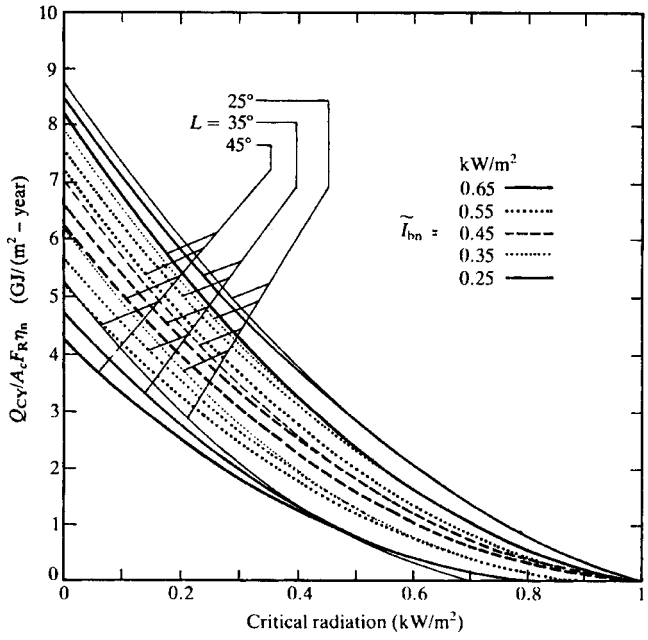


**FIGURE 6.4.14** Yearly total energy delivered by flat-plate collectors with tilt equal to latitude. (From Gordon, J.M. and Rabl, A., Design, analysis, and optimization of solar industrial process heat plants without storage, *Solar Energy*, 28, 519, 1982. With permission.)

$$\tilde{I}_{bn} = 1.37\ \tilde{K} - 0.34 \tag{6.4.27}$$

where $\tilde{I}_{bn}$ is in kW/m² and $\tilde{K}$ is the annual average clearness index of the location. Values of $\tilde{K}$ for several locations worldwide are given in Reddy (1987).

This correlation is strictly valid for latitudes ranging from 25° to 48°. If used for lower latitudes, the correlation is said to lead to overprediction. Hence, it is recommended that for such lower latitudes a value of 25° should be used to compute $Q_{CY}$.

A direct comparison of the yearly performance of different collector types is given in Figure 6.4.15 (from Rabl, 1981). A latitude of 35°N is assumed and plots of $Q_{cy}$ vs. $(T_{ci} - T_a)$ have been generated in a sunny climate with $\tilde{I}_{bn}$ = 0.6 kW/m². Relevant collector performance data are given in Figure 6.4.15. The cross-over point between flat-plate and concentrating collectors is approximately 25°C above ambient temperature whether the climate is sunny or cloudy.

## 6.4.3 Solar Systems

### Classification

Solar thermal systems used for HVAC can be divided into two categories: standalone or solar supplemented. They can be further classified by means of energy collection as active or passive, and by the type of storage they use into seasonal or daily systems.

#### *Standalone and Solar Supplemented Systems*

*Standalone systems* are systems in which solar energy is the only source of energy input used to meet the required load. Such systems are normally designed for applications where a certain amount of tolerance is permissible concerning the load requirement; in other words, where it is not absolutely imperative that the specified load be met each and every instant. This leniency is generally admissible in the case of certain residential and agricultural applications. The primary reasons for using such systems are their low cost and simplicity of operation.

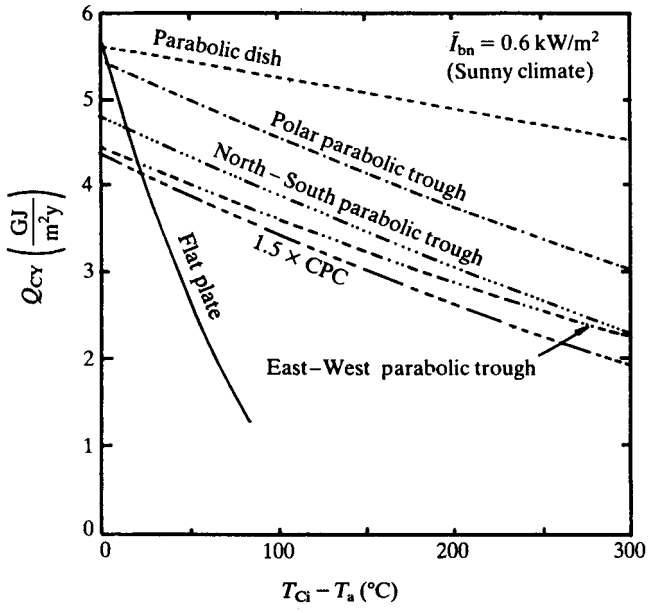


**FIGURE 6.4.15** Figure illustrating the comparative performance (yearly collectible energy) of different collector types as a function of the difference between collector inlet temperature and ambient collector performance parameters $F'\eta_0$ and $F'U_L$ in W/(m² °C) are: flat plate (0.70 and 5.0), CPC (0.60 and 0.75), parabolic trough (0.65 and 0.67), and parabolic dish (0.61 and 0.27). (From Rabl, A., Yearly average performace of the principal solar collector types, *Solar Energy*, 27, 215, 1981. With permission.)

*Solar-supplemented systems*, widely used for both industrial and residential purposes, are those in which solar energy supplies part of the required heat load, the rest being met by an auxiliary source of heat input. Due to the daily variations in incident solar radiation, the portion of the required heat load supplied by the solar energy system may vary from day to day. However, the auxiliary source is so designed that at any instant it is capable of meeting the remainder of the required heat load. It is normal practice to incorporate an auxiliary heat source large enough to supply the entire heat load required. Thus, the benefit in the solar subsystem is not in its capacity credit (i.e., not that a smaller capacity conventional system can be used), but rather that a part of the conventional fuel consumption is displaced. The solar subsystem thus acts as a fuel economizer.

Solar-supplemented energy systems will be the primary focus of this chapter. Designing such systems has acquired a certain firm scientific rationale, and the underlying methodologies have reached a certain maturity and diversity, which may satisfy professionals from allied fields. On the other hand, unitary solar apparatus are not discussed here, since these are designed and sized based on local requirements, material availability, construction practices and practical experience. Simple rules of thumb based on prior experimentation are usually resorted to for designing such systems.

### *Active and Passive Systems*

*Active systems* are those systems that need electric pumps or blowers to collect solar energy. It is evident that the amount of solar energy collected should be more than the electrical energy used. Active systems are invariably used for industrial applications and for most domestic and commercial applications as well. *Passive systems* are those systems that collect or use solar energy without direct recourse to any source of conventional power, such as electricity, to aid in the collection. Thus, either such systems operate by natural thermosyphon (for example domestic water heating systems) between collector, storage, and load or, in the case of space heating, the architecture of the building is such as to favor optimal use of solar energy. Use of a passive system for space heating applications, however, in no way precludes the use of a back-up auxiliary system. This chapter deals with active solar systems.

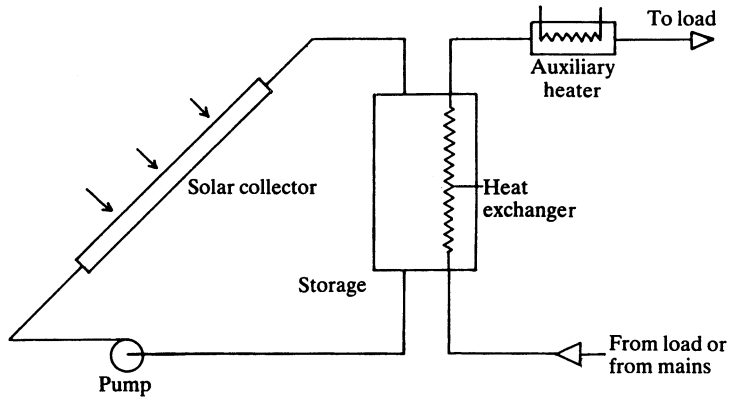


**FIGURE 6.4.16** Schematic of a closed-loop solar system.

### *Daily and Seasonal Storage*

By *daily storage* is meant systems having capacities equivalent to at most a few days of demand (i.e., just enough to tide over day-to-day climatic fluctuations). In *seasonal storage*, solar energy is stored during the summer for use in winter. The present-day economics of seasonal storage units do not usually make such systems an economical proposition except for community heating in cold climates.

## Closed-Loop and Open-Loop Systems

The two possible configurations of solar thermal systems with daily storage are classified as closed-loop or open-loop systems. Though different authors define these differently, we shall define these as follows. A *closed-loop system* has been defined as a circuit in which the performance of the solar collector is directly dependent on the storage temperature. Figure 6.4.16 gives a schematic of a closed-loop system in which the fluid circulating in the collectors does not mix with the fluid supplying thermal energy to the load. Thus, these two subsystems are distinct in the sense that any combination of fluids (water or air) is theoretically feasible (a heat exchanger, as shown in the figure, is of course imperative when the fluids are different). However, in practice, only water–water or water–air combinations are used. From the point of system performance, the storage temperature normally varies over the day and, consequently, so does collector performance. Closed-loop system configurations have been widely used to date for domestic hot water and space heating applications. The flow rate per unit collector area is generally around 50 kg/(h $m^2$) for liquid collectors. The storage volume makes about 5 to 10 passes through the collector during a typical sunny day, and this is why such systems are called *multipass* systems. The temperature rise for each pass is small, of the order of 2 to 5°C for systems with circulating pumps and about 10°C for thermosyphon systems. An expansion tank and a check valve to prevent reverse thermosyphoning at nights, although not shown in the figure, are essential for such system configurations.

Figure 6.4.17 illustrates one of the possible configurations of *open-loop or single-pass systems*. Open-loop systems are defined as systems in which the collector performance is independent of the storage temperature. The working fluid may be rejected (or a heat recuperator can be used) if contaminants are picked up during its passage through the load. Alternatively, the working fluid could be directly recalculated back to the entrance of the solar collector field. In all these open-loop configurations, the collector is subject to a given or known inlet temperature specified by the load requirements.

If the working fluid is water, instead of having a continuous flow rate (in which case the outlet temperature of the water will vary with insolation), a control valve can be placed just at the exit of the collector, set so as to open when the desired temperature level of the fluid in the collector is reached. The water is then discharged into storage, and fresh water is taken into the collector. The solar collector will thus operate in a discontinuous manner, but this will ensure that the temperature in the storage is always at the desired level. An alternative way of ensuring uniform collector outlet temperature is to vary

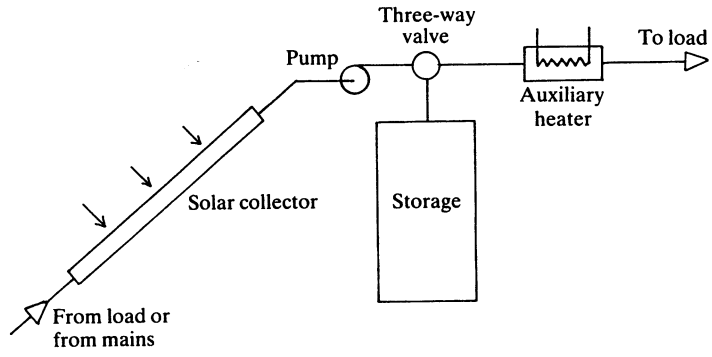


**FIGURE 6.4.17** Schematic of an open-loop solar system.

the flow rate according to the incident radiation. One can collect a couple of percent more energy than with constant rate single-pass designs (Gordon and Zarmi, 1985). However, this entails changing the flow rate of the pump more or less continuously. Of all the three variants of the open-loop configuration, the first one, namely the single-pass open-loop solar thermal system configuration with constant flow rate and without a solenoid valve, is the most common. The single-pass design is not recommended for *variable* loads. The tank size is based on yearly daily load volumes, and efficient use of storage requires near-total depletion of the daily collected energy each day. If the load draw is markedly lower than its average value, the storage would get full relatively early the next day and solar collection would cease. It is because industrial loads tend to be more uniform, both during the day and over the year, than domestic applications that the single-pass open-loop configuration is recommended for such applications.

## Description of a Typical Closed-Loop System

Figure 6.4.18 illustrates a typical closed-loop solar-supplemented liquid heating system. The useful energy is often (but not always) delivered to the storage tank via a collector–heat exchanger, which separates the collector fluid stream and the storage fluid. Such an arrangement is necessary either for antifreeze protection or to avoid corrosion of the collectors by untreated water containing gases and salts. A safety relief valve is provided because the system piping is normally nonpressurized, and any steam produced in the solar collectors will be let off from this valve. When this happens, energy dumping is said to take place. Fluid from storage is withdrawn and made to flow through the load–heat exchanger when the load calls for heat. Whenever possible, one should withdraw fluid directly from the storage and pass it through the load, and avoid incorporating the load–heat exchanger, since it introduces additional thermal penalties and involves extra equipment and additional parasitic power use. Heat is withdrawn from the storage tank at the top and reinjected at the bottom in order to derive maximum benefit from the thermal stratification that occurs in the storage tank. A bypass circuit is incorporated prior to the load heat exchanger and comes into play

1. When there is no heat in the storage tank (i.e., storage temperature $T_S$ is less than the fluid temperature entering the load heat exchanger $T_{Xi}$)
2. When $T_S$ is such that the temperature of the fluid leaving the load heat exchanger is greater than that required by the load (i.e., $T_{Xo} > T_{Li}$, in which case the three-way valve bypasses part of the flow so that $T_{Xo} = T_{Li}$). The bypass arrangement is thus a differential control device which is said to modulate the flow such that the above condition is met. Another operational strategy for maintaining $T_{Xo} = T_{Li}$ is to operate pump in a "bang-bang" fashion (i.e., by short cycling the pump). Such an operation is not advisable, however, since it would lead to premature pump failure.

An auxiliary heater of the *topping-up type* supplies just enough heat to raise $T_{Xo}$ to $T_{Li}$. After passing through the load, the fluid (which can be either water or air) can be recirculated or, in case of liquid contamination through the load, fresh liquid can be introduced. The auxiliary heater can also be placed

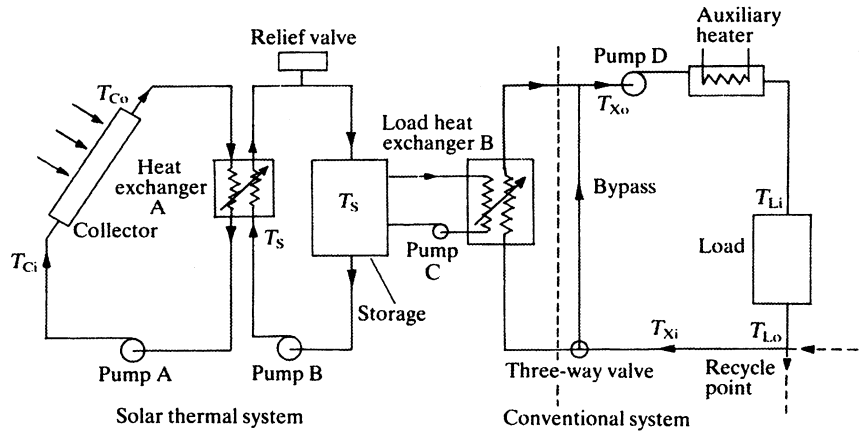


**FIGURE 6.4.18** Schematic of a typical closed-loop system with auxiliary heater placed in series (also referred to as a topping-up type).

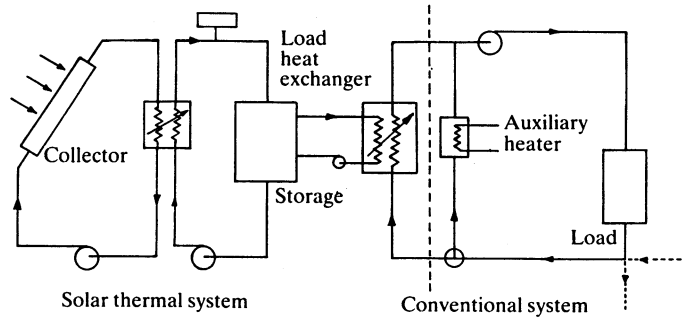


**FIGURE 6.4.19** Schematic of a typical closed-loop system with auxiliary heater placed in parallel (also referred to as an all-or-nothing type).

in parallel with the load (see Figure 6.4.19) in which case it is called an *all-or-nothing type*. Although such an arrangement is thermally less efficient than the topping-up type, this type is widely used during the solar retrofit of heating systems because it involves little mechanical modifications or alterations to the auxiliary heater itself.

It is obvious that there could also be solar-supplemented energy systems that do not include a storage element in the system. Figure 6.4.20 shows such a system configuration with the auxiliary heater installed in series. The operation of such systems is not very different from that of systems with storage, the primary difference being that whenever instantaneous solar energy collection exceeds load requirements (i.e., $T_{Co} > T_{Li}$), energy dumping takes place. It is obvious that by definition there cannot be a closed-loop, no-storage solar thermal system. Solar thermal systems without storage are easier to construct and operate, and even though they may be effective for 8 to 10 hours a day, they are appropriate for applications such as process heat in industry.

Active closed-loop solar systems as described earlier are widely used for service hot water systems, that is for domestic hot water and process heat applications as well as for space heat. There are different variants to this generic configuration. A system without the collector–heat exchanger is referred to having collectors *directly coupled* to the storage tank (as against *indirect coupling* as in Figure 6.4.16). For domestic hot water systems, the system can be simplified by placing the auxiliary heater (which is simply an electric heater) directly inside the storage tank. One would like to maintain stratification in the tank so that the coolest fluid is at the bottom of the storage tank, thereby enhancing collection efficiency. Consequently, the electric heater is placed at about the upper third portion of the tank so as to assure good collection

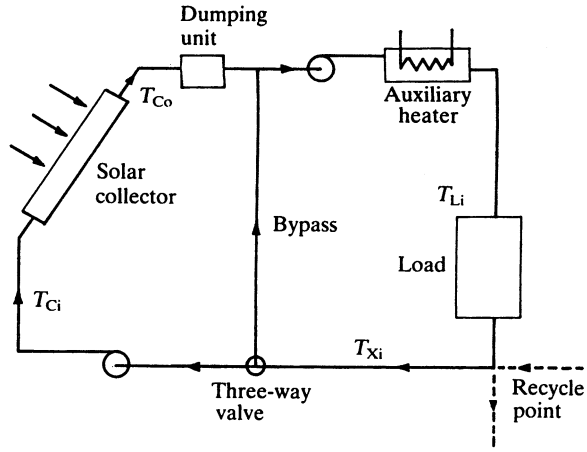


**FIGURE 6.4.20** Simple solar thermal system without storage.

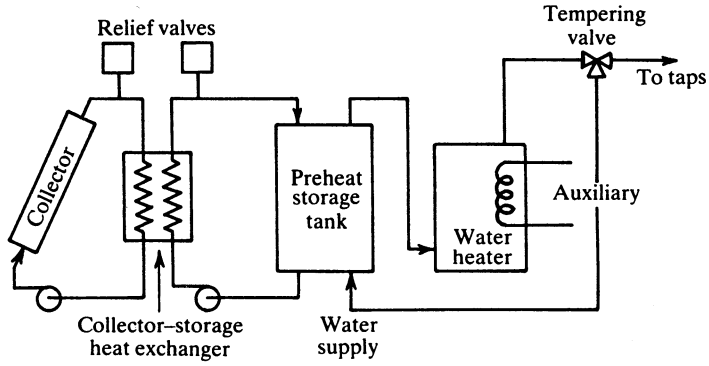


**FIGURE 6.4.21** Schematic of a standard domestic hot-water system with double tank arrangement.

efficiency while assuring adequate hot water supply to the load. A more efficient but expensive option is widely used in the United States: the *double tank system*, shown in Figure 6.4.21. Here the functions of solar storage and auxiliary heating are separated, with the solar tank acting as a preheater for the conventional gas or electric unit. Note that a further system simplification can be achieved for domestic applications by placing the load heat exchanger directly inside the storage tank. In certain cases, one can even eliminate the heat exchanger completely.

Another system configuration is the *drain-back* (also called drain-out) system, where the collectors are emptied each time the solar system shuts off. Thus the system invariably loses collector fluid at least once, and often several times, each day. No collector–heat exchanger is needed, and freeze protection is inherent in such a configuration. However, careful piping design and installation, as well as a two-speed pump, are needed for the system to work properly (Newton and Gilman, 1977). The drain-back configuration may be either open (vented to atmosphere) or closed (for better corrosion protection). Long-term experience in the United States with the drain-back system has shown it to be very reliable if engineered properly. A third type of system configuration is the *drain-down* system, where the fluid from the collector array is removed only when adverse conditions, such as freezing or boiling, occur. This design is used when freezing ambient temperatures are only infrequently encountered.

Active solar systems of the type described above are mostly used in countries such as the United States and Canada. Countries such as Australia, India, and Israel (where freezing is rare) usually prefer thermosyphon systems. No circulating pump is needed, the fluid circulation being driven by density

difference between the cooler water in the inlet pipe and the storage tank and the hotter water in the outlet pipe of the collector and the storage tank. The low fluid flow in thermosyphon systems enhances thermal stratification in the storage tank. The system is usually fail-proof, and a study by Liu and Fanney (1980) reported that a thermosyphon system performed better than several pumped service hot water systems. If operated properly, thermosyphon and active solar systems are comparable in their thermal performance. A major constraint in installing thermosyphon systems in already existing residences is the requirement that the bottom of the storage tank be at least 20 cm higher than the top of the solar collector in order to avoid reverse thermosyphoning at night. To overcome this, spring-loaded one-way valves have been used, but with mixed success.

## Thermal Storage Systems

Low-temperature solar thermal energy can be stored in liquids, solids, or phase change materials (PCMs). Water is the most frequently used liquid storage medium because of its low cost and high specific heat. The most widely used solid storage medium is rocks (usually of uniform circular size 25 to 40 mm in diameter). PCM storage is much less bulky because of the high latent heat of the PCM material, but this technology has yet to become economical and safe for widespread use.

Water storage would be the obvious choice when liquid collectors are used to supply hot water to a load. When hot air is required (for space heat or for convective drying), one has two options: an air collector with a pebble-bed storage or a system with liquid collectors, water storage, and a load heat exchanger to transfer heat from the hot water to the working air stream. Though a number of solar air systems have been designed and operated successfully (mainly for space heating), water storage is very often the medium selected. Water has twice the heat capacity of rock, so water storage tanks will be smaller than rock-bed containers. Moreover, rock storage systems require higher parasitic energy to operate, have higher installation costs and require more sophisticated controls. Water storage permits simultaneous charging and discharging while such an operation is not possible for rock storage systems. The various types of materials used as containers for water and rock-bed storage and the types of design, installation, and operation details one needs to take care of in such storage systems are described by Mueller Associates (1985) and SERI (1989).

Sensible storage systems, whether water or rock-bed, exhibit a certain amount of thermal stratification. Standard textbooks present relevant equations to model such effects. In the case of active closed-loop multipass hot water systems, storage stratification effects can be neglected for long-term system performance with little loss of accuracy. Moreover, this leads to conservative system design (i.e., solar contribution is underpredicted if stratification is neglected). A designer who wishes to account for the effect of stratification in the water storage can resort to a formulation by Phillips and Dave (1982), who showed that this effect can be fairly well modeled by introducing a *stratification coefficient* (which is a system constant that needs to be determined only once) and treating the storage subsystem as fully mixed. However, this approach is limited to the specific case of no (or very little) heat withdrawal from storage during the collection period. Even when water storage systems are highly stratified, simulation studies seem to indicate that modeling storage as a one-dimensional plug-flow three-node heat transfer problem yields satisfactory results of long-term solar system performance.

The thermal losses $q_w$ from the storage tank can be modeled as

$$q_w = \left(UA_S\right)\left(T_S - T_{\text{env}}\right) \tag{6.4.28}$$

where $(UA_S)$ is the storage overall heat loss per unit temperature difference and $T_{\text{env}}$ is the temperature of the air surrounding the storage tank. Note that $(UA_S)$ depends on the storage size, which is a parameter to be sized during system design, and on the configuration of the storage tank (i.e., on the length by diameter ratio in case of a cylindrical tank). For storage tanks, this ratio is normally in the range of 1.0 to 2.0.

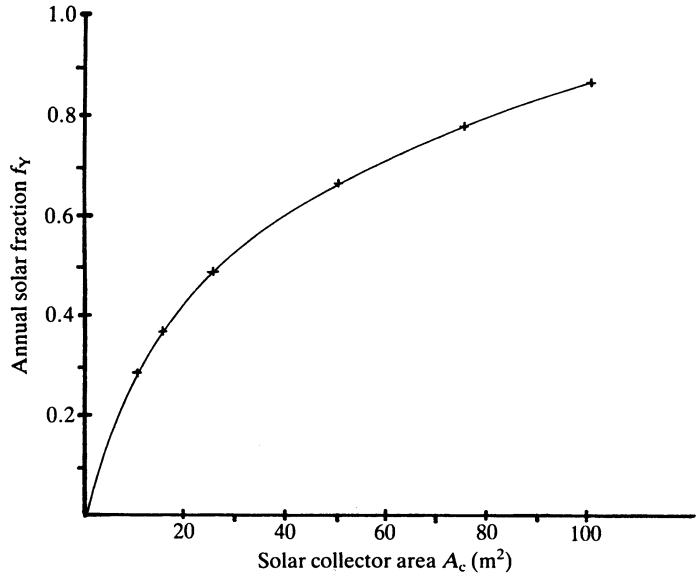


**FIGURE 6.4.22** A typical solar system production function.

## 6.4.4 Solar System Sizing Methodology

Sizing of solar systems primarily involves determining the collector area and storage size that are most cost effective. We shall address standalone and solar-supplemented systems separately since the basic design problem is somewhat different.

### Solar-Supplemented Systems

***Production Functions***

Because of the annual variation of incident solar radiation, it is not normally economical to size a solar subsystem such that it provides 100% of the heat demand. Most solar energy systems follow the *law of diminishing returns*. This implies that increasing the size of the solar collector subsystem results in a less than proportional increase in the annual fuel savings (or alternatively, in the annual solar fraction).

Any model has two types of variables: exogenous and endogenous. The *exogenous parameters* are also called the input variables, and these in turn may be of two kinds. *Variable* exogenous parameters are the collector area $A_C$, the collector performance parameters $F_R\eta_n$ and $F_RU_L$, the collector tilt, the thermal storage capacity $(Mc_p)_S$, the heat exchanger size, and the control strategies of the solar thermal system. On the other hand, the climatic data specified by radiation and the ambient temperature, as well as the end-use thermal demand characteristics, are called *constrained* exogenous parameters because they are imposed externally and cannot be changed. The *endogenous* parameters are the output parameters whose values are to be determined, the annual solar fraction being one of the parameters most often sought.

Figure 6.4.22 illustrates the law of diminishing results. The annual solar fraction $f_Y$ is seen to increase with collector area but at a decreasing rate and at a certain point will reach saturation. Variation of any of the other exogenous parameters also exhibit a similar trend. The technical relationship between $f_Y$ and one or several variable exogenous parameters for a given location is called the *yearly production function*.

It is only for certain simple types of solar thermal systems that an analytical expression for the production can be deduced directly from theoretical considerations. The most common approach is to carry out computer simulations of the particular system (solar plus auxiliary) over the complete year for several combinations of values of the exogenous parameters. The production function can subsequently be determined by an empirical curve fit to these discrete sets of points.

***Economic Analysis***

It is widely recognized that *discounted cash flow analysis* is most appropriate for applications such as sizing an energy system. This analysis takes into account both the initial cost incurred during the installation of the system and the annual running costs over its entire life span.

The economic objective function for optimal system selection can be expressed in terms of either the energy cost incurred or the energy savings. These two approaches are basically similar and differ in the sense that the objective function of the former has to be minimized while that of the latter has to be maximized. In our analysis, we shall consider the latter approach, which can further be subdivided into the following two methods:

1. Present worth or life cycle savings, wherein all running costs are discounted to the beginning of the first year of operation of the system
2. Annualized life cycle savings, wherein the initial expenditure incurred at the start as well as the running costs over the life of the installation are expressed as a yearly mean value.

Chapter 3.2 described the details. The optimization methods for Chapter 3.2 (see Figure 3.2.6) must be used. The HVAC designer must complete such a calculation for solar sizing since solar systems do not meet peak loads unlike fossil fuel based systems.

## 6.4.5 Solar System Design Methods

### Classification

Design methods may be separated into three generic classes. The *simple* category, usually associated with the prefeasibility study phase (see the introduction) involves quick manual calculations of solar collector/system performance and rule-of-thumb engineering estimates. For example, the generalized yearly correlations proposed by Rabl (1981) and described in Section 6.4.2 could be conveniently used for year-round, more or less constant loads. The approach is directly valid for open-loop solar systems, while it could also be used for closed-loop systems if an *average* collector inlet temperature could be determined. A simple manner of selecting this temperature $\overline{T}_{\mathrm{m}}$ for domestic closed-loop multipass systems is to assume the following empirical relation:

$$\overline{T}_m = T_{\mathrm{mains}}/3 + \left(2/3\right) T_{\mathrm{set}} \tag{6.4.29}$$

where $T_{\mathrm{mains}}$ is the average annual supply temperature and $T_{\mathrm{set}}$ is the required hot water temperature (about 60 to 80°C in most cases).

These manual methods often use general guidelines, graphs, and/or tables for sizing and performance evaluation. The designer should have a certain amount of knowledge and experience in solar system design in order to make pertinent assumptions and simplifications regarding the operation of the particular system.

*Mid-level* design methods are resorted to during the feasibility phase of a project. The main focus of this chapter has been toward this level, and a few of these design methods will be presented in this section. A personal computer is best suited to these design methods because they could be conveniently programmed to suit the designer's tastes and purpose (spreadsheet programs, or better still one of the numerous equation-solver software packages, are most convenient). Alternatively, commercially available software packages such as f-chart (Beckman et al., 1977) could also be used for certain specific system configurations.

*Detailed* design methods involve performing hourly simulations of the solar system over the entire year from which accurate optimization of solar collector and other equipment can be performed. Several simulation programs for active solar energy systems are available, TRNSYS (Klein et al., 1975, 1979) developed at the University of Wisconsin—Madison being perhaps the best known. This public-domain software has technical support and is being constantly upgraded. TRNSYS contains simulation models

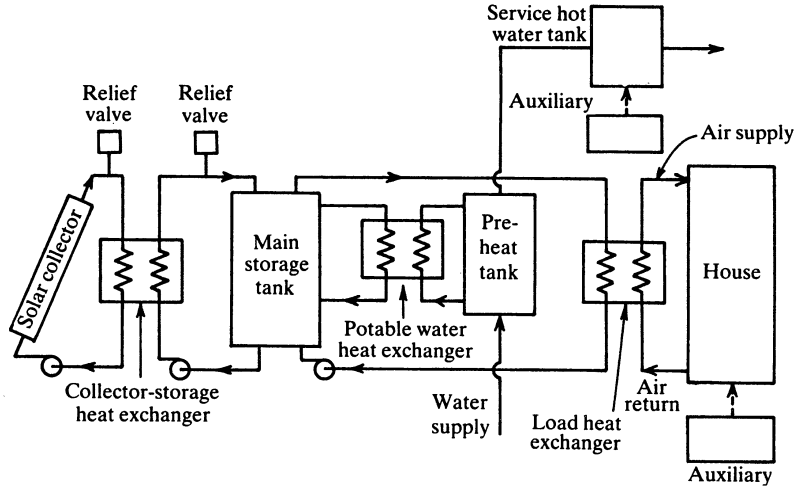


**FIGURE 6.4.23** Schematic of the standard space heating liquid system configuration for the f-chart method. (From Duffie, J.A. and Beckman, W.A., *Solar Engineering of Thermal Processes*, Wiley Interscience, New York. Copyright 1980. Reprinted with permission of John Wiley & Sons, Inc.).

of numerous subsystem components (solar radiation, solar equipment, loads, mechanical equipment, controls, etc.) that comprise a solar energy system. A user can conveniently hook up components representative of a particular solar system to be analyzed and then simulate that system's performance at a level of detail that the user selects. Thus TRNSYS provides the design with large flexibility, diversity and convenience of usage.

As pointed out by Rabl (1985), the detailed computer simulations approach, though a valuable tool, has several problems. Judgment is needed both in the selection of the input and in the evaluation of the output. The very flexibility of big simulation programs has drawbacks. So many variables must be specified by the user that errors in interpretation or specification are common. Also, learning how to use the program is a time-consuming task. Because of the numerous system variables to be optimized, the program may have to be run for numerous sets of combinations, which adds to expense and time. The inexperienced user can be easily misled by the second-order details while missing first-order effects. For example, uncertainties in load, solar radiation, and economic variables are usually very large, and long-term performance simulation results are only accurate to within a certain degree. Nevertheless, detailed simulation programs, if properly used by experienced designers, can provide valuable information on system design and optimization aspects at the final stages of a project design.

There are basically three types of mid-level design approaches: the empirical correlation approach, the analytical approach, and the one-day repetitive methods approach (described fully in Reddy, 1987). We shall illustrate their use by means of specific applications.

## Active Space Heating

The solar system configuration for this particular application has become more or less standardized. For example, for a liquid system, one would use the system shown in Figure 6.4.23. One of the most widely used design methods is the f-chart method (Beckman et al., 1977; Duffie and Beckman, 1980), which is applicable for standardized liquid and air heating systems as well as for standardized domestic hot water systems. The f-chart method basically involves using a simple algebraic correlation that has been deduced from numerous TRNSYS simulation runs of these standard solar systems subject to a wide range of climates and solar system parameters. Correlations were developed between monthly solar fractions and two easily calculated dimensionless variables $X$ and $Y$, where

$$X = \left(A_C \; F_R' \, U_L \left(T_{\text{Ref}} - \overline{T}_a\right)\Delta t\right) \Big/ Q_{LM} \tag{6.4.30}$$

$$Y = A_C F_R' \overline{\eta}_0 \overline{H}_T N / Q_{LM} \tag{6.4.31}$$

where $A_C$ = collector area ($m^2$)
$F_R'$ = collector-heat exchanger heat removal factor
$U_L$ = collector overall loss coefficient (W/($m^2$ °C)
$\Delta t$ = total number of seconds in the month = $3{,}600 \times 24 \times N = 86{,}400 \times N$
$\overline{T}_a$ = monthly average ambient temperature (°C)
$T_{Ref}$ = an empirically derived reference temperature, taken as 100°C
$Q_{LM}$ = monthly total heating load for space heating and/or hot water (J)
$\overline{H}_T$ = monthly average daily radiation incident on the collector surface per unit area ($J/m^2$)
$N$ = number of days in the month
$\overline{\eta}_0$ = monthly average collector optical efficiency

The dimensionless variable $X$ is the ratio of reference collector losses over the entire month to the monthly total heat load; the variable $Y$ is the ratio of the monthly total solar energy absorbed by the collectors to the monthly total heat load. It will be noted that the collector area and its performance parameters are the predominant exogenous variables that appear in these expressions. For changes in secondary exogenous parameters, the following corrective terms $X_C$ and $Y_C$ should be applied for liquid systems:

1. for changes in storage capacity:

$$X_C / X = \left(\text{actual storage capacity} / \text{standard storage capacity}\right)^{-0.25} \tag{6.4.32}$$

   where the standard storage volume is 75 $L/m^2$ of collector area.

2. for changes in heat exchanger:

$$Y_C / Y = 0.39 + 0.65 \ \exp\left[-\left(0.139 \ (UA)_B \Big/ \left(E_L \left(mc_p\right)_{\min}\right)\right)\right] \tag{6.4.33}$$

The monthly solar fraction for liquid space heating can then be determined from the following empirical correlation:

$$f_M = 1.029\,Y - 0.065\,X - 0.245\,Y^2 + 0.0018\,X^2 + 0.0215\,Y^3 \tag{6.4.34}$$

subject to the conditions that $0 \le X \le 15$ and $0 \le Y \le 3$. This empirical correlation is shown graphically in Figure 6.4.24.

A similar correlation has also been proposed for space heating systems using air collectors and pebble-bed storage. The procedure for exploiting the preceding empirical correlations is as follows. For a predetermined location, specified by its 12 monthly radiation and ambient temperature values, Eq. (6.4.34) is repeatedly used for each month of the year for a particular set of variable exogenous parameters. The monthly solar fraction $f_M$ and the annual thermal energy delivered by the solar thermal system are easily deduced. Subsequently, the entire procedure is repeated for different values and combinations of variable exogenous parameters. Finally, an economic analysis is performed to determine optimal sizes of various solar system components. Care must be exercised that the exogenous parameters considered are not outside the range of validity of the f-chart empirical correlations.

### Domestic Water Heating

The f-chart correlation can also be used to predict the monthly solar fraction for domestic hot water systems provided the water mains temperature $T_{mains}$ is between 5 and 20°C and the minimum acceptable

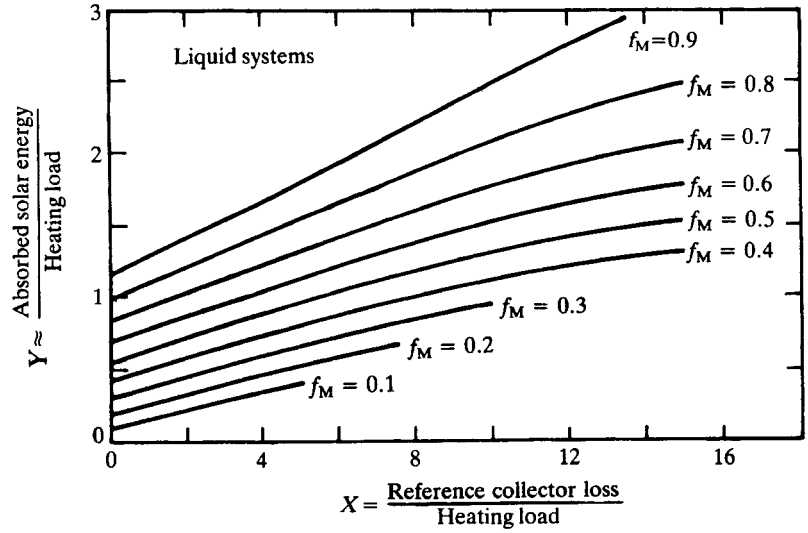


**FIGURE 6.4.24** The f-chart correlation for liquid system configuration. (From Duffie, J.A. and Beckman, W.A., *Solar Engineering of Thermal Processes*, Wiley Interscience, New York. Copyright 1980. Reprinted with permission of John Wiley & Sons, Inc.)

hot water temperature drawn from the storage for end use (called the set water temperature $T_w$) is between 50 and 70°C. Further, the dimensionless parameter $X$ must be corrected by the following ratio

$$X_w / X = \left(11.6 + 1.8\,T_w + 3.86\,T_{\text{mains}} - 2.32\,\overline{T}_a\right) \Big/ \left(100 - \overline{T}_a\right) \tag{6.4.35}$$

In case the domestic hot water load is much smaller than the space heat load, it is recommended that Eq. (6.4.34) be used without the above correction.

## Industrial Process Heat

### *Open-Loop Single-Pass Systems*

The advantages offered by open-loop single-pass systems over closed-loop multipass systems for meeting constant loads has been described in Section 6.4.3 under "Closed-Loop and Open-Loop Systems." Because industrial loads operate during the entire sun-up hours or even for 24 hours daily, the simplest solar thermal system is one with no heat storage. A sizable portion (between 25 and 70%) of the daytime thermal load can be supplied by such systems and consequently, the sizing of such systems will be described below (Gordon and Rabl, 1982). We shall assume that $T_{\text{Li}}$ and $T_{\text{Xi}}$ are constant for all hours during system operation. Because no storage is provided, excess solar energy collection (whenever $T_{\text{Ci}} > T_{\text{Li}}$) will have to be dumped out.

The maximum collector area $\hat{A}_C$ for which energy dumping does not occur at any time of the year can be found from the following instantaneous heat balance equation:

$$P_L = \hat{A}_C\,\hat{F}_R\left[I_{\max}\,\eta_n - U_L\left(T_{Ci} - T_a\right)\right] \tag{6.4.36}$$

where $P_L$ the instantaneous thermal heat demand of the load (say, in kW) is given by

$$P_L = m_L\,c_p\left(T_{Li} - T_{Xi}\right) \tag{6.4.37}$$

and $F_R$ is the heat removal factor of the collector field when its surface area is $\hat{A}_C$. Since $\hat{A}_C$ is as yet unknown, the value of $\hat{F}_R$ is also undetermined. (Note that though the *total* fluid flow rate is known, the flow rate per unit collector area is not known.) Recall that the plate efficiency factor $F'$ for liquid collectors

can be assumed constant and independent of fluid flow rate per unit collector area. Equation (6.4.36) can be expressed in terms of critical radiation level $I_C$:

$$P_L = \hat{A}_C \hat{F}_R \eta_n \left(I_{\max} - I_C\right) \tag{6.4.38}$$

or

$$\hat{A}_C \hat{F}_R \eta_n = P_L \Big/ \left(I_{\max} - I_C\right) \tag{6.4.39}$$

Substituting for $F_R$ and rearranging yields

$$\hat{A}_C = -\left(m_L c_p \Big/ F' U_L\right) \ln\left[1 - P_L U_L \Big/ \eta_n \left(I_{\max} - I_C\right) m_L c_p\right] \tag{6.4.40}$$

If the actual collector area $A_C$ exceeds this value, dumping will occur as soon as the radiation intensity reaches a value $I_D$, whose value is determined from the following heat balance:

$$P_L = A_C F_R \eta_n \left(I_D - I_C\right) \tag{6.4.41}$$

Hence

$$I_D = I_C + P_L \Big/ \left(A_C F_R \eta_n\right) \tag{6.4.42}$$

Note that the value of $I_D$ decreases with increasing collector area $A_C$, thereby indicating that increasing amounts of solar energy will have to be dumped out.

Since the solar thermal system is operational during the entire sunshine hours of the year, the yearly total energy collected can be directly determined by the Rabl correlation given by Eq. (6.4.26). Similarly, the yearly total solar energy collected by the solar system which has got to be dumped out is

$$Q_{DY} = A_C F_R \eta_n \left(\tilde{a} + \tilde{b} I_D + \tilde{c} I_D^2\right) \tag{6.4.43}$$

The yearly total solar energy delivered to the load is

$$\begin{aligned} Q_{UY} &= Q_{CY} - Q_{DY} \\ &= A_C F_R \eta_n \left[\tilde{b} \cdot \left(I_C - I_D\right) + \tilde{c} \cdot \left(I_C^2 - I_D^2\right)\right] \end{aligned} \tag{6.4.44}$$

$$= -\left(\tilde{b} + 2\tilde{c} I_C\right) P_L - \tilde{c} P_L^2 \Big/ \left(A_C F_R \eta_n\right) \tag{6.4.45}$$

Replacing the value of $F_R$ given by Eq. (6.4.3), the annual production function in terms of $A_C$ is

$$Q_{UY} = -\left(\tilde{b} + 2\tilde{c} I_C\right) P_L - \frac{\tilde{c} P_L^2}{\left(\dfrac{F' \eta_n}{F' U_L}\right) \cdot \left(m_L c_p\right) \left[1 - \exp\left(-\dfrac{F' U_L A_C}{m_L c_p}\right)\right]} \tag{6.4.46}$$

subject to the condition that $A_C > \hat{A}_C$. If the thermal load is not needed during all days of the year due to holidays or maintenance shut-down, the production function can be reduced proportionally.

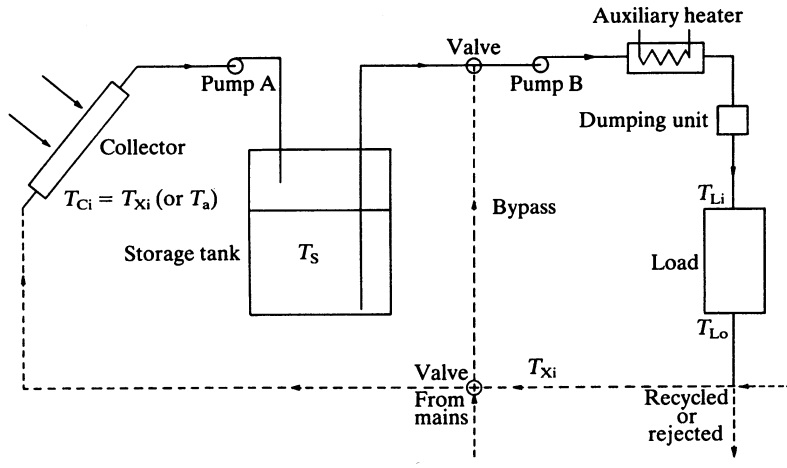


**FIGURE 6.4.25** Open-loop solar industrial hot-water system with storage.

**TABLE 6.4.3** Percentage of Total System Cost by Component

| Cost Component | Percentage Range |
|---|---|
| Collectors | 15–30 |
| Collector installation | 5–10 |
| Collector support structure | 5–20[a] |
| Storage tanks | 5–7 |
| Piping and specialties | 10–30 |
| Pumps | 1–3 |
| Heat exchangers | 0–5[b] |
| Chiller | 5–10 |
| Miscellaneous | 2–10 |
| Instrumentation | 1–3 |
| Insulation | 2–8 |
| Control subsystem | 4–9 |
| Electrical | 2–6 |

[a] For collectors mounted directly on a tilted roof.
[b] For systems without heat exchangers.
*Source:* From Mueller and Associates, 1985.

## 6.4.6 Design Recommendations and Costs

### Design Recommendations

Design methods reduce computational effort compared to detailed computer simulations. Even with this decrease, the problem of optimal system design and sizing remains formidable due to:

1. The presence of several solar thermal system configuration alternatives.
2. The determination of optimal component sizes for a given system.
3. The presence of certain technical and economic constraints.
4. The choice of proper climatic, technical and economic input parameters.
5. The need to perform sensitivity analysis of both technical and economic parameters.

For most practical design work, a judicious mix of theoretical expertise and practical acumen is essential. Proper focus right from the start on the important input variables as well as the restriction of the normal range of variation would lead to a great decrease in design time and effort.

Several examples of successful case studies and system design recommendations are described in the published literature (see, for example, Kutcher et al., 1982).

### Solar System Costs

How the individual components of the solar system contribute to the total cost can be gauged from Table 6.4.3. We note that collectors constitute the major fraction (from 15 to 30%), thus suggesting that collectors should be selected and sized with great care. Piping costs are next with other collector-related costs like installation and support structure being also important.

Costs vary by location. The HVAC designer should consult R.S. Means *Mechanical Cost Data* issued annually. Solar costs are in Division 13, "Period Construction," Section 13600.

## References


Anderson, B. (1977). *Solar Energy: Fundamentals in Building Design*, McGraw-Hill, New York.

ASHRAE Standard 93-77 (1978). *Methods of Testing to Determine the Thermal Performance of Solar Collectors*, American Society of Heating, Refrigeration and Air Conditioning Engineers, New York.

ASHRAE (1985). *Fundamentals*, American Society of Heating, Refrigeration and Air Conditioning Engineers, New York.

Beckman, W.A., Klein, S.A. and Duffie, J.A. (1977). *Solar Heating Design by the f-Chart Method*, Wiley Interscience, New York.

Charters, W.W.S. and Pryor, T.L. (1982). *An Introduction to the Installation of Solar Energy Systems*, Victoria Solar Energy Council, Melbourne, Australia.

Chiam, H.F. (1981). Planar concentrators for flat-plate solar collectors, *Solar Energy*, 26, p. 503.

Clark, D.R., Klein, S.A. and Beckman, W.A. (1983). Algorithm for evaluating the hourly radiation utilizability function. *ASME Journal of Solar Energy Eng.*, 105, p. 281.

Collares-Pereira, M. and Rabl, A. (1979). Derivation of method for predicting the long-term average energy delivery of solar collectors, *Solar Energy*, 23, p. 223.

Collares-Pereira, M., Gordon, J.M., Rabl, A. and Zarmi, Y. (1984). Design and optimization of solar industrial hot water systems with storage, *Solar Energy*, 32, p. 121.

Connelly, M., Giellis, R., Jenson, G. and McMorchie, R. (1976). Solar heating and cooling computer analysis—A simplified method for non-thermal specialists, Proc. of the Int. Solar Energy Society Conf., Winnipeg, Canada.

de Winter (1975). Heat exchanger penalties in double loop solar water heating systems, *Solar Energy*, 17, p. 335.

Duffie, J.A. and Beckman, W.A. (1980). *Solar Engineering of Thermal Processes*, Wiley Interscience, New York.

Edwards, D.K., Nelson, K.E., Roddick, R.D. and Gier, J.T. (1960). Basic Studies on the Use of Solar Energy, Report no. 60-93, Dept. of Engineering, Univ. of California at Los Angeles, CA.

Emery, M. and Rogers, B.A. (1984) On a solar collector thermal performance test method for use in variable conditions, *Solar Energy*, 33, p. 117.

Feuermann, D., Gordon, J.M. and Zarmi, Y. (1985). A typical meteorological day (TMD) approach for predicting the long-term performance of solar energy systems, *Solar Energy*, 35, p. 63.

Gordon, J.M. and Zarmi, Y. (1981). Technical note: Thermosyphon systems: Single vs. multipass, *Solar Energy*, 27, p. 441.

Gordon, J.M. and Rabl, A. (1982). Design, analysis and optimization of solar industrial process heat plants without storage, *Solar Energy*, 28, p. 519.

Gordon, J.M. and Zarmi, Y. (1985). An analytic model for the long-term performance of solar thermal systems with well-mixed storage, *Solar Energy*, 35, p. 55.

Gordon, J.M. and Rabl, A. (1986). Design of solar industrial process heat systems, in *Reviews of Renewable Energy Sources*, M.S. Sodha, S.S. Mathur, M.A.S. Malik and T.C. Kandpal (eds.) Ch. 6, Wiley Easter, New Delhi.

Gordon, J.M. and Saltiel, C. (1986). Analysis and optimization of multistage solar collector systems, *ASME Journal of Solar Energy Eng.*, 108, p. 92.

Gordon, J.M. (1987). Optimal sizing of stand-alone photovoltaic systems, *Solar Cells*, 20, p. 295.

Grassie, S.L. and Sheridan, N.R. (1977). The use of planar reflectors for increasing the energy yield of flat-plate collectors, *Solar Energy*, 19, p. 663.
Hollands, K.G.T. (1965). Honeycomb devices in flat-plate solar collectors, *Solar Energy*, 9, p. 159.
Klein, S.A., Cooper, P.I., Freeman, T.L., Beekman, D.M., Beckman, W.A. and Duffie, J.A. (1975). A method of simulation of solar processes and its applications, *Solar Energy*, 17, p. 29.
Klein, S.A. (1978). Calculation of flat-plate collector utilizability, *Solar Energy*, 21, p. 393.
Klein, S.A. et al. (1979). TRNSYS-A Transient System Simulation User's Manual, University of Wisconsin-Madison Engineering Experiment Station Report 38-10.
Klein, S.A. and Beckman, W.A. (1979). A general design method for closed-loop solar energy systems, *Solar Energy*, 22, p. 269.
Kreider, J.F. (1979). *Medium and High Temperature Solar Processes*, Academic Press, New York.
Kutcher, C.F., Davenport, R.L., Dougherty, D.A., Gee, R.C., Masterson, P.M. and May, E.K. (1982). Design Approaches for Solar Industrial Process Heat Systems, SERI/TR-253-1356, Solar Energy Research Institute, Golden, CO.
Larson, D.C. (1980). Optimization of flat-plate collector flat mirror system, *Solar Energy*, 24, p. 203.
Larson, R.W. Vignola, F. and West, R. (1992). *Economics of Solar Energy Technologies*, American Solar Energy Society Report, Boulder, CO.
Liu, B.Y.H. and Jordan, R.C. (1960). The inter-relationship and characteristic distribution of direct, diffuse and total solar radiation, *Solar Energy*, 4, p. 1.
Liu, B.Y.H. and Jordan, R.C. (1963). A rational procedure for predicting the long-term average performance of flat-plate solar energy collectors, *Solar Energy*, 7, p. 53.
Liu, S.T. and Fanney, A.H. (1980). Comparing experimental and computer-predicted performance for solar hot water systems, *ASHRAE Journal*, 22, No. 5, p. 34.
Meyer, B.A. (1978). Natural convection heat transfer in small and moderate aspect ratio enclosures — An application to flat-plate collectors, in *Thermal Storage and Heat Transfer in Solar Energy Systems*, F. Kreith, R. Boehm, J. Mitchell and R. Bannerot (eds.), American Society of Mechanical Engineers, New York.
Mitchell, J.C., Theilacker, J.C. and Klein, S.A. (1981). Technical note: Calculation of monthly average collector operating time and parasitic energy requirements, *Solar Energy*, 26, p. 555.
Mueller Associates (1985). *Active Solar Thermal Design Manual*, funded by U.S. DOE (no. EG-77-C-01-4042), SERI(XY-2-02046-1) and ASHRAE (project no. 40), Baltimore, MD.
Newton, A.B. and Gilman, S.H. (1977). *Solar Collector Performance Manual*, funded by U.S. DOE (no. EG-77-C-01-4042), SERI(XH-9-8265-1) and ASHRAE (project no. 32, Task 3).
OTA (1991). Office of Technology Assessment, U.S. Congress, Washington, D.C.
Phillips, W.F. and Dave, R.N. (1982). Effect of stratification on the performance of liquid-based solar heating systems, *Solar Energy*, 29, p. 111.
Rabl, A. (1981). Yearly average performance of the principal solar collector types, *Solar Energy*, 27, p. 215.
Rabl, A. (1985). *Active Solar Collectors and Their Applications*, Oxford University Press, New York.
Reddy, T.A., Gordon, J.M. and de Silva, I.P.D. (1988). MIRA: A one-repetitive day method for predicting the long-term performance of solar energy systems, *Solar Energy*, 39, no. 2, p. 123.
Reddy, T.A. (1987). *The Design and Sizing of Active Solar Thermal Systems*, Oxford University Press, Oxford, U.K.
Saunier, G.Y. and Chungpaibulpatana, S. (1983). A new inexpensive dynamic method of testing to determine solar thermal collector performance, Int. Solar Energy Society World Congress, Perth, Australia.
SERI (1989). *Engineering Principles and Concepts for Active Solar Systems*, Hemisphere Publishing Company, New York.
Symons, J.G. (1976). *The Direct Measurement of Heat Loss from Flat-Plate Solar Collectors on an Indoor Testing Facility*, Technical Report TR7, Division of Mechanical Eng., Commonwealth Scientific and Industrial Research Organisation, Melbourne, Australia.

Theilacker, J.C. and Klein, S.A. (1980). Improvements in the utilizability relationships, American Section of the International Solar Energy Society Meeting Proceedings, P. 271, Phoenix, AZ.